| AD NUMBER |
| --- |
| **AD502325** |
| CLASSIFICATION CHANGES |
| TO: **UNCLASSIFIED** |
| FROM: **CONFIDENTIAL** |
| LIMITATION CHANGES |
| TO:<br>**Approved for public release; distribution is unlimited.** |
| FROM:<br>**Distribution authorized to DoD only; Administrative/Operational Use; MAR 1969. Other requests shall be referred to Army Aviation Material Labs., Fort Eustis, VA.** |
| AUTHORITY |
| **USAAMRDL ltr 21 May 1973; USAAMRDL ltr 21 May 1973** |

# SECURITY MARKING

**The classified or limited status of this report applies to each page, unless otherwise marked.**
**Separate page printouts MUST be marked accordingly.**

CONFIDENTIAL

AD

# USAAVLABS TECHNICAL REPORT 68-90A

# SINGLE-STAGE AXIAL COMPRESSOR COMPONENT DEVELOPMENT FOR SMALL GAS TURBINE ENGINES (U)

## VOLUME I. DESIGN (U)
## PHASE I REPORT



By
C. H. Muller
W. Litke
A. Sabatiuk
H. Weiser

March 1969



U. S. ARMY AVIATION MATERIEL LABORATORIES
FORT EUSTIS, VIRGINIA
CONTRACT DA 44-177-AMC-392(T)
WRIGHT AERONAUTICAL DIVISION
CURTISS-WRIGHT CORPORATION
WOOD-RIDGE, NEW JERSEY



CONFIDENTIAL

## Disclaimers

The findings in this report are not to be construed as an official Department of the Army position unless so designated by other authorized documents.

When Government drawings, specifications, or other data are used for any purpose other than in connection with a definitely related Government procurement operation, the United States Government thereby incurs no responsibility nor any obligation whatsoever; and the fact that the Government may have formulated, furnished, or in any way supplied the said drawings, specifications, or other data is not to be regarded by implication or otherwise as in any manner licensing the holder or any other person or corporation, or conveying any rights or permission, to manufacture, use, or sell any patented invention that may in any way be related thereto.

## Disposition Instructions

When this report is no longer needed, Department of the Army organizations will destroy it in accordance with the procedures given in AR 380-5.

DEPARTMENT OF THE ARMY
U. S. ARMY AVIATION MATERIEL LABORATORIES
FORT EUSTIS, VIRGINIA 23604

(U) Appropriate technical personnel of this Command have reviewed this report and concur with the conclusions contained herein.

(U) The findings and recommendations outlined herein were considered in planning the subsequent phases of the program.

Task 1G162203D14413
Contract DA 44-177-AMC-392(T)
USAAVLABS Technical Report 68-90A
March 1969

# SINGLE-STAGE AXIAL COMPRESSOR COMPONENT DEVELOPMENT FOR SMALL GAS TURBINE ENGINES (U)

Volume I. Design (U)

Phase I Report

WAD: R608/PF-1

By

C. H. Muller
W. Litke
A. Sabatiuk
H. Weiser



Prepared by

Wright Aeronautical Division
Curtiss-Wright Corporation
Wood-Ridge, New Jersey

for

U. S. ARMY AVIATION MATERIEL LABORATORIES
FORT EUSTIS, VIRGINIA

## (U) SUMMARY

The overall objective of this program is to advance and demonstrate high-pressure-ratio axial compressor technology to the point where an engine designer has sufficient design data to incorporate the axial compressor in a small gas turbine engine. The analysis and results of the designs and studies conducted under Phase I of this program are presented in this report.

The design of a single-stage axial supersonic compressor has been completed. The predicted performance for this compressor stage is:

| | |
|---|---|
| stage pressure ratio | 2.8:1 |
| adiabatic efficiency | 82.0 percent |
| corrected airflow | 4.0 pounds per second |
| design speed | 50,700 RPM |

A gas generator performance study has been conducted to evaluate non-regenerated designs with 16:1 pressure ratio compressors and turbine inlet temperatures between 2500°F and 3000°F. The design point specific fuel consumption of the engines studied ranged from 0.415 to 0.438 pound per horsepower per hour. At 50 percent power, this range increased to 0.465 and 0.534 respectively. The engine configuration which indicated the lowest specific fuel consumption has a two-spool gas generator and variable stator free power turbine.

The preliminary design of a two-stage 16:1 axial/centrifugal compressor has been completed, and the design point performance for this compressor is:

| | |
|---|---|
| pressure ratio | 16:1 |
| adiabatic efficiency | 77.5 percent |
| corrected airflow | 4.0 pounds per second |
| design speed | 50,700 RPM |

The preliminary design of an advanced two-spool gas generator which incorporates the 16:1 axial/centrifugal compressor has been completed. This non-regenerated engine is a two-spool gas generator with a variable stator two-stage free power turbine and a 2500°F turbine inlet temperature. The design point performance is:

| | |
|---|---|
| specific fuel consumption | 0.431 pound per horsepower per hour |
| horsepower | 785 |
| airflow | 4.0 pounds per second |

A preliminary design study of a variable-geometry axial compressor rotor has also been conducted, and two mechanical schemes of a variable-geometry rotor have evolved. The performance analysis of this concept indicates that part-speed pressure ratio and efficiency of the axial rotor can be improved considerably and that the engine airflow can be varied substantially to improve part-speed matching with succeeding stages on the same shaft. The performance of the variable-geometry airfoil together

with the performance of very highly cambered and high diffusing rotors needs to be established experimentally before the full extent of the performance potential can be assessed.

Appendix I to this report describes the experimental results of a 2:1 supersonic axial compressor program currently being conducted at the Wright Aeronautical Division of Curtiss-Wright. The technology being developed and advanced in this program is closely related and of direct benefit to the U.S. Army Aviation Materiel Laboratories (USAAVLABS) program and establishes a firm basis for the design procedures utilized in the more advanced 2.8:1 pressure ratio supersonic compressor stage.

## (U) FOREWORD

United States Army Contract DA 44-177-AMC-392(T) (Task 1G162203D14413) is being performed by the Curtiss-Wright Corporation, Wright Aeronautical Division to advance and demonstrate high-pressure-ratio axial compressor technology for small gas turbines. This contract is administered under the direction of the Propulsion Division of the U.S. Army Aviation Materiel Laboratories. The Phase I effort for this program is discussed in this report. This phase consisted of the design of a single-stage supersonic axial compressor and test rig and an analytical evaluation of its performance potential as a compressor boost stage for small gas turbine engines. Experimental investigation and development of the rotor performance of this compressor will be performed in Phase II. The experimental investigation of the total stage performance is scheduled for Phase III.

The manager of the Small Gas Turbine Engine Program is T. Schober, and the manager of this Compressor Technology Contract is C. H. Muller. Principal contributing engineers are L. Cox, W. Litke, H. Weiser, A. Corrado, and T. Lutringer. The overall guidance and technical direction provided by Mr. A. Sabatiuk and the direction of Mr. S. Lombardo are gratefully acknowledged. The guidance of Mr. J. White, Mr. L. Hubert, and Mr. D. Cale of USAAVLABS is also gratefully acknowledged.

(U) CONTENTS

## (U) ILLUSTRATIONS

## (U) ILLUSTRATIONS (Cont'd)

## (U) ILLUSTRATIONS (Cont'd)

## (U) ILLUSTRATIONS (Cont'd)

## (U) ILLUSTRATIONS (Cont'd)

## (U) TABLES

## (U) SYMBOLS

| | |
|---|---|
| $A/A^*$ | isentropic area ratio - dimensionless |
| $A^*$ | area at which sonic flow would occur - square inches |
| $A_{ann}$ | annular area - square inches |
| $A_{flow}$ | flow area - square inches |
| a | acoustic velocity (based on static temperature) - feet per second |
| $a_t$ | acoustic velocity (based on total temperature) - feet per second |
| $C_p$ | specific heat for a constant pressure process - BTU per pound per degree Rankine |
| D | diameter - inches |
| $D_m$ | mean diameter - inches |
| g | acceleration of gravity - feet per second squared |
| h | hub streamtube |
| I.C. | iron-constantan thermocouple |
| I.D. | inside diameter - inches |
| i | incidence angle - degrees |
| i′ | modified incidence angle - degrees |
| J | work constant (778 foot-pounds per BTU) |
| K | continuity equation constant (0.26048 pound degrees Rankine per square inch per inch of mercury) |
| k | spring rate - pounds per inch |
| M | Mach number - dimensionless |
| m | mean streamtube |
| N | rotational speed - revolutions per minute |
| O.D. | outside diameter - inches |
| $P_s$ | static pressure - inches of mercury |

| | |
|---|---|
| $P_T$ | total pressure - inches of mercury |
| R | radius of curvature in meridional plane - inches (or gas constant, 53.4 foot-pounds per pound degree Rankine, when occurs in the expression $\sqrt{KgRT_s}$) |
| REC | total pressure recovery - ratio of total pressure remaining after losses through blade row passage to initial total pressure at blade row inlet - dimensionless |
| r | radius from compressor axis - inches |
| $T_s$ | static temperature - degrees Rankine |
| $T_T$ | total temperature - degrees Rankine |
| t | tip streamtube |
| $t_c$ | ratio of maximum blade thickness to the chord length |
| U | rotor blade section speed - feet per second |
| V | velocity - feet per second |
| $V_{ax}$ | axial velocity component - feet per second |
| $V_{tan}$ | tangential velocity component - feet per second |
| W | airflow - pounds per second |
| $\alpha$ | tangential airflow angle relative to the compressor axis - degrees |
| $\beta$ | tangential angle to blade camber line - degrees |
| $\beta'$ | tangential angle to blade suction surface - degrees |
| $\delta$ | deviation angle - degrees (or ratio of local total pressure to a reference pressure, when occurs in $(W\sqrt{\theta})/\delta$ - dimensionless) |
| $\Delta$ | change of a quantity across a blade row - dimensionless |
| $\epsilon$ | airflow slope angle in meridional plane - degrees |
| $\eta_{ad}$ | adiabatic efficiency - dimensionless |
| $\gamma$ | ratio of specific heats - dimensionless |

| | |
|---|---|
| $\phi$ | blade camber angle - degrees |
| $\rho$ | density - pounds per cubic foot |
| $\theta$ | air turning angle through a blade row - degrees (or ratio of local total temperature to a reference temperature, when occurs in either $N/\sqrt{\theta}$ or $(W\sqrt{\theta})/\delta$ - dimensionless) |

Subscripts

| | |
|---|---|
| amb | ambient conditions |
| o | station at entrance to inlet guide vanes |
| 1 | absolute conditions (relative to non-rotating reference) at a station representing exit of inlet guide vanes and inlet to rotor |
| 2 | entrance conditions to rotor relative to the rotating rotor blade |
| 3 | exit conditions from the rotor relative to the rotating rotor blade |
| 4 | absolute conditions (relative to non-rotating reference) at a station representing the rotor exit and inlet to the exit stator |
| 5 | absolute conditions at a station representing the exit of the exit stator and interconnecting duct |

## (U) INTRODUCTION

The overall objective of the U.S. Army Aviation Materiel Laboratories in the field of small gas turbine engines has been stated on numerous occasions. In general, it is the advancement of technology in the major component areas to the point where a small gas turbine engine can be designed to provide a non-regenerated engine with a specific fuel consumption of less than 0.460 pound per horsepower per hour. The compressor component required to make this performance goal possible must be capable of high pressure ratio (16:1 range) at good component efficiencies and, in addition, must be designed for simplicity, ruggedness, durability, and minimum cost.

The objective of this program is to advance and demonstrate high-pressure-ratio axial compressor technology to the level that, when matched analytically with the advanced centrifugal compressor technology supplied by USAAVLABS, will provide a 16:1 compressor which offers the desired engine performance. Specifically, this program addresses the development of a supersonic axial compressor to serve as the boost or supercharging stage. Since the part-power performance of these engines is also critical, several study tasks have been included in the program to gain some insight into the important off-design parameters and trade-offs which should influence the axial compressor development when considered in the overall compressor and engine operation.

The program is scheduled in three phases. Phase I involves (1) the design of the supersonic axial stage compressor and test rig; (2) an analytical study to evaluate the performance potential and characteristics of various compressor and engine configurations; and (3) the preliminary design of an advanced 16:1 axial/centrifugal compressor, an advanced gas generator incorporating this compressor, and a variable-geometry compressor rotor. In Phase II, the inlet guide vanes and compressor rotor will be procured and developed through experimental testing. In Phase III, the design of the exit stator and interconnecting duct for the supersonic axial stage will be finalized, and this hardware will be procured and developed through experimental testing. Also in the final phase, an advanced inlet guide vane will be designed, the hardware will be procured and its improvement of stage performance experimentally evaluated.

The pressure ratio for the axial boost compressor of the 16:1 axial/centrifugal configuration is required to be in excess of 2.5:1. Minimizing the number of stages required to achieve the high-performance goals of these compressors offers the advantages of smaller engine envelope, reduced costs, and increased reliability. On this basis, a single-stage axial compressor is most attractive.

Subsonic and transonic compressors do not possess the rotor blade section speeds necessary to achieve pressure ratios of 2.5:1 per stage. The transonic compressor is limited to stage pressure ratios of 2:1. The

supersonic compressor is, therefore, the only category of axial compressor which offers the potential of a pressure ratio in excess of 2.5:1 in one stage.

There are two basic types of supersonic axial compressors. These are the impulse rotor and the shock-in-rotor designs. In the impulse rotor, the air enters and exits at supersonic relative Mach numbers. This approach offers the highest potential pressure ratio per stage (in excess of 4:1); therefore, investigation of this type has been far more extensive in the past than for the shock-in-rotor type, which is limited to less than 4:1. The demonstrated rotor performance of the impulse type has been very high, but the exit stator losses associated with the diffusion from supersonic to subsonic Mach numbers have been excessive (as high as 50 percent total pressure loss in some cases) and have resulted in relatively low overall stage efficiencies.

The stage pressure ratio potential of the shock-in-rotor type of axial supersonic compressor easily meets the goal (>2.5:1) of the boost stage to be developed in this program. The air enters this type of rotor at supersonic relative Mach numbers but shocks down in the rotor passage to subsonic exit Mach numbers for both the relative and the absolute vectors. The exit stator losses are, therefore, expected to be comparable to those in transonic stages (>3 percent total pressure loss). The rotor pressure losses at the supersonic relative inlet Mach numbers are expected to be higher than those for rotors with transonic or subsonic relative inlet Mach numbers. However, even with the higher rotor pressure losses, stage efficiencies of 80 percent to 85 percent are predicted for the shock-in-rotor type of supersonic compressors as a result of the high pressure ratio developed in the stage.

The number and scope of past experimental investigations, to advance the shock-in-rotor type of supersonic compressor, were relatively limited, and efficiencies of 80 percent or higher were not achieved. Curtiss-Wright believes that the ranges of cascade parameters explored in those programs do not offer the optimum performance potential. Specifically, the selection of rotor parameters to provide higher solidities and minimum passage divergence (nearly constant area passage) and the utilization of body forces (from hub and tip curvature and blade lean and sweep) to control pressure gradients are required to achieve the desired efficiencies.

Concurrent with the initiation of the subject contract, an experimental evaluation of a 2:1 supersonic compressor was initiated under a program being conducted at the Wright Aeronautical Division of the Curtiss-Wright Corporation. The design of this compressor incorporates the approach to the advanced cascade design parameters discussed in the previous paragraph. Initial experimental results from these tests are very encouraging and thus support the design approach and projected performance potential.

Based on the high performance potential, the merits of achieving the boost pressure ratio in a single stage, and the encouraging data from the

current experimental program discussed above, a single-stage shock-in-rotor supersonic compressor has been chosen as the axial boost compressor to be advanced and demonstrated under this contract. The design goals of this compressor are:

| | |
|---|---|
| pressure ratio | 2.8:1 |
| adiabatic efficiency | 82.0 percent |
| corrected airflow | 4.0 pounds per second |

## (C) GAS GENERATOR PERFORMANCE ANALYSIS (U)

(U) The integration of the 16:1 pressure ratio axial/centrifugal compressor into the design of an optimum small gas turbine engine requires an appreciation for the trade-offs associated with its configuration, efficiency, and characteristic operation. An analytical study has been conducted to provide these trade-off data. The design point and part-power cycle performance of non-regenerated engines has been determined to evaluate several axial/centrifugal compressor configurations.

(U) The engine design parameters for this study were:

| | |
|---|---|
| specific fuel consumption at design point | 0.46 pound per horsepower per hour |
| airflow | 4.0 pounds per second |
| turbine inlet temperature | 2500°F to 3000°F |
| compressor pressure ratio at design point | 16:1 |

### (C) COMPRESSOR CONFIGURATIONS AND PERFORMANCE (U)

(U) The 16:1 compressor consists of an axial compressor followed by either a centrifugal or a radial outflow compressor. Three axial, one centrifugal, and a radial outflow compressor were included in this investigation. The three axial compressors are Curtiss-Wright designs. The predicted performance for the centrifugal and radial outflow stages was supplied by USAAVLABS and was developed under Army Contracts DA 44-177-AMC-173(T) and DA 44-177-AMC-180(T) respectively. The design parameters and designations for these components are shown in Table I. The compressor maps are presented in Figures 1 through 5.

TABLE I. (U) COMPRESSOR STAGES FOR ENGINE STUDY

| Type | Designation | Description | Atmospheric Corrected Design Air-Flow (lb/sec) | Design Pressure Ratio | Design Adiabatic Efficiency |
|---|---|---|---|---|---|
| Axial | SSC (2.0) | Curtiss-Wright single-stage supersonic | 4.0 | 2.1:1 | 79.3 |
| Axial | SSC (2.8) | Curtiss-Wright single-stage supersonic | 4.0 | 2.8:1 | 82.2 |
| Axial | TST | Curtiss-Wright two-stage transonic (TST) | 4.0 | 2.0:1 | 85.5 |
| Centrifugal | RF-1 | Radial flow* | 4.0 | 10:1 | 79.0 |
| Radial Outflow | ROC-1 | Radial outflow with variable guide vanes* | 4.0 | 11:1 | 82.5 |

*Scaled to match axial compressor outlet conditions

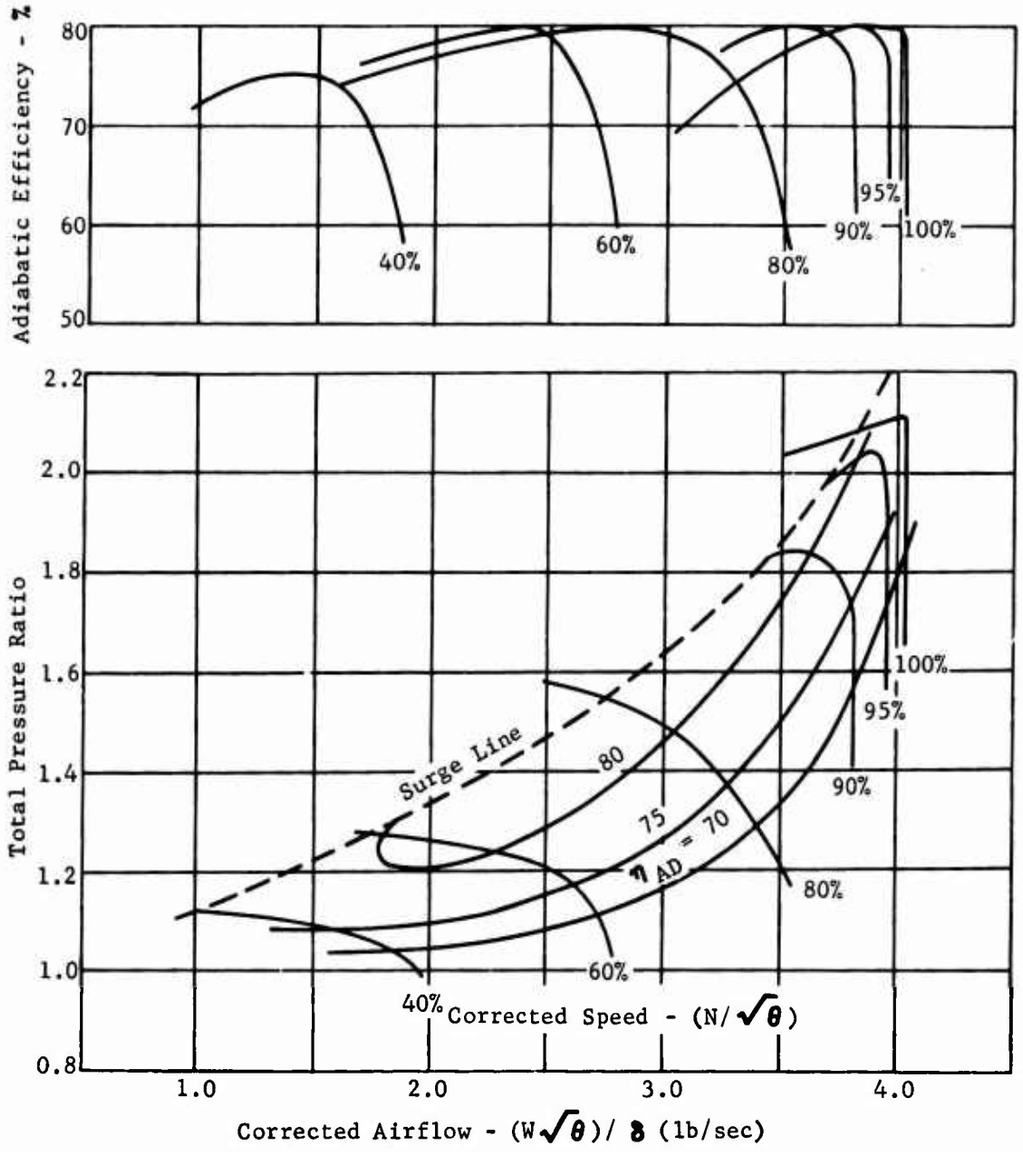


Figure 1. (U) 2:1 Single-Stage Supersonic Compressor - SSC (2.0) Predicted Performance Map.

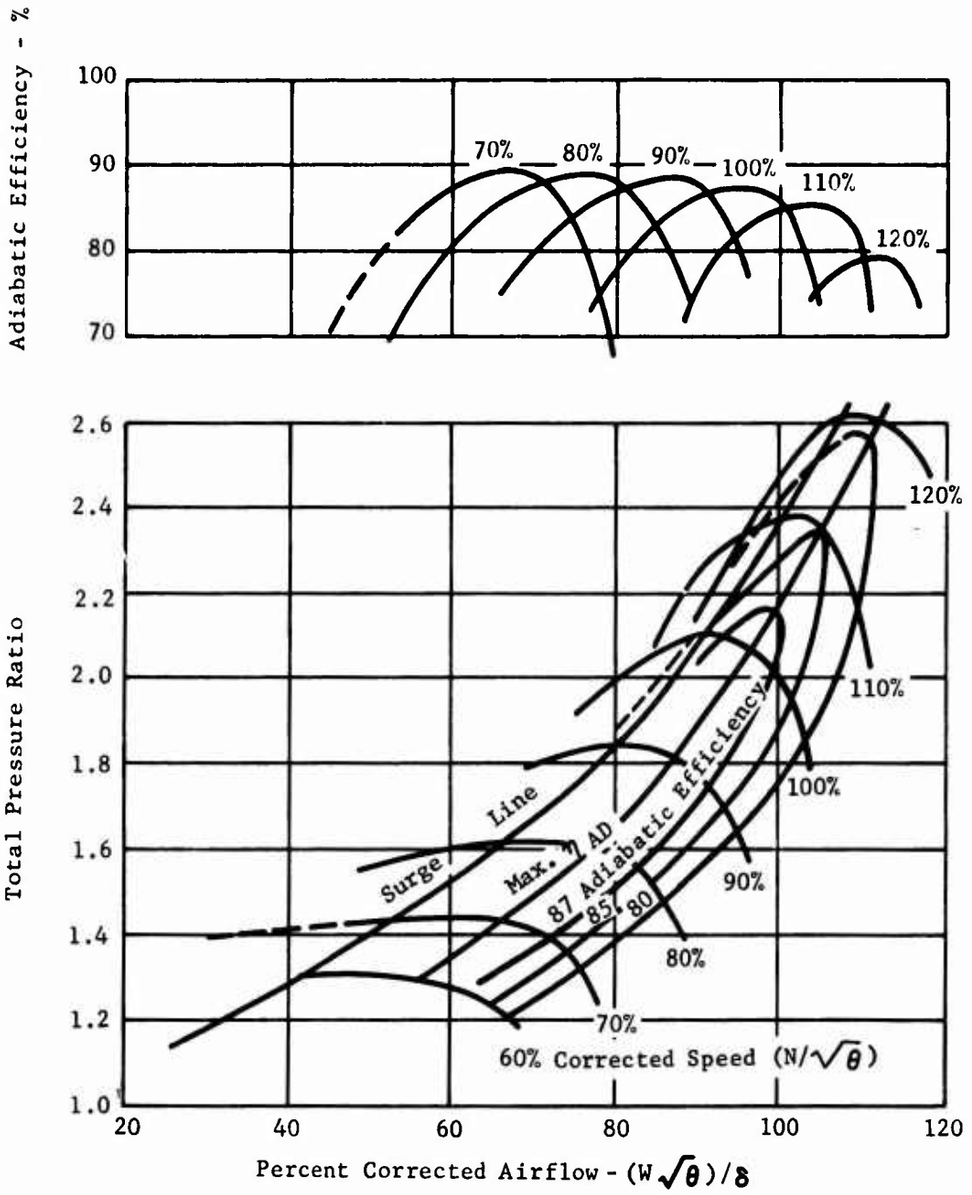


Figure 2. (U) Two-Stage Transonic Axial Compressor - (TST) Predicted Performance Map.

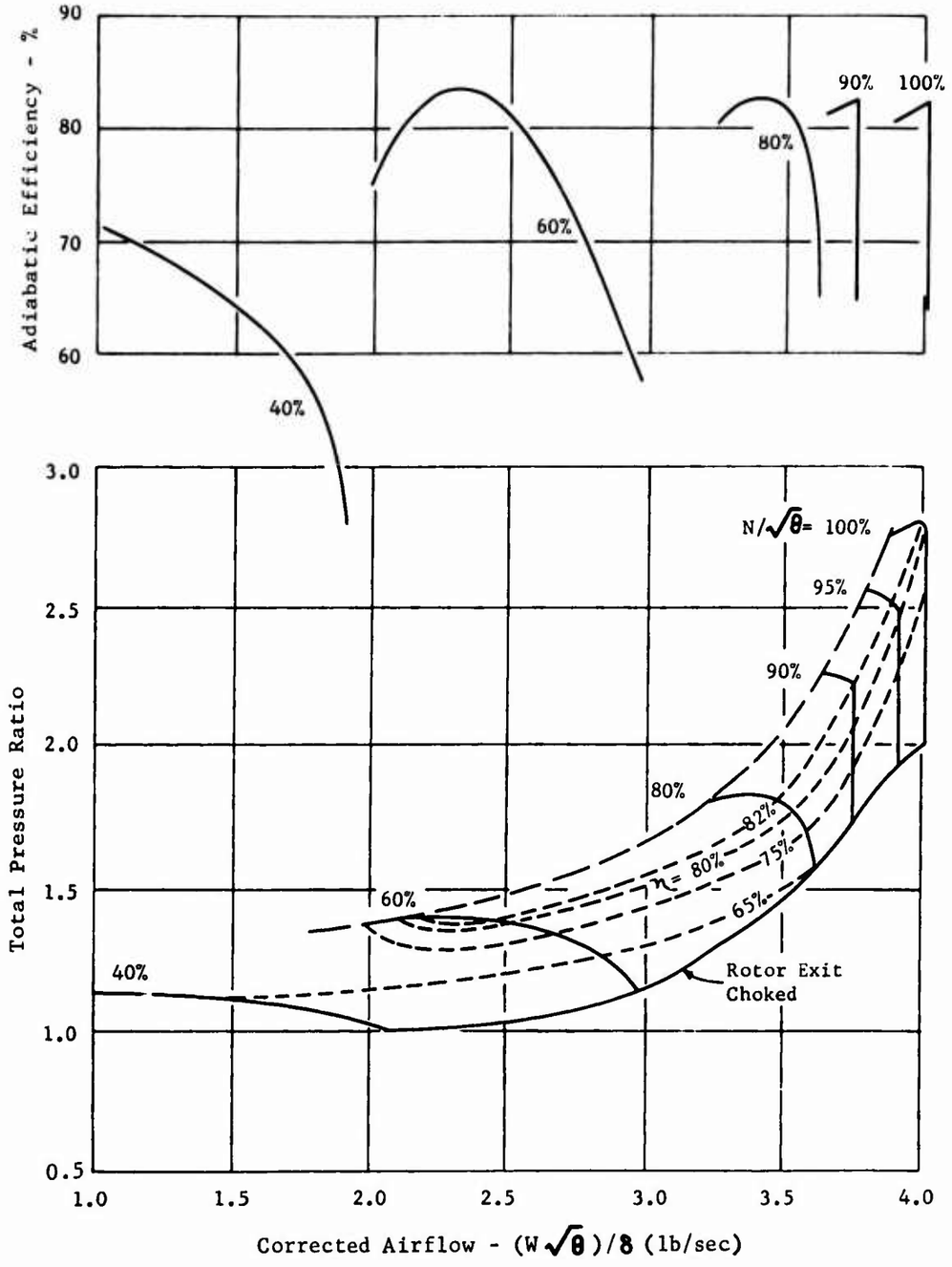


Figure 3. (U) 2.8:1 Single-Stage Supersonic Compressor - SSC (2.8) Predicted Performance Map.

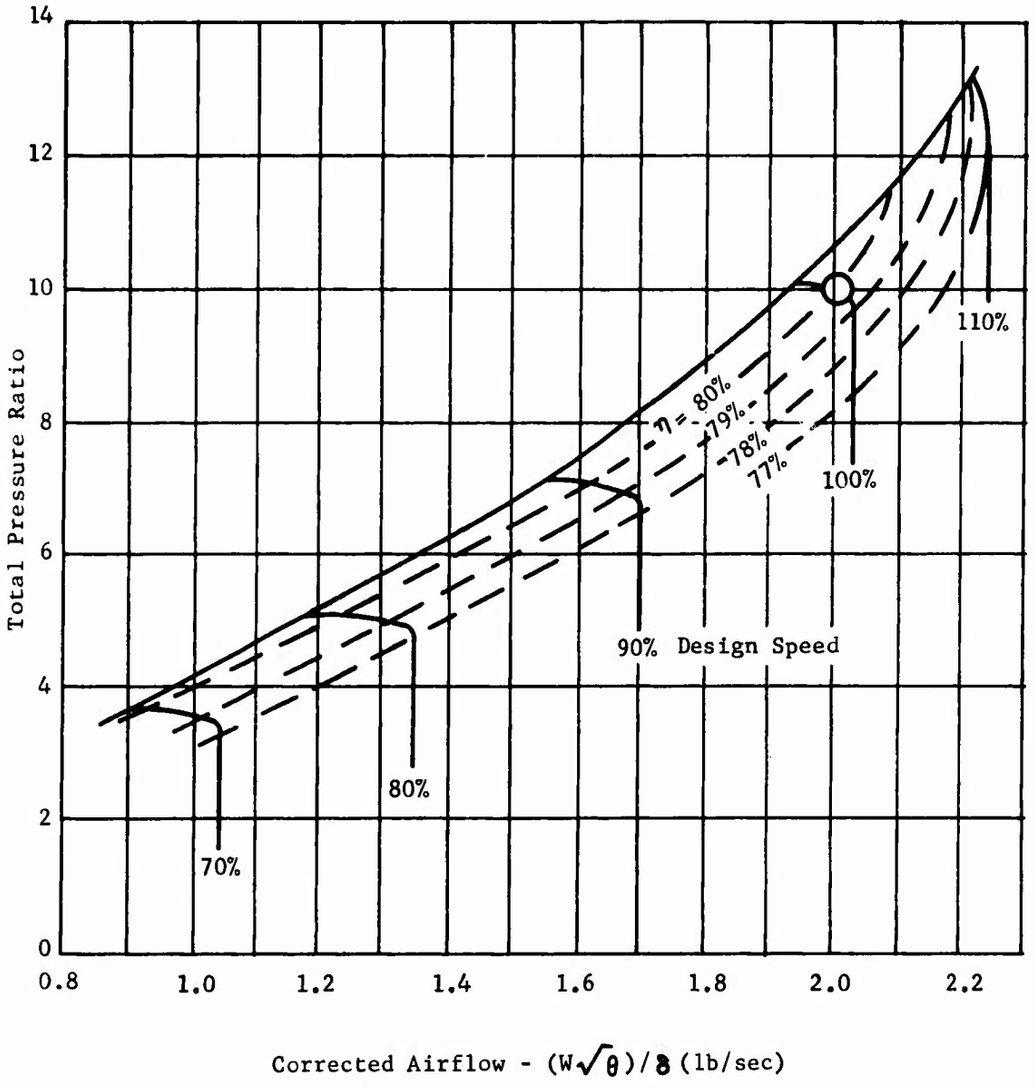


Figure 4. (U) 10:1 Centrifugal Compressor - (RF-1)
Predicted Performance Map.

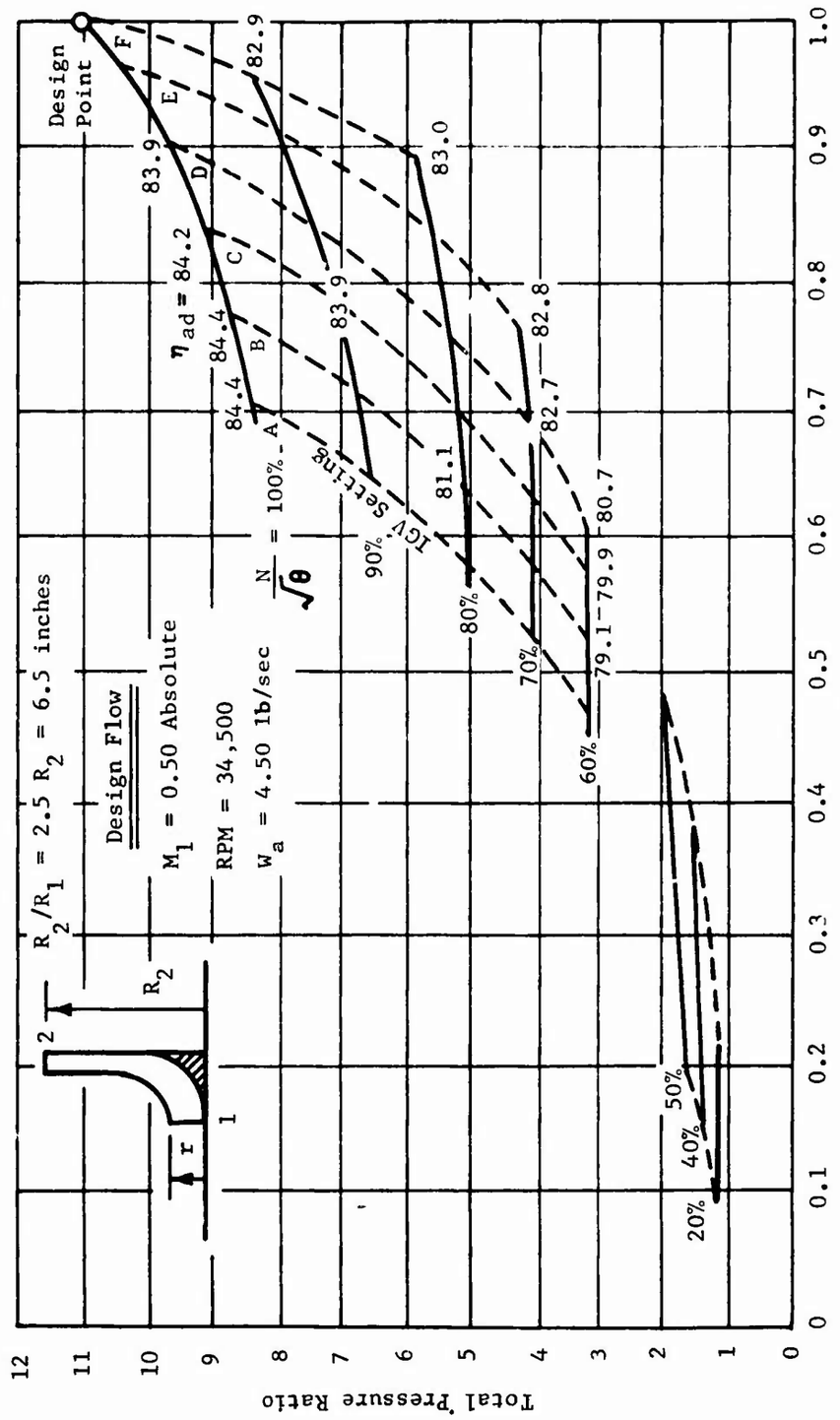


Figure 5. (C) 11:1 Radial Outflow Compressor - (ROC-1)
Predicted Performance Map. (U)

(U) The compressors listed in Table I have been combined into the five axial/centrifugal 16:1 configurations listed in Table II.

TABLE II. (U) COMPRESSOR CONFIGURATIONS FOR ENGINE STUDY

| Compressor Configuration No. | Number of Compressor Spools | Low Pressure (LP) Compressor | High Pressure (HP) Compressor | Overall Design Point Pressure Ratio |
|---|---|---|---|---|
| 1 | 2 | SSC (2.0) | RF-1 | 16:1 |
| 2 | 2 | TST (2.0) | RF-1 | 16:1 |
| 3 | 2 | SSC (2.0) | ROC-1 | 16:1 |
| 4 | 2 | SSC (2.8) | RF-1 | 16:1 |
| 5* | 1 (with interstage bleed) | SSC (2.8) | RF-1 | 16:1 |
| 5a* | 1 (with variable-geometry rotor and reduced bleed) | SSC (2.8) | RF-1 | 16:1 |

*Two approaches were investigated for configuration 5 and are designated 5 and 5a respectively.

(U) Configuration 5 employs interstage bleed at the exit stator of the axial stage for surge-free part-power operation. In configuration 5a, a variable-geometry axial rotor is incorporated which reduces considerably the required interstage bleed. The interstage bleed for these configurations is assumed to be dumped overboard in the performance calculations. Figure 6 presents the compressor map for configuration 5. The airflow presented on this figure is the remainder after interstage bleed corrected to standard inlet conditions, and the efficiency represents the ideal work of compression for only the airflow which passes through both the axial and centrifugal stages divided by the summation of the actual work on the total airflow passing through the axial stage (including bleed flow) and that on the remaining flow through the centrifugal stage.

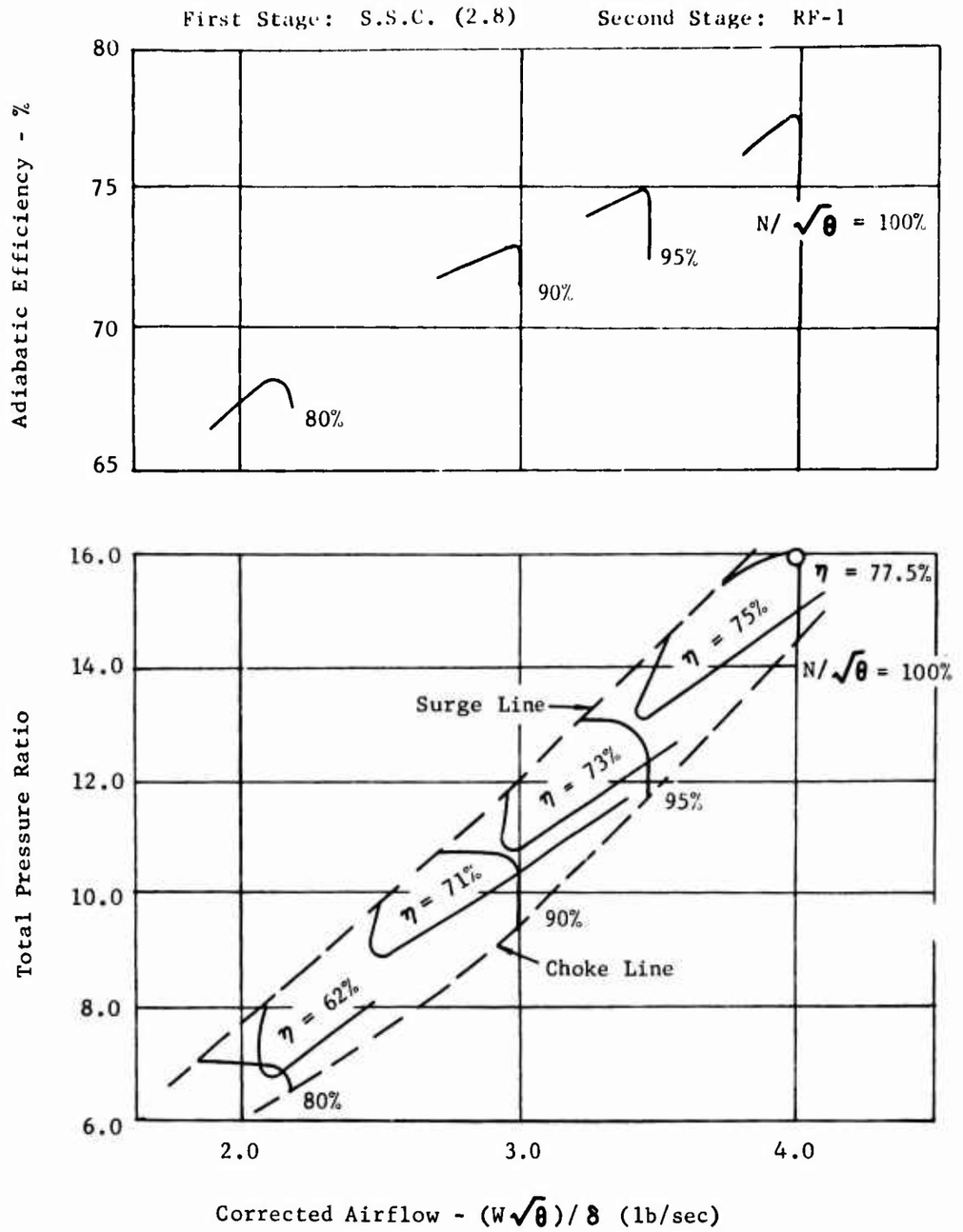


Figure 6. (U) Axial/Centrifugal Single Spool Compressor - Configuration 5 With Interstage Bleed at Part Speed Predicted Performance Map.

(U) COMPONENT PERFORMANCE AND BASIS OF ANALYSIS

(U) All of the engine performance calculations were based on sea level, static, standard day conditions. The various component efficiencies at maximum power were estimated as follows:

| | |
|---|---|
| Axial Compressors (Adiabatic) | Noted above |
| Centrifugal Compressors (Adiabatic) | Noted above |
| HP Turbine (Adiabatic) | 90 Percent |
| LP Turbine (Adiabatic) | 89 Percent |
| Power Turbine (Adiabatic) | 87 Percent |
| Combustor | 98 Percent |
| HP Turbine, Mechanical | 99 Percent |
| LP Turbine, Mechanical | 100 Percent |
| Gear - Output Shaft | 97 Percent |

(U) Turbine performance maps were programmed and utilized to establish the matched off-design operating conditions. Turbine cooling air was included as required, and stator and rotor blades were assumed to be transpiration cooled where blade cooling was necessary. The cooling air percentages given in Table III remain constant over the operating power range.

TABLE III. (U) TURBINE COOLING AIR FOR ENGINE STUDY

| | 2500°F | 2700°F | 3000°F |
|---|---|---|---|
| 1st Stator | 6.25% | 7.25% | 8.5% |
| 1st Rotor, Blades | 4.75 | 5.5 | 6.5 |
| 1st Rotor, Disc | 1.0 | 1.0 | 1.0 |
| 1st Rotor, Leakage | 1.0 | 1.0 | 1.0 |
| 2nd Stator | - | 3.25 | 4.5 |
| 2nd Rotor, Blades | - | 2.25 | 3.25 |
| 2nd Rotor, Disc | 1.5 | 1.0 | 1.0 |
| 2nd Rotor, Leakage | - | 1.0 | 1.0 |
| Power Turbine Stator | - | - | - |
| Power Turbine Rotor, Blades | - | - | - |
| Power Turbine Rotor, Disc | 1.25 | 1.5 | 1.75 |
| Power Turbine Rotor, Leakage | - | - | - |
| Total | 15.75% | 23.75% | 28.50% |

(U) The turbine cooling air is treated as follows in the calculation of the cycle performance:

1. The high-pressure (HP) turbine stator cooling air was returned to the cycle mass flow at the HP turbine rotor inlet.

2. The HP turbine rotor cooling and internal seal leakage air and the low-pressure (LP) turbine stator cooling air were returned at the LP turbine rotor inlet.

3. The LP turbine rotor cooling air and internal seal leakage air were returned at the power turbine rotor inlet.

4. The power turbine rotor disc cooling air and internal seal leakage air were returned at the jet nozzle inlet.

(U) The component pressure loss percentages remained constant, as listed below, over the operating power range.

| | Pressure Losses |
|---|---|
| Inlet | None |
| Exhaust | 1.5 Percent |
| Combustor | 3 Percent |
| Diffuser (Power Turbine) | 1 Percent |

The fuel lower heating value of 18,400 British thermal units per pound was used.

(U) Engine design and off-design performance was computed using an IBM 704 digital computer. The following digital programs were utilized in the applicable portions of the program:

Curtiss-Wright Log 776 - Turboshaft Design Point Program.

Curtiss-Wright Log 903 - Single-Spool Turboshaft Engine Performance.

Curtiss-Wright Log 792 - Two-Spool Turboshaft Engine Performance.

(U) ENGINE CONFIGURATIONS STUDIED

(U) For each of the gas generator configurations studied, three power turbine arrangements were evaluated: (1) the power turbine rotor on a shaft independent from the gas generator shafts (free-power turbine) and fixed inlet stators (fixed stator); (2) a free-power turbine with stators which can be varied to vary the stator flow area (variable stators); and (3) the power turbine rotor on a shaft which is locked or integral with the low-pressure spool gas generator shaft and a fixed stator. The performance of the fixed-stator free-power turbine engines was obtained by computing the specific fuel consumption and shaft horsepower as a function of power turbine speed for several speeds of the low-pressure gas generator spool. The locus of minimum specific fuel consumption points was then selected to establish the off-design performance. The variable-stator free-power turbine performance was determined by repeating this procedure for several reduced area settings of the power turbine stator and establishing the minimum specific fuel consumption for each respective speed of the low-pressure gas generator spool. All engine configurations were evaluated at turbine inlet temperatures of 2500°F, 2700°F, and 3000°F. Table IV lists the engines evaluated.

TABLE IV. (U) ENGINE CONFIGURATIONS FOR PERFORMANCE ANALYSIS

| Engine Number | Compressor Configuration | Number of Gas Generator Spools | Power Turbine Configuration | Power Turbine Stator | Inlet Temp. HP Turbine Stator °F |
|---|---|---|---|---|---|
| 1,2,3 | 1 | 2 | Independent Spool (Free) | Fixed | 2500,2700,3000 |
| 4,5,6 | | | | Variable | 2500,2700,3000 |
| 7,8,9 | | | Coupled to LP Spool | Fixed | 2500,2700,3000 |
| 10,11,12 | 2 | 2 | Independent Spool (Free) | Fixed | 2500,2700,3000 |
| 13,14,15 | | | | Variable | 2500,2700,3000 |
| 16,17,18 | | | Coupled to LP Spool | Fixed | 2500,2700,3000 |
| 19,20,21 | 3 | 2 | Independent Spool (Free) | Fixed | 2500,2700,3000 |
| 22,23,24 | | | | Variable | 2500,2700,3000 |
| 25,26,27 | | | Coupled to LP Spool | Fixed | 2500,2700,3000 |
| 28,29,30 | 4 | 2 | Independent Spool (Free) | Fixed | 2500,2700,3000 |
| 31,32,33 | | | | Variable | 2500,2700,3000 |
| 34,35,36 | | | Coupled to LP Spool | Fixed | 2500,2700,3000 |
| 37,38,39 | 5 (with interstage bleed) | 1 | Independent Spool (Free) | Fixed | 2500,2700,3000 |
| 40,41,42 | | | | Variable | 2500,2700,3000 |
| 43,44,45 | | | Coupled to LP Spool | Fixed | 2500,2700,3000 |
| 46,47,48 | 5 (with variable axial rotor) | 1 | Independent Spool (Free) | Fixed | 2500,2700,3000 |
| 49,50,51 | | | | Variable | 2500,2700,3000 |
| 52,53,54 | | | Coupled to LP Spool | Fixed | 2500,2700,3000 |

(U) RESULTS AND CONCLUSIONS

(U) The results of this study are presented in Figures 7 through 23. The performance for each of the five compressor configurations is summarized in a series of three figures. The first figure of the series compares the engine performance of the three power turbine arrangements for a 2500°F design point turbine inlet temperature. The performance data from the computer runs with design point turbine inlet temperatures of 2700°F and 3000°F exhibit essentially the same relationship between the three power turbine arrangements as at the 2500°F turbine inlet temperature. The second figure of the series compares the performance of the variable-stator free-power turbine engines at turbine inlet temperatures of 2500°F, 2700°F, and 3000°F. The last figure of the series presents the low-pressure compressor performance map with the engine operating lines or points indicated. A fourth figure (Figure 18) has been prepared for compressor configuration 4, which differs from the second in the series in that the specific fuel consumption is plotted as a function of percent power instead of absolute power, and the performance at the three temperature levels is compared on this basis. The specific fuel consumption of the highest performance engines for each of the five compressor configurations is compared in Figure 23 at both 100 percent power and 50 percent power.

(U) An analysis of these results leads to the following conclusions for the axial/centrifugal 16:1 compressors:

1. The engine specific fuel consumption with compressor configuration 3 is 5.5 percent lower at maximum power than with compressor configuration 1 (see Figure 23). The difference is attributed to the predicted efficiency of the radial outflow second stage of configuration 3 being three points higher than that of the centrifugal second stage of configuration 1.

2. At 50 percent power, the specific fuel consumption of the engine with configuration 3 is only 3.5 percent lower than that with configuration 1. Since configuration 3 had variable guide vanes to the second-stage compressor while configuration 1 did not, it is concluded that variable guide vanes to the centrifugal stage do not offer significant benefit in a two-spool arrangement.

3. Two-spool gas generators offer lower specific fuel consumption at part-power than the single-spool configurations.

4. The engine specific fuel consumption with compressor configuration 2 is 2.3 percent lower at maximum power than with compressor configuration 1, which is attributable to a 6.5 point higher axial stage efficiency for configuration 2.

5. The 2500°F turbine inlet temperature resulted in the lowest specific fuel consumption; 3000°F, second lowest; and 2700°F, highest. It should be noted that the increase in specific fuel consumption between turbine inlet temperatures of 2500°F and 2700°F is attributed to the shift in required blade cooling from one to two turbine stages between these two temperature levels. The specific fuel consumption resumes a decreasing trend as the turbine inlet temperature is increased from 2700°F to 3000°F.

6. The maximum horsepower at the design airflow increases with increasing turbine inlet temperature (see Figures 8, 11, 14, 17, 21).

7. The variable-stator free-power turbine provided the lowest specific fuel consumption, with the fixed stator free and coupled arrangements following in that order (see Figures 7, 10, 13, 16, 20).

8. The coupled and variable-stator free-power turbines provide the widest margin to the low-pressure compressor surge line for the two-spool gas generators (see Figures 9, 12, 15).

9. The operating line for the two-stage transonic axial compressor provides a wider margin to the surge line than for the single-stage supersonic axial compressor.

10. The operating line on the supersonic stage (SSC 2.0) in compressor configuration 1, for engines with fixed-stator free-power turbines, falls in the surge region at part-power based on the predicted surge line. Initial experimental results, however, indicate that the actual surge lines for these compressors may provide more margin than predicted (see Figure 9).

11. The operating lines on the supersonic stage (SSC 2.8) in compressor configuration 4, for two-spool engines with fixed- and variable-stator free-power turbines, cross into the surge region based on the predicted surge line while the coupled turbine line does not (see Figure 19). As mentioned in conclusion 10, however, initial experimental results indicate wider surge margins than predicted for the supersonic compressors.

12. The high interstage bleed required in the single-spool compressor configuration 5 results in a 7 percent higher specific fuel consumption at 50 percent power compared to the two-spool configuration 4 (see Figure 23).

13. The part-power engine specific fuel consumption with the variable-geometry axial compressor rotor and reduced interstage bleed in configuration 5a is halfway between that of configurations 4 and 5. (See Figure 23.)

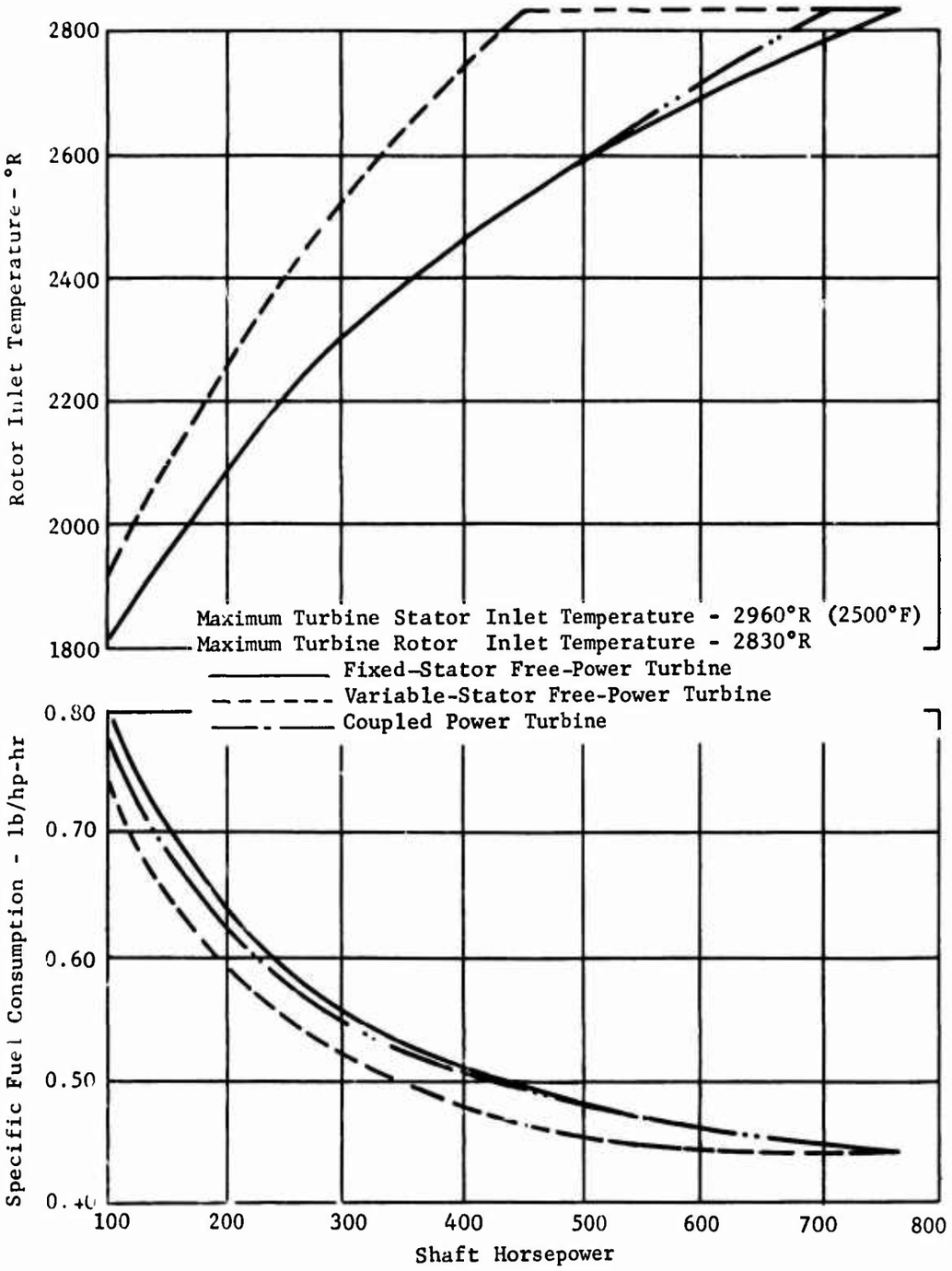


Figure 7. (U) Estimated Engine Performance - Compressor Configuration 1 (USAAVLABS).

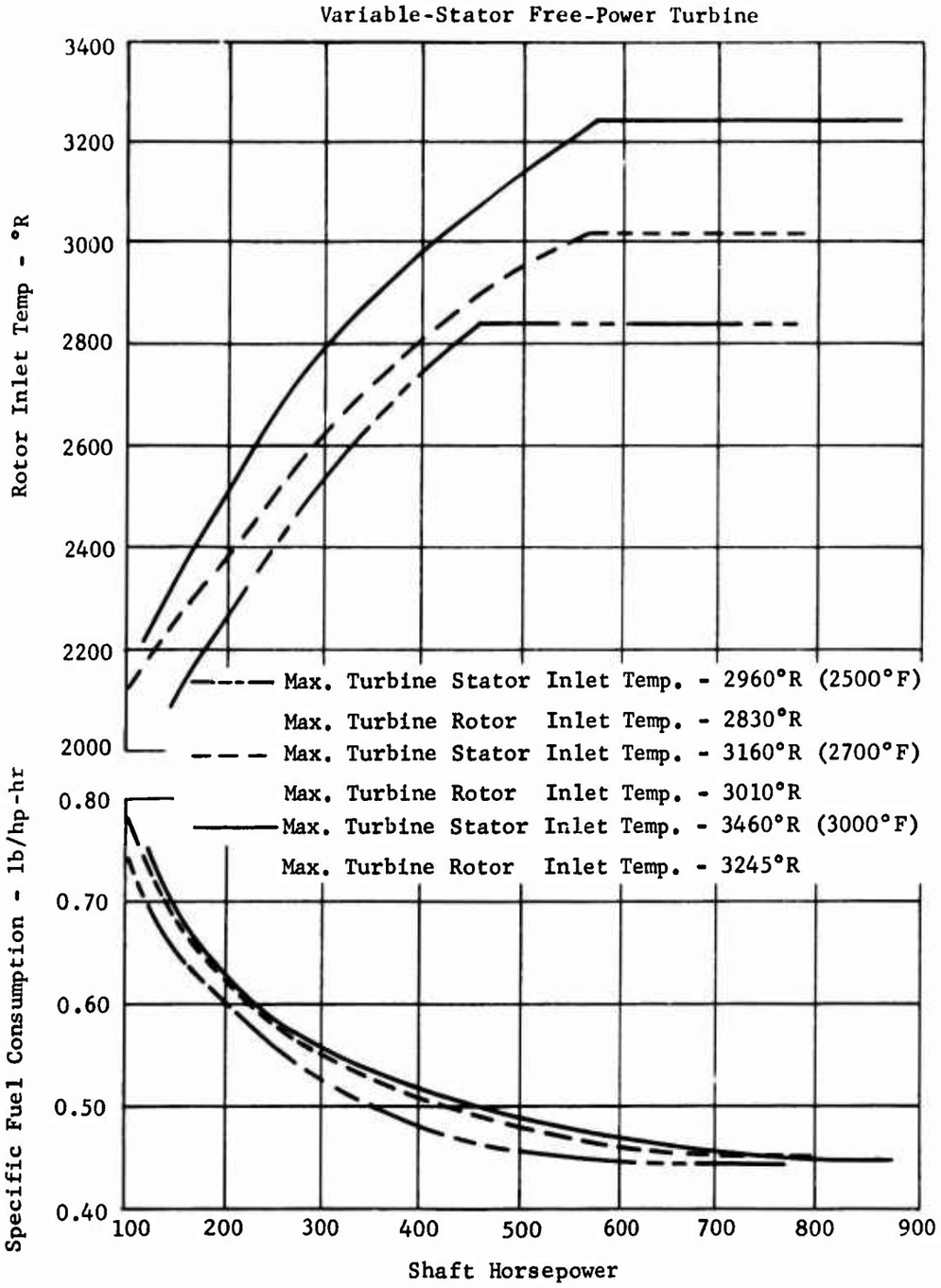


Figure 8. (U) Estimated Engine Performance - Compressor Configuration 1 (USAAVLABS).

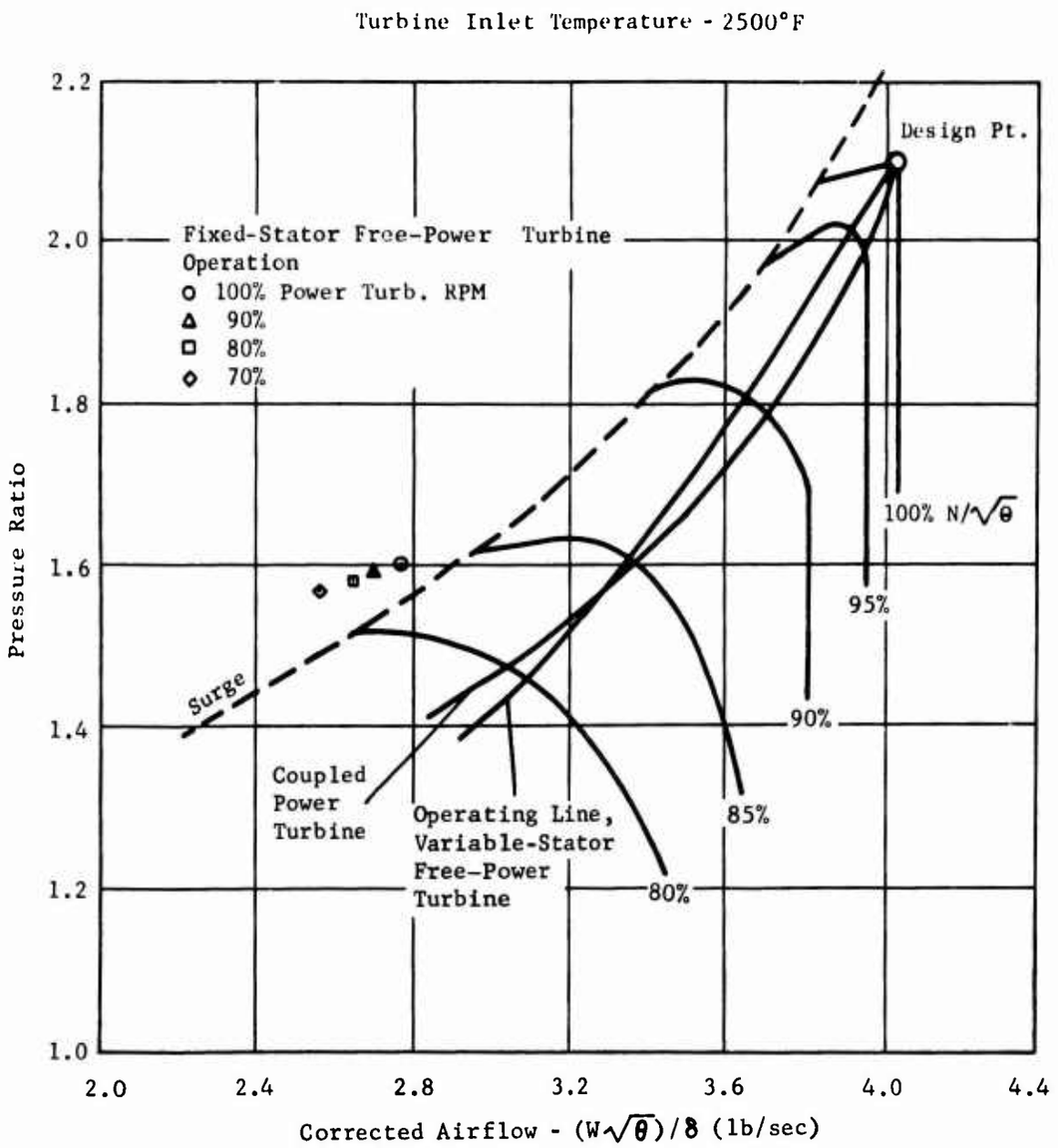


Figure 9. (U) LP Operating Line SSC (2.0) - Compressor Configuration 1.

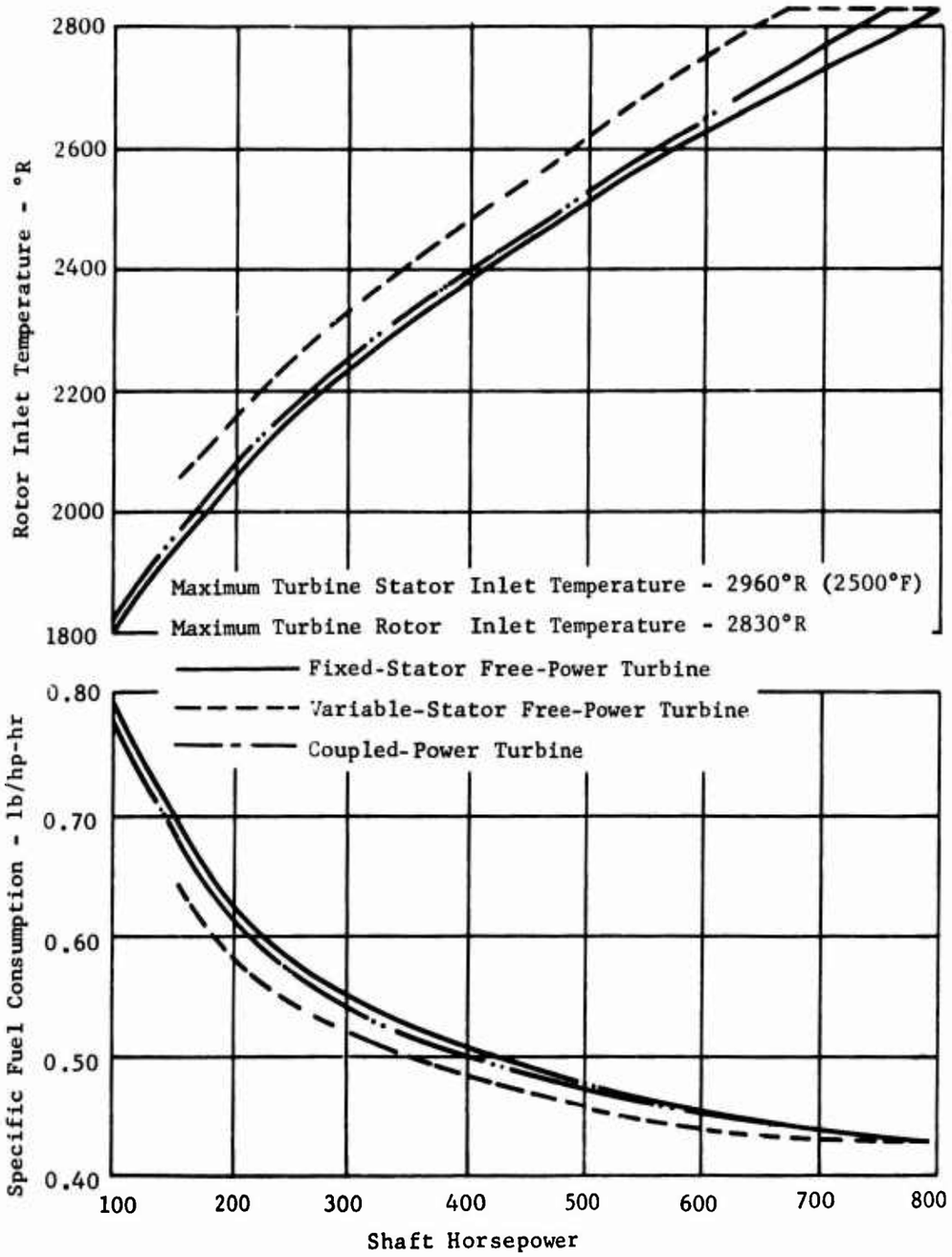


Figure 10. (U) Estimated Engine Performance - Compressor Configuration 2 (USAAVLABS).

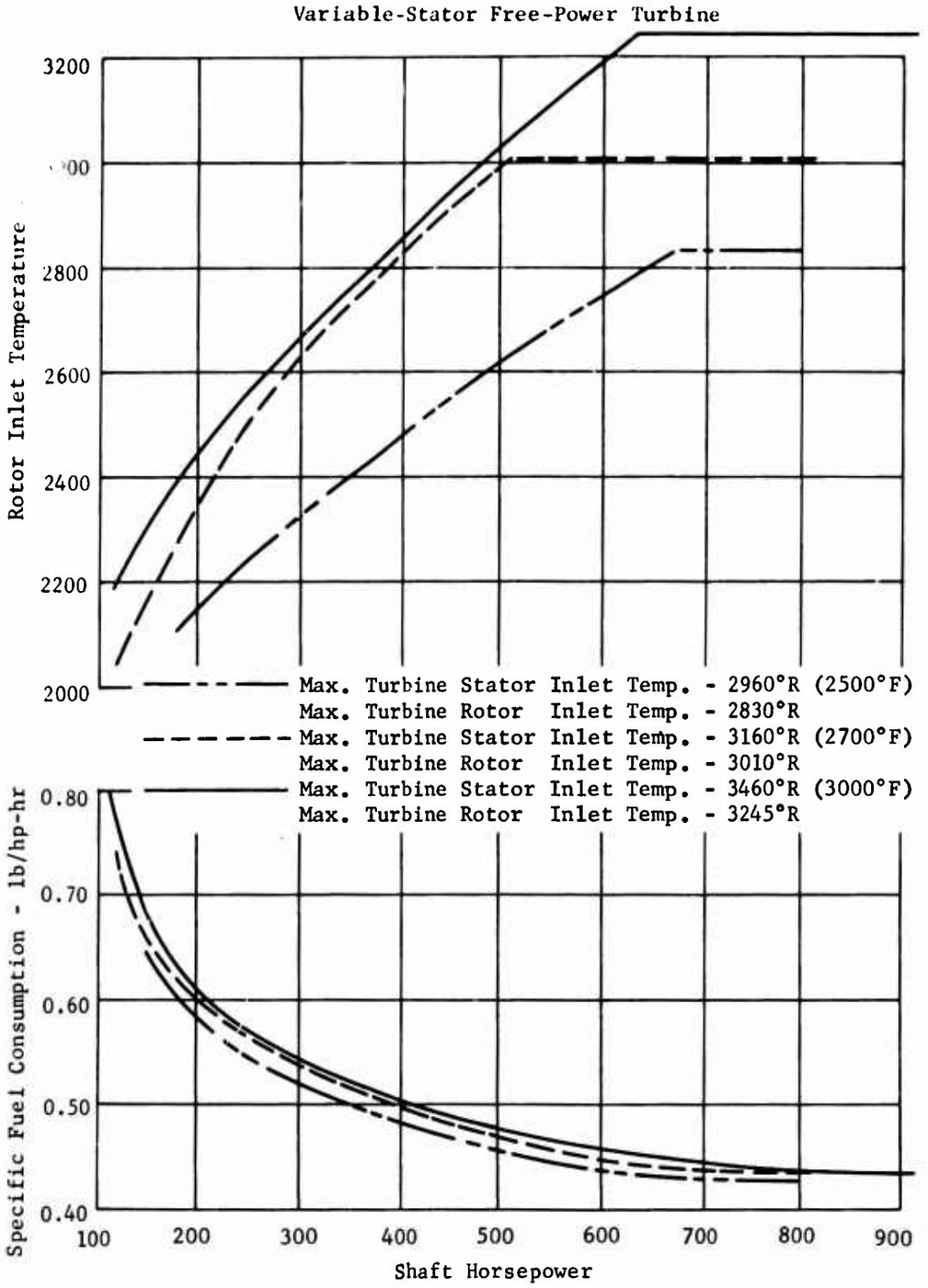


Figure 11. (U) Estimated Engine Performance - Compressor Configuration 2 (USAAVLABS).

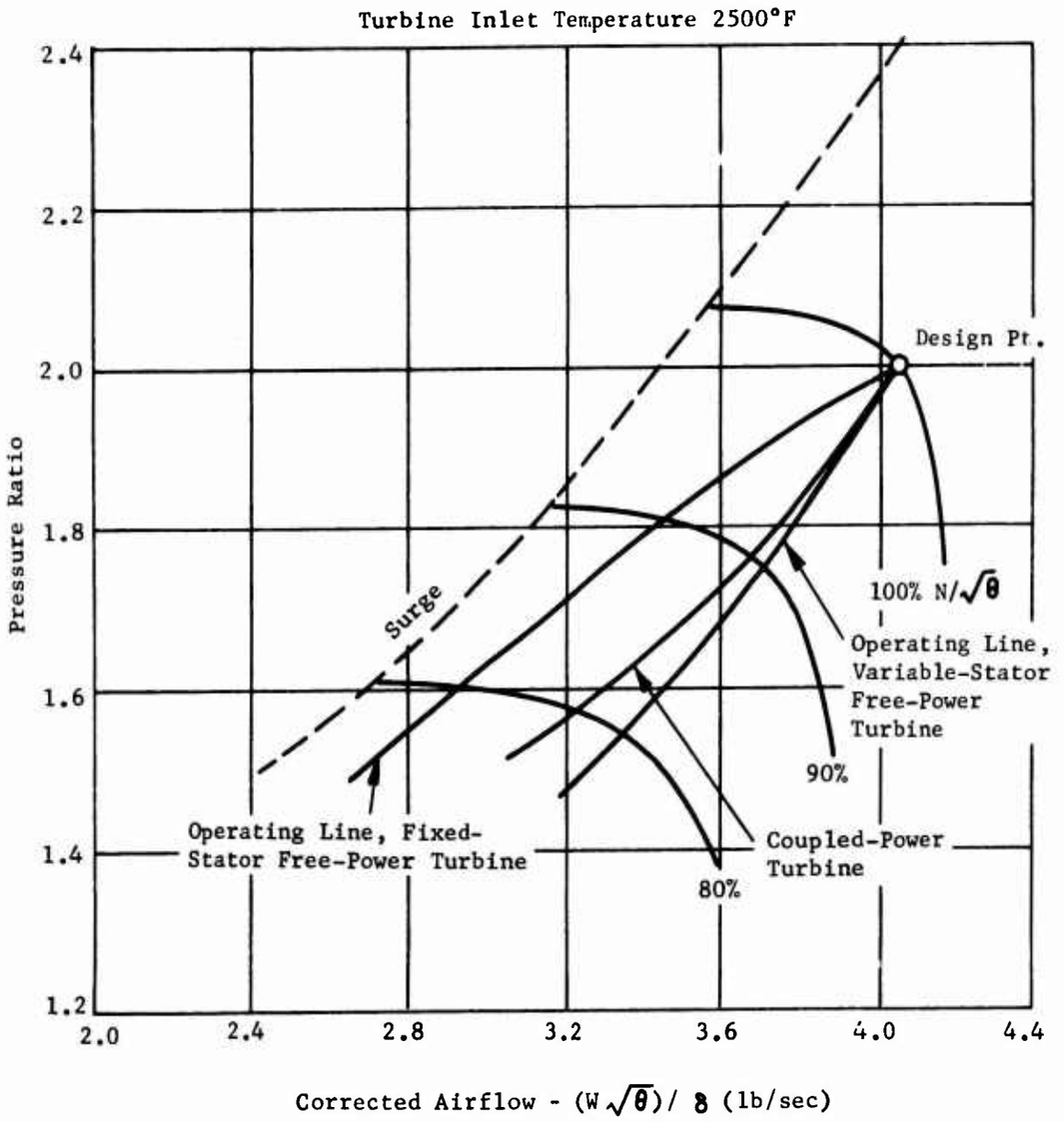


Figure 12. (U) LP Operating Line (TST) - Compressor Configuration 2.

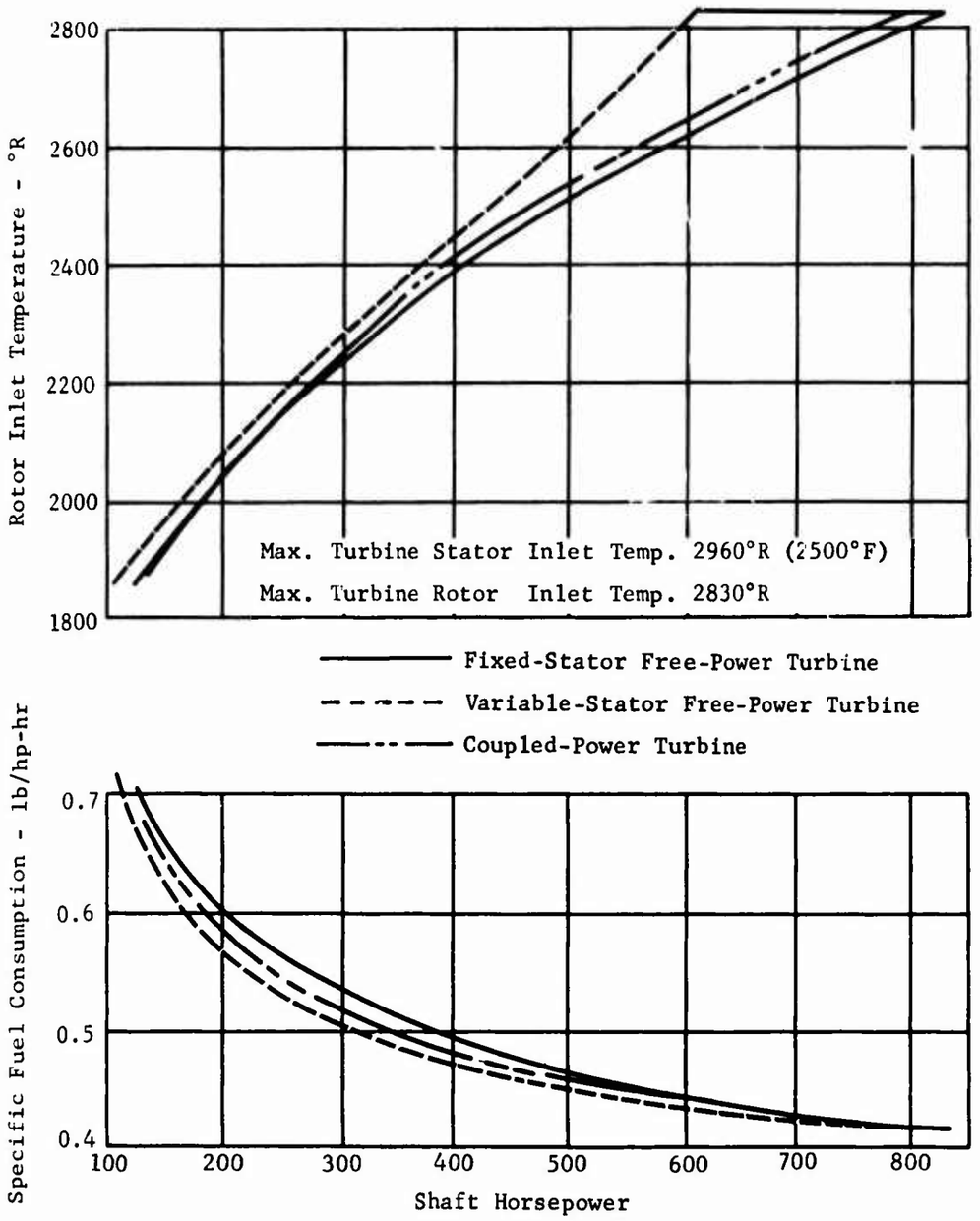


Figure 13. (U) Estimated Engine Performance - Compressor Configuration 3 (USAAVLABS).

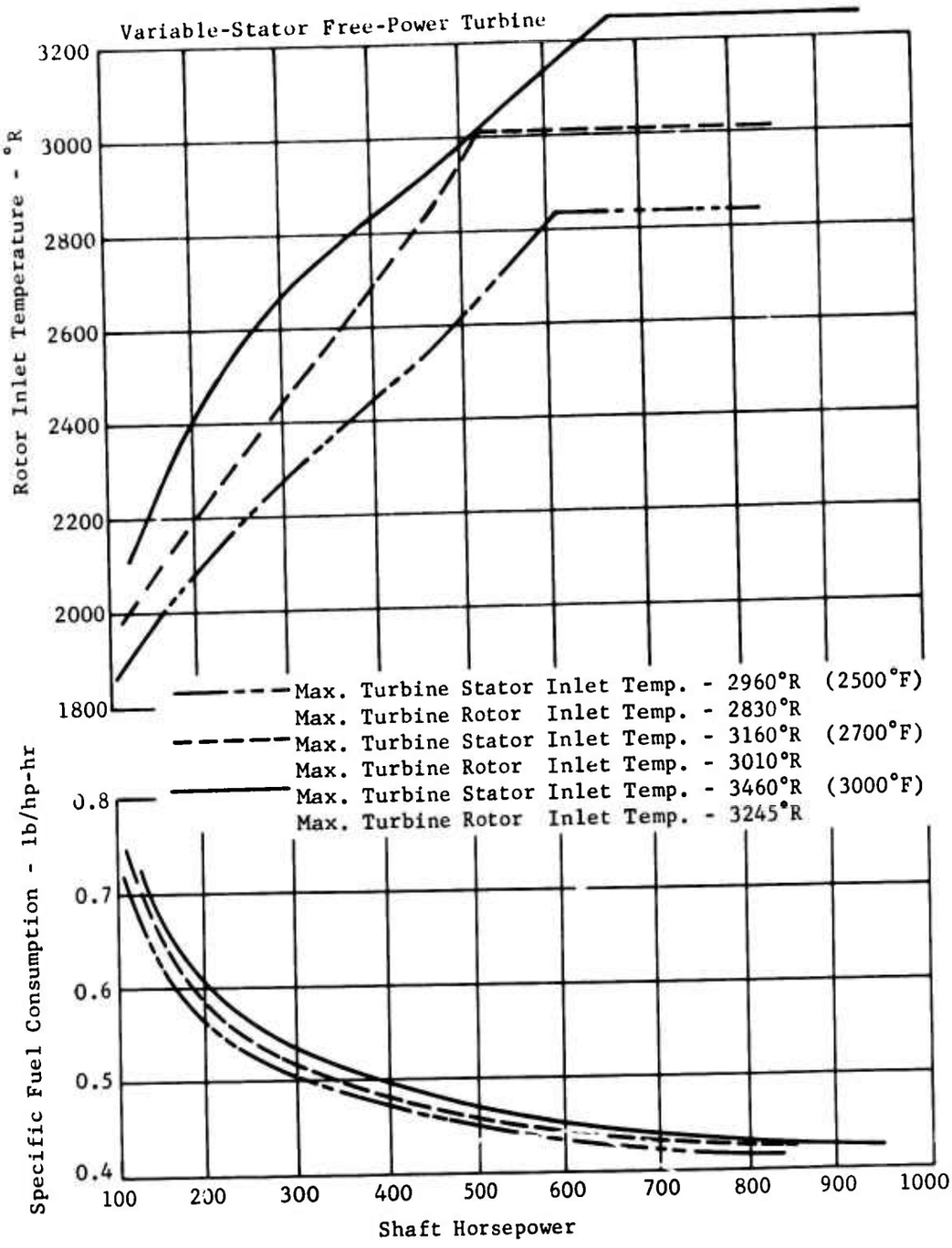


Figure 14. (U) Estimated Engine Performance - Compressor Configuration 3 (USAAVLABS).

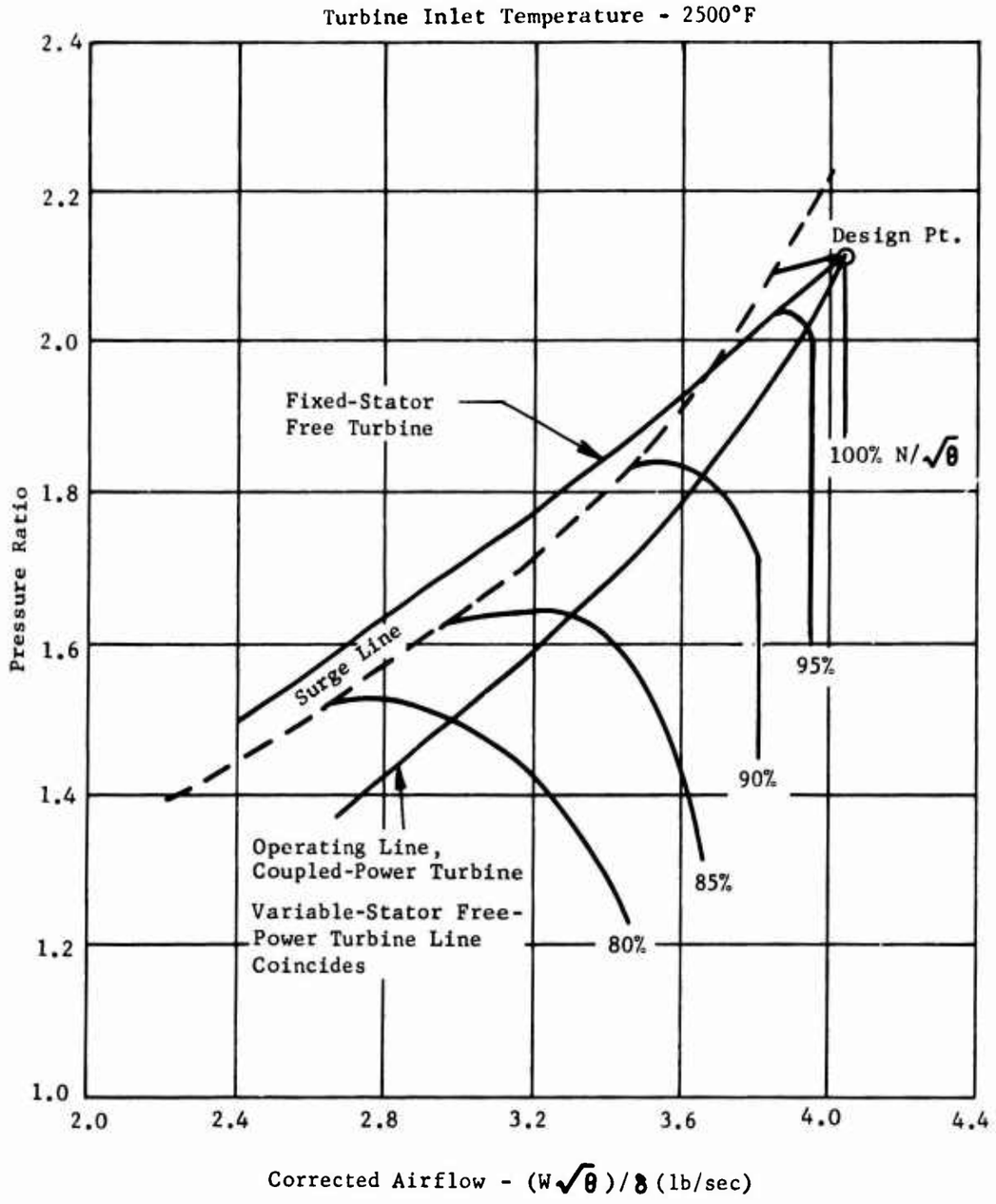


Figure 15. (U) LP Operating Line SSC (2.0) - Compressor Configuration 3.

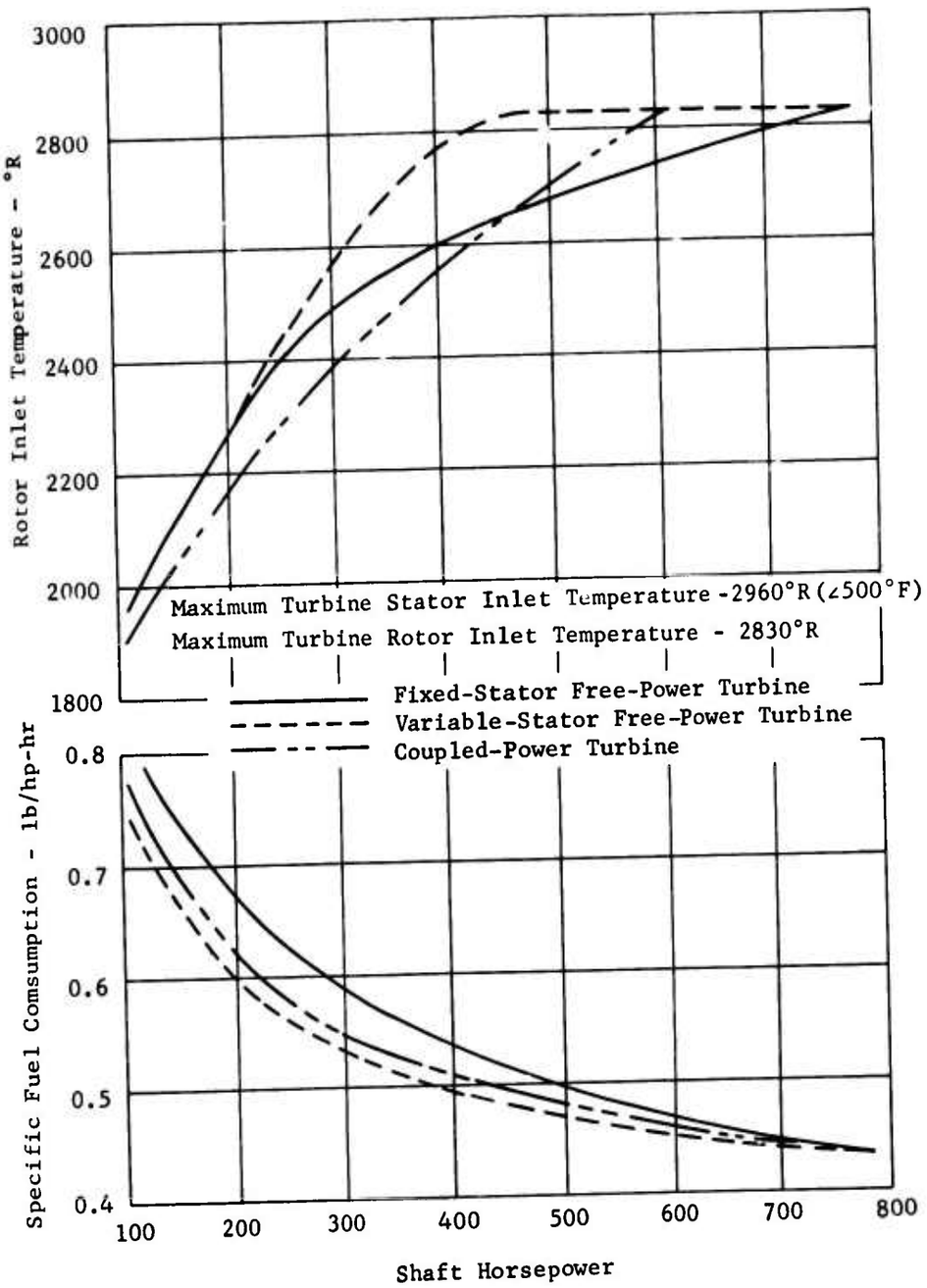


Figure 16. (U) Estimated Engine Performance - Compressor Configuration 4 (USAAVLABS).

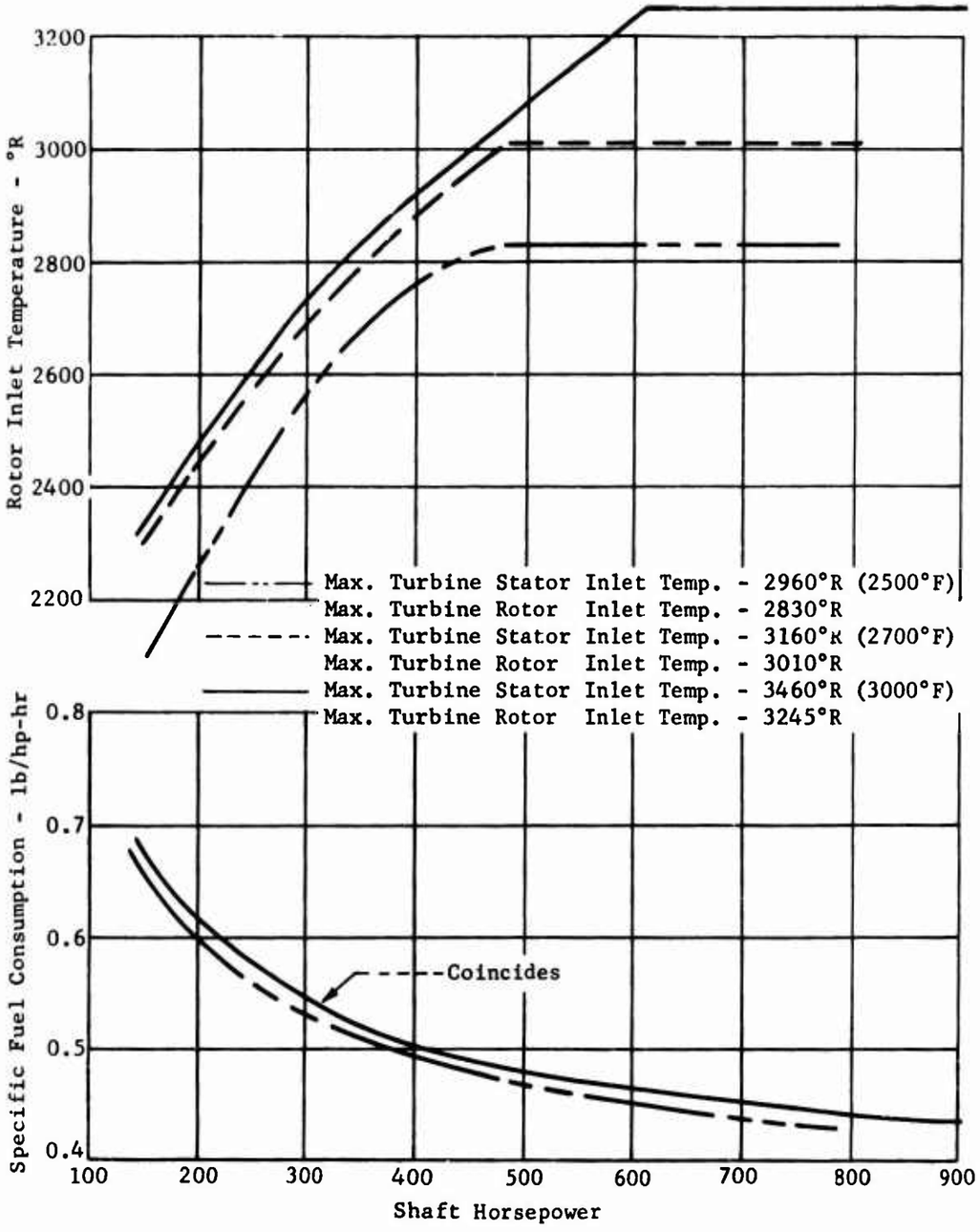


Figure 17. (U) Estimated Engine Performance - Compressor Configuration 4 (USAAVLABS).

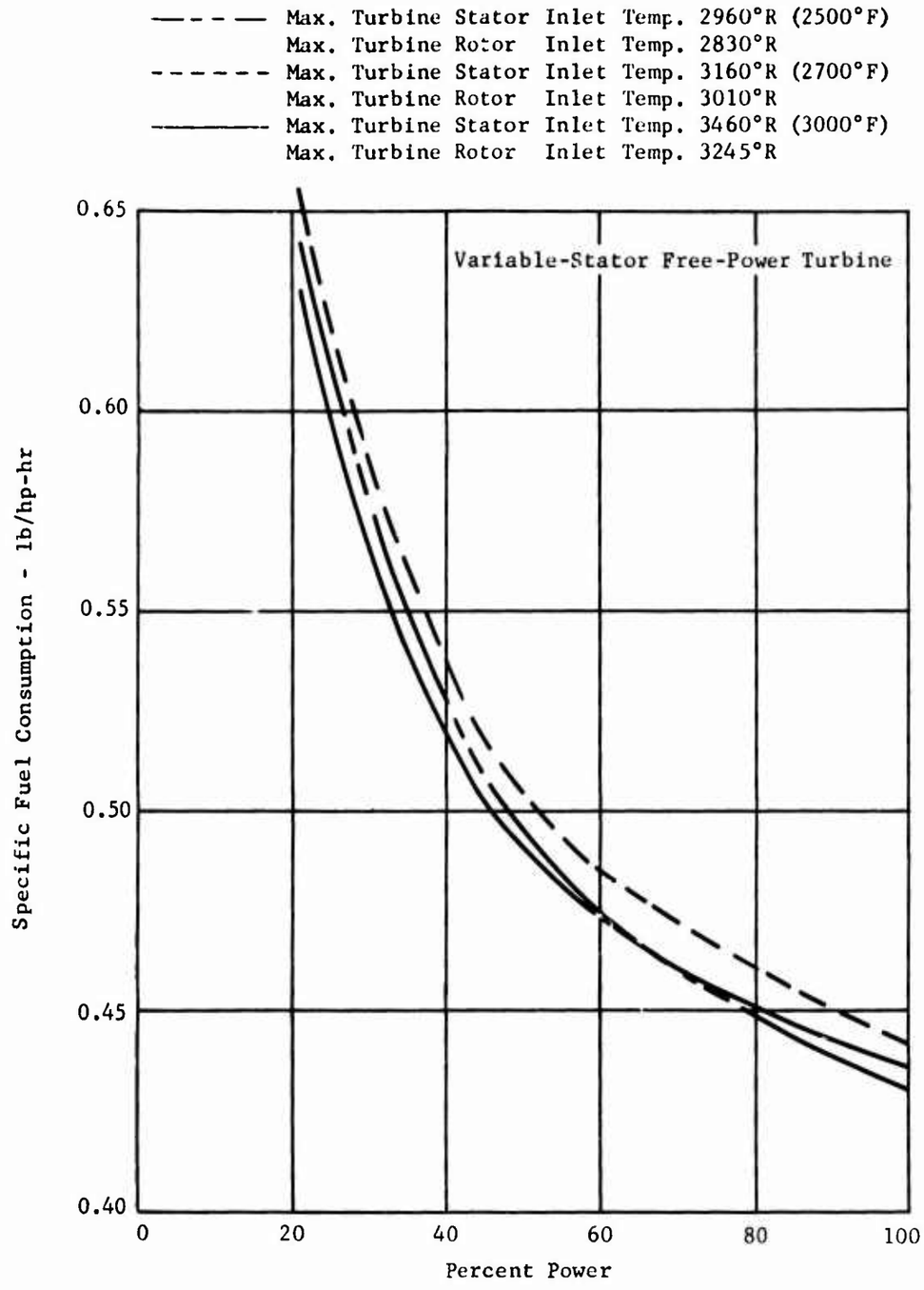


Figure 18. (U) Estimated Engine Performance - Compressor Configuration 4 (USAAVLABS).

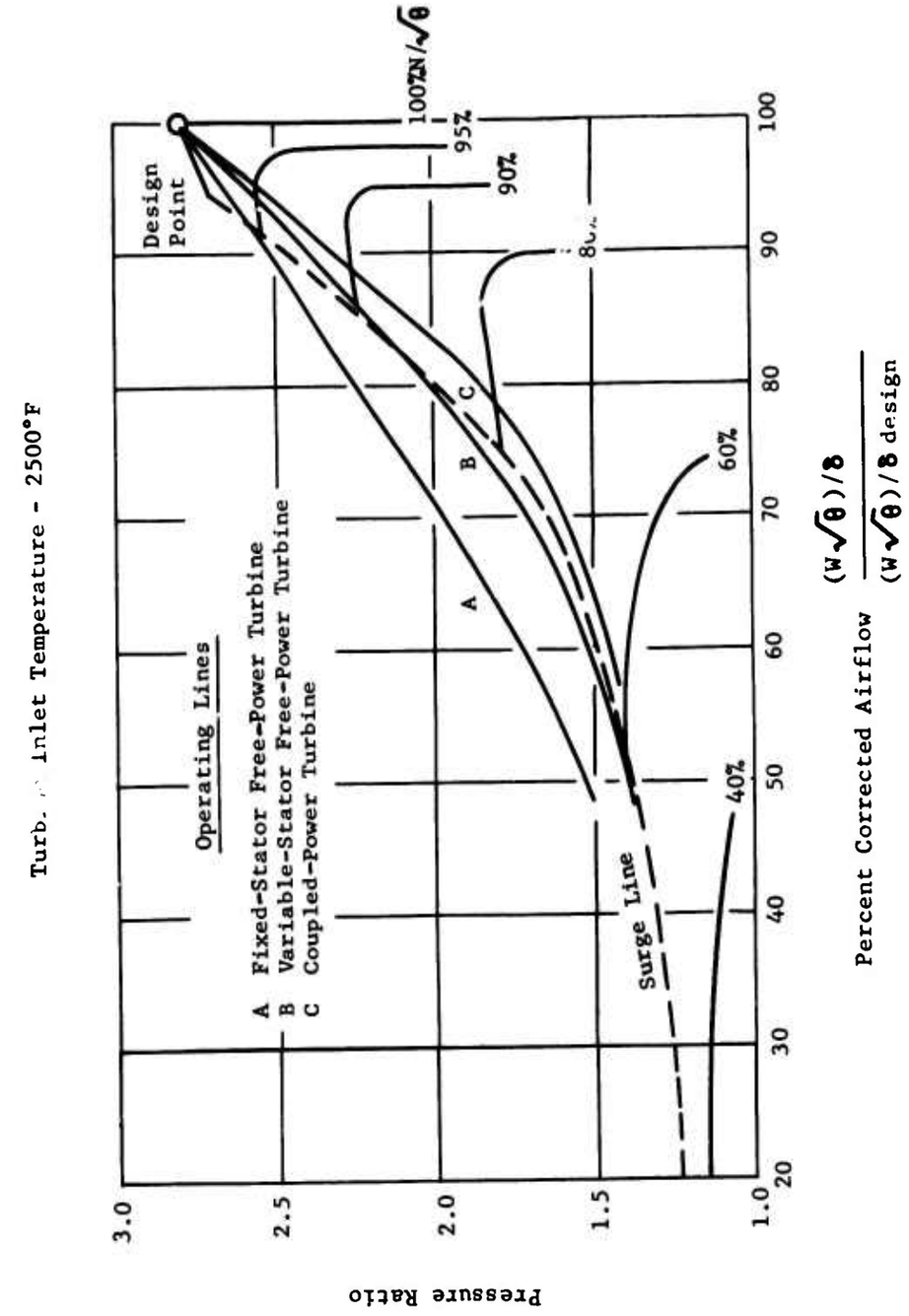


Figure 19. (U) LP Operating Line SSC (2.8) - Compressor Configuration 4.

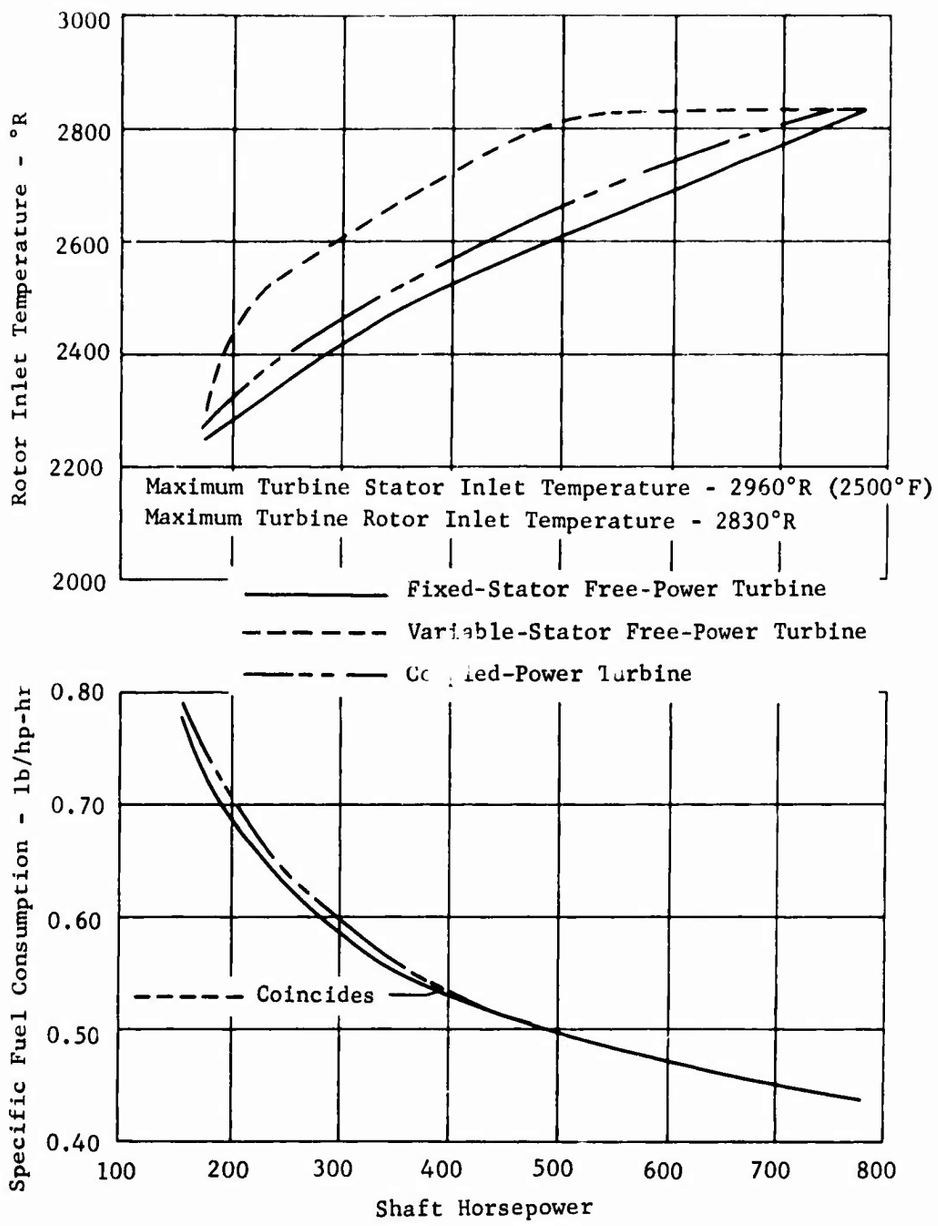


Figure 20. (U) Estimated Engine Performance - Compressor Configuration 5 (USAAVLABS).

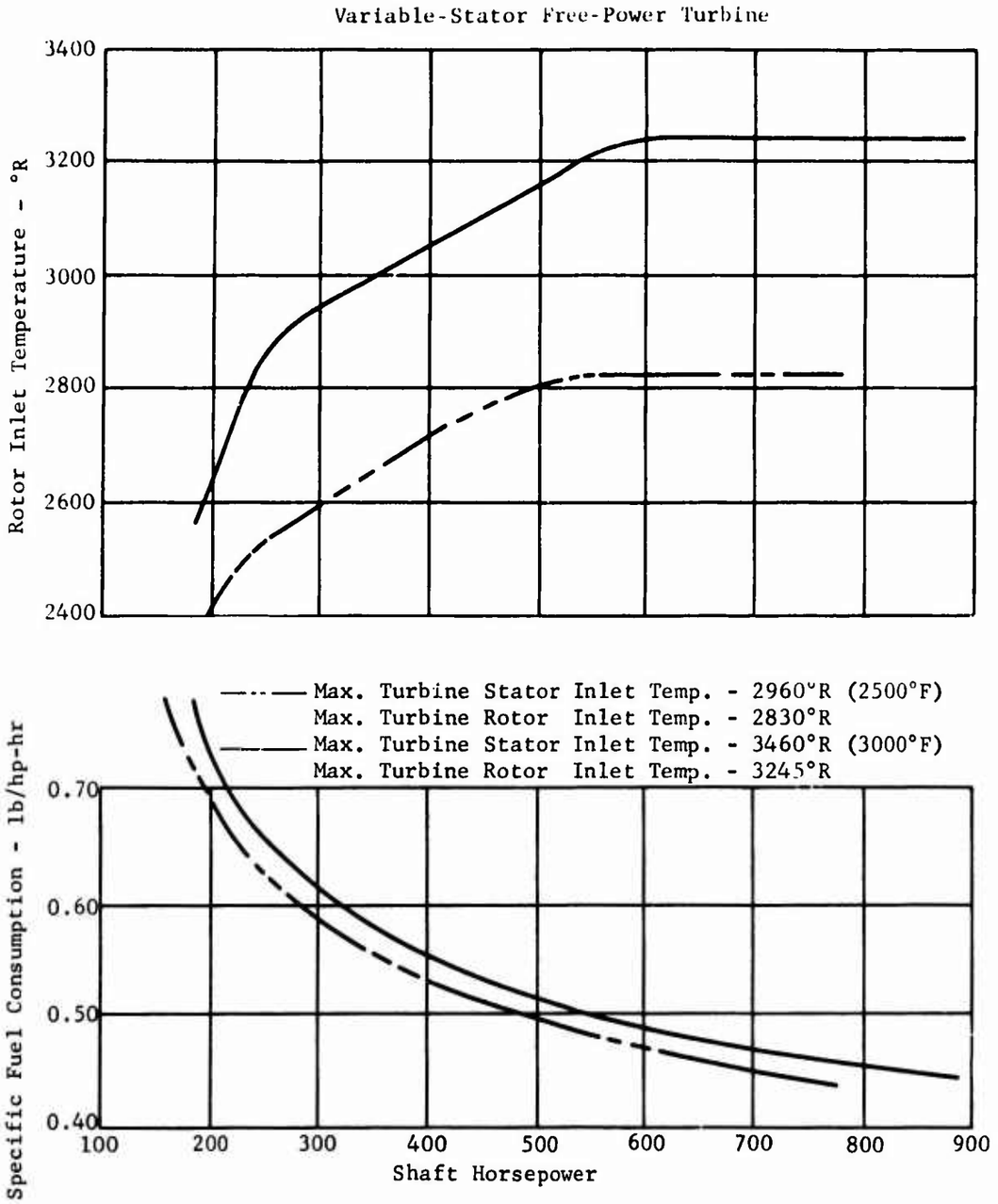


Figure 21. (U) Estimated Engine Performance - Compressor Configuration 5 (USAAVLABS).

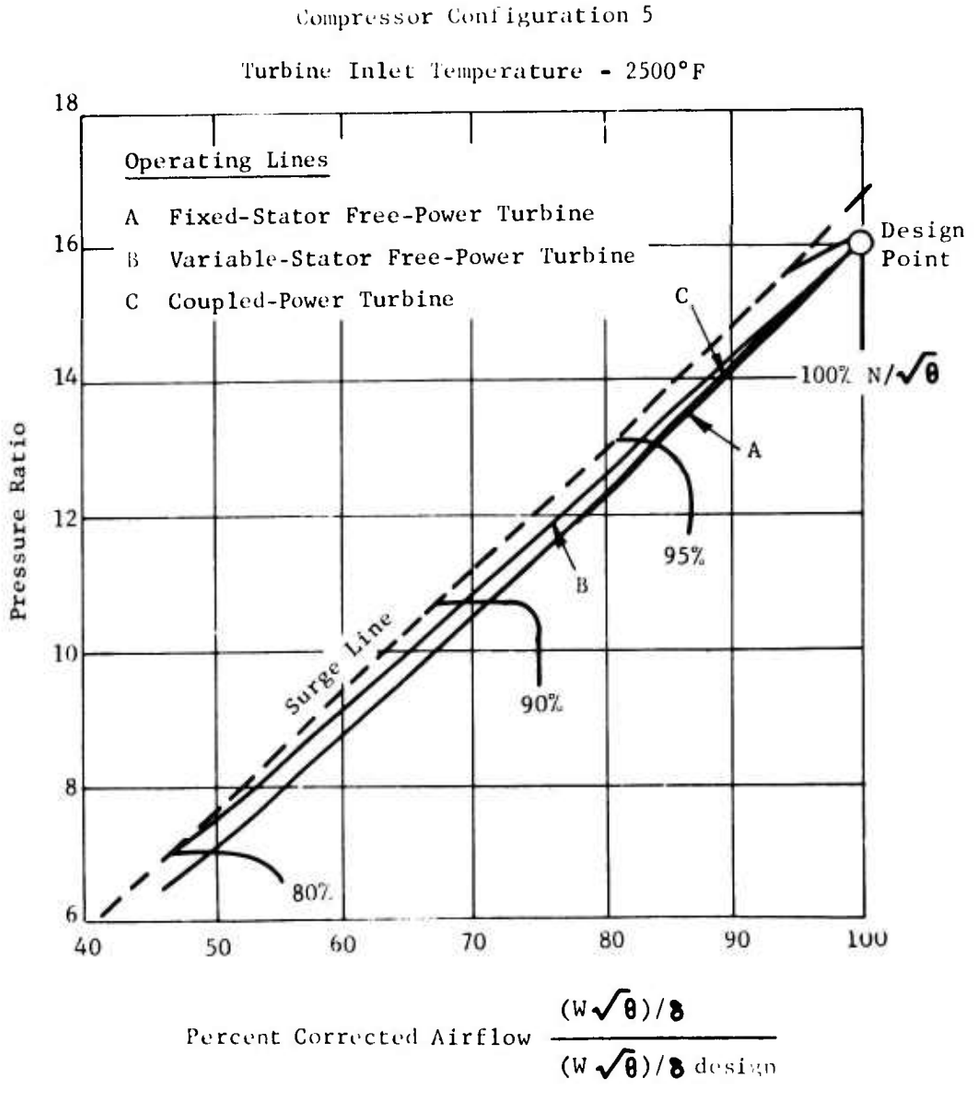


Figure 22. (U) Axial Stage Operating Line SSC (2.8) - Single-Spool Axial/ Centrifugal Compressor.

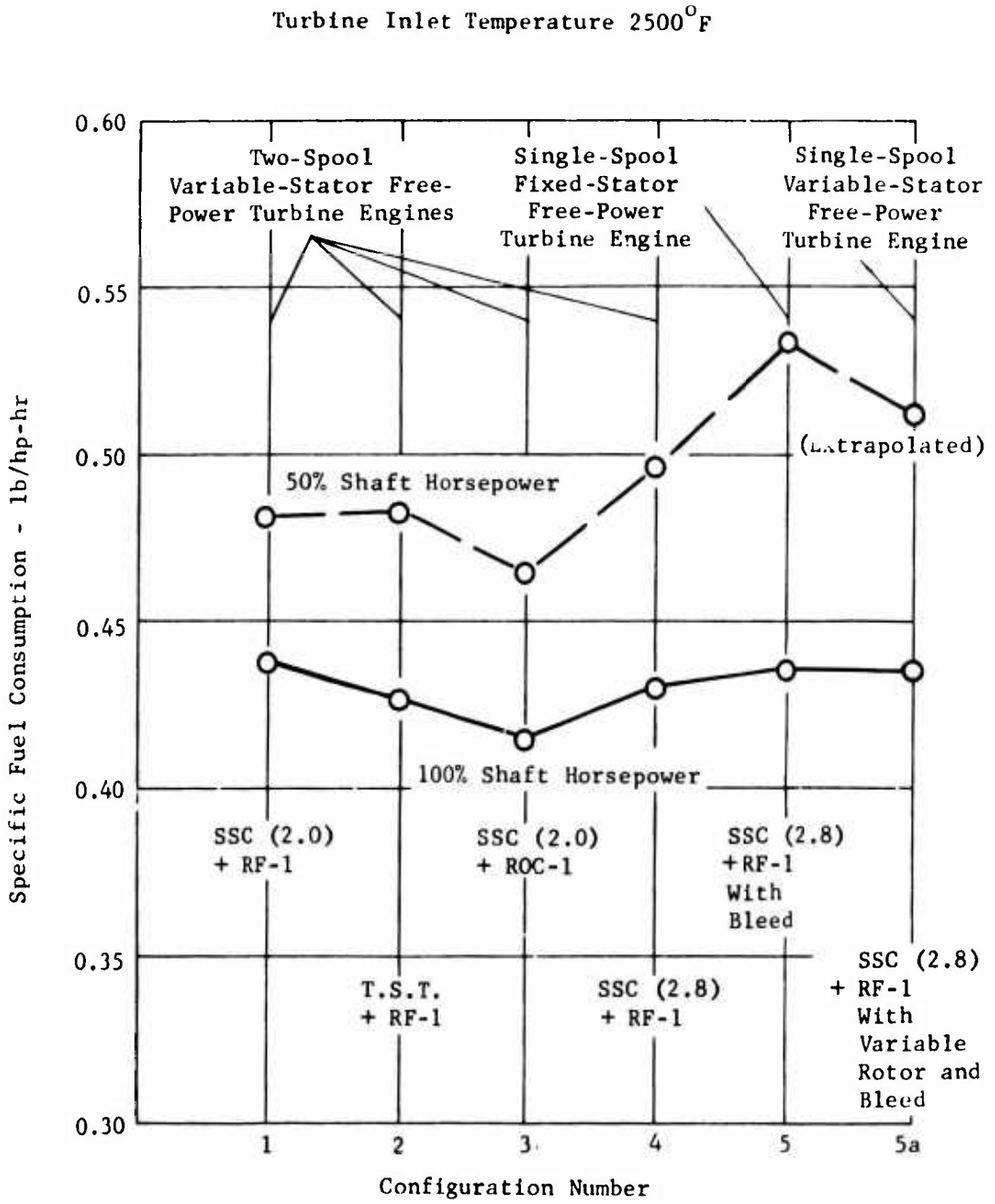


Figure 23. (U) Engine Study Performance Summary, Comparison of the Minimum Engine SFC for Each of the Five Compressor Configurations.

## (U) PRELIMINARY DESIGNS

The axial compressor stage being developed under this contract is intended to serve as a boost stage for advanced centrifugal compressors. The combination of the axial boost stage and the advanced centrifugal stage will provide a 16:1 pressure ratio capability for future small gas turbine engines. The advanced centrifugal compressor technology is currently being developed under other Army contracts. The preliminary design study of both an advanced 16:1 compressor and an engine incorporating such a compressor has been conducted to establish in some detail their performance, design considerations, and operating characteristics. This information provides the basis for guiding the design and development of the axial stage compressor toward an optimum engine.

The preliminary design study of a variable-geometry rotor for the axial stage compressor has also been conducted. This concept offers the potential of significantly improving the part-power performance of a high-pressure-ratio engine with a single-spool compressor.

These preliminary designs are discussed below.

### ADVANCED 16:1 COMPRESSOR

#### Selection of Components

The advanced 16:1 axial/centrifugal compressor consists of a 2.8:1 pressure ratio single-stage axial supersonic compressor and a single-stage 10:1 centrifugal compressor. The 2.8:1 supersonic axial stage is the compressor to be advanced and demonstrated under this contract. The selection of this component is discussed in the section titled Supersonic Axial Compressor. The predicted performance maps of two compressors were supplied by USAAVLABS for consideration as the second stage of the 16:1 compressor. These were the RF-1 centrifugal and the ROC-1 radial outflow compressors referred to in the section on the gas generator studies. Initial investigations included the matching of the axial stage to each of the two second stages. In neither case did the interstage duct, which joins the flow paths of the two stages, result in a straight-through configuration. The misalignment of the axial/radial outflow (ROC-1) compressor was much more severe than that of the axial/centrifugal (RF-1) compressor. This was the primary criterion by which the centrifugal compressor was chosen as the second stage for the 16:1 compressor preliminary design. A parametric study was conducted to see if the choice of design point conditions affected the misalignment between the annuli of the axial stage exit and the centrifugal stage inlet. The design weight flow, overall pressure ratio, and pressure ratio split between the two stages were varied, and the matched configurations were determined. It was established that within the ranges investigated, the degree of annuli misalignment did not change appreciably, as illustrated in Figure 24. Therefore, the interconnecting duct need not be a significant factor in the choice of the design point conditions. Consequently, a design speed of 50,700 revolutions per minute and an airflow of 4.0 pounds per second were selected so as to be the same as those of the 2:1 supersonic compressor currently being

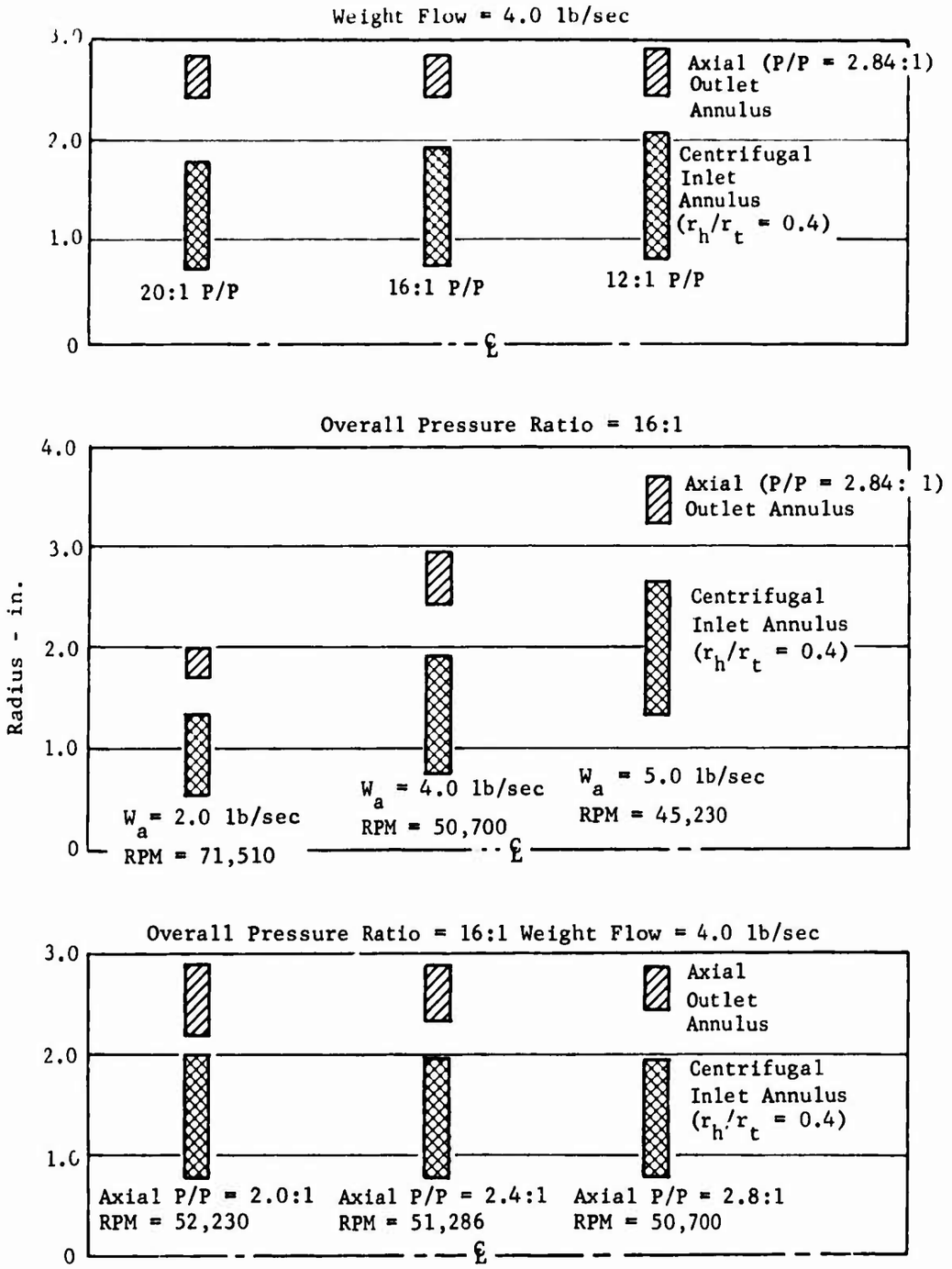


Figure 24. Comparison of Matched Configurations for Axial/Centrifugal Compressor.

veloped. Under these conditions, the 2.8:1 supersonic compressor is identical to the 2:1 compressor in size and configuration from the inlet to the rotor leading edge. This approach permits a direct comparison of 2.8:1 compressor test results with those of the 2:1 compressor, which will be of considerable advantage to the development of the 2.8:1 compressor.

Figures 47 through 50 present the vector diagrams and aerodynamic design data for the axial compressor stage. This design is discussed in detail in the section on Supersonic Axial Compressors. The predicted design point performance of the finalized axial stage design is:

| | |
|---|---|
| pressure ratio | 2.8:1 |
| adiabatic efficiency | 82.2 percent |
| inlet correct airflow | 4.0 pounds per second |
| inlet corrected speed | 50,700 RPM |

The centrifugal compressor (RF-1) had two alternate impeller configurations with hub/tip ratios of 0.6 and 0.4 respectively. The hub/tip ratio of 0.6 was chosen because this configuration results in a more favorable interconnecting duct. The centrifugal stage was sized as follows:

1. The initial one-dimensional aerodynamic design for the axial stage indicated a design point performance of 2.84 pressure ratio, 84 percent efficiency, and 4.0 pounds per second airflow. These values were used to scale the centrifugal (RF-1) compressor so as to match the axial stage.

2. On this basis, a centrifugal stage pressure ratio of 5.634 is required to achieve a 16:1 overall pressure ratio. The corrected airflow $(W\sqrt{\theta})/\delta$ at the second-stage inlet is 1.681 based on 4.0 pounds per second, a total temperature of 741°R, and a total pressure of 85 inches of mercury.

3. Choosing an operating point on the centrifugal compressor map at a corrected airflow of 1.360 and a pressure ratio of 5.634, the respective rotational speed and blade section speeds are established.

4. The geometric scale factor which will achieve the required corrected flow is calculated as the square root of the desired to original corrected airflow $\sqrt{\frac{1.681}{1.360}}$. The factor is 1.237.

5. The rotational speed is computed for the new scaled diameter by maintaining the blade section speeds at the same values computed in step 3. A speed of 50,570 revolutions per minute was calculated on this basis, and this was considered to be within

sufficient accuracy of the 50,700 axial design speed for a valid match point.

6. The minor variation in predicted performance from the one-dimensional design to the final design of the axial stage does not affect this match point significantly.

7. The geometry of the Boeing diffuser vane, designated DI-1, was the only one available, and the radius ratios of the vaneless space and vane were used as 1.06 and 1.8 respectively.

The compressor preliminary design is of a single-spool configuration (Figure 25). The basic flow path is essentially independent of the spooling arrangement, and the same compressor is shown as a two-spool arrangement in the engine preliminary design (Figure 27). The part-speed operation of the single-spool compressor was investigated by referencing the corrected airflows and speeds from the axial stage map to the conditions at the axial stage exit (centrifugal stage inlet). In this manner the two compressor maps can be compared on a common basis. It can be seen in Figure 26 that at part-speed, the axial stage surge line is at a much higher weight than the centrifugal stage can pass at wide-open throttle. Interstage bleed is therefore required so that axial stage will not be forced to operate in surge when the two stages operate at the same part speed as that imposed by a single-spool arrangement. Figure 6 presents the compressor map for the single-spool compressor with sufficient interstage bleed to effectively have the surge lines of both stages coincide. The percentage of bleed is 40 percent at 80 percent speed. The exit area required to pass the bleed is computed to be 7.86 square inches. The area was computed assuming that the bleed total pressure is the static pressure at the axial rotor exit at 80 percent speed and that the bleed vents to ambient. The exit stator blades are planned with a porous metal skin to serve as the bleed surface. The percentage of open area of the metal would be selected so as to satisfy the bleed area.

## DESCRIPTION OF COMPRESSOR AND MECHANICAL CONSIDERATIONS

The compressor shown in Figure 25 consists of a single-axial stage followed by a single-stage centrifugal wheel. The centrifugal wheel is splined to the integral shaft of the axial rotor, and the complete rotor assembly is straddle mounted on rolling element bearings.

The six-spoke inlet housing serves as the front main bearing support and also contains the inlet guide vanes of the axial rotor and the inlet bullet. The struts are hollowed to provide passages for the bearing oil, the thrust balance, and the seal pressurizing air.

The inlet guide vanes are trapped between the compressor housing and the inner ring of the front bearing support housing. The vanes are cast integral with an inner and outer shroud ring; the unit is precision cast in 17-4PH steel (AMS 5643). The inner shroud ring doubles as the seal

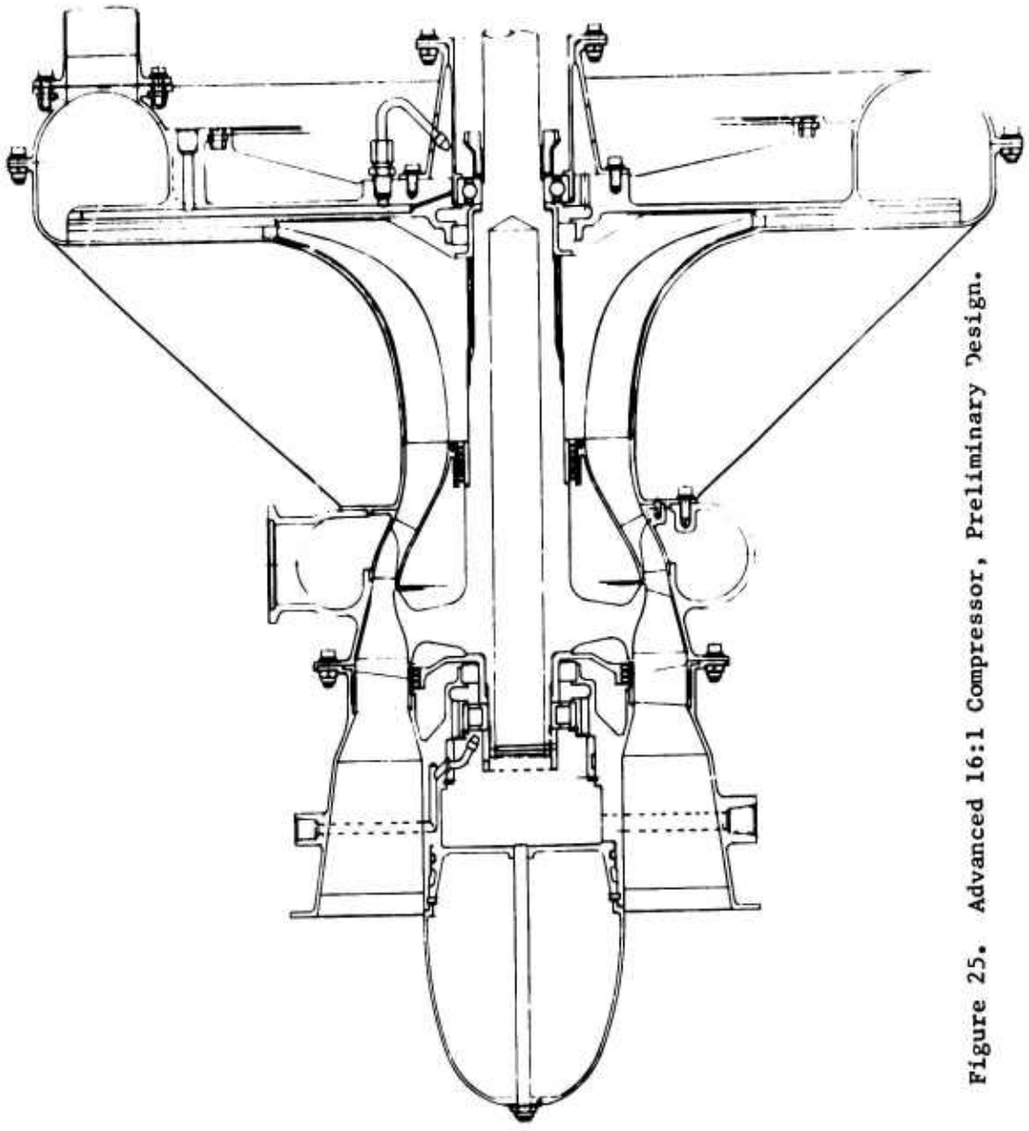

Figure 25. Advanced 16:1 Compressor, Preliminary Design.

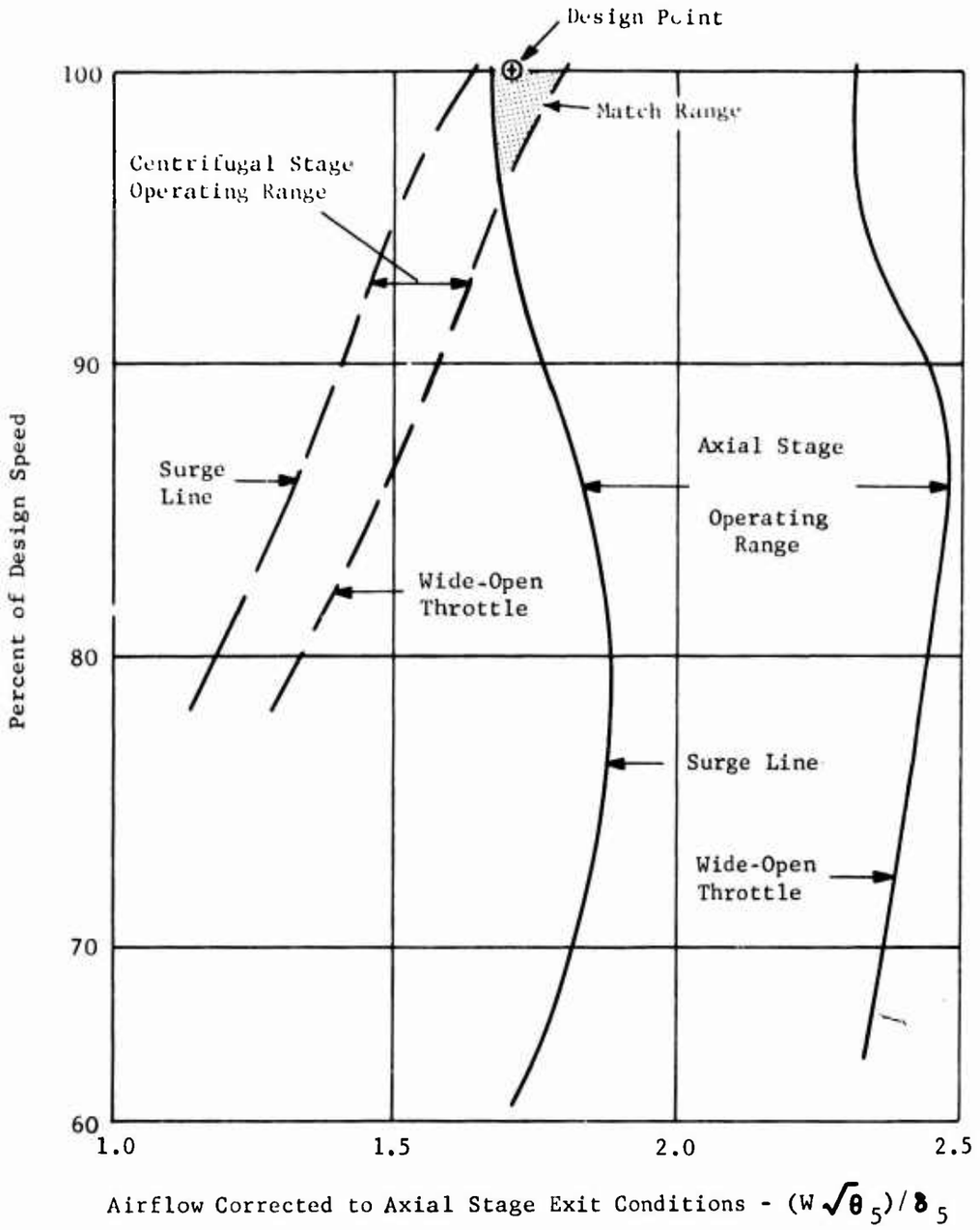


Figure 26. Airflow Range Characteristics - Axial Stage SSC (2.8) Compared to Centrifugal Stage (RF-1).

runner for the front thrust balance labyrinth seal. An aluminum-graphite type rub-tolerant material is deposited on the inner diameter (I.D.) of this ring to permit small seal clearances without risk of seal damage.

The axial stage rotor housing is a 360 degree precision casting in 17-4PH. It incorporates a bleed manifold to accommodate interstage air bleed. The area of the housing immediately over the rotor is coated with an aluminum-graphite material which is readily abradable. This will permit operation with the small clearances so necessary in this size compressor.

The exit stator is precision cast in a full 360-degree arc with shroud rings at the root and tip of the blades. The stator assembly is axially contained between the rotor housing and the compressor delivery housing. The stator vanes themselves are partially hollow in order to direct the interstage bleed air into the manifold. The inner shroud ring of the stator doubles as the seal runner for the interstage labyrinth seal. Again, an aluminum-graphite type rub-tolerant material is deposited on the I.D. of this ring to allow very small seal clearances without risk of seal damage.

The compressor delivery housing is composed of two full 360-degree arc sections. The housing as shown is intended for a rear-end-mounted combustor and is the reason for the individual air outlets from the collector. The vanes of the diffuser are intended to be integral with the rear section of the delivery housing, with the two housing sections being bolted together. One of the bolt circles would pass through a thick section of the diffuser vanes, while the other is at the outer diameter (O.D.) of the manifold collector as shown. The compressor delivery housing also serves as the thrust bearing support structure.

A critical speed analysis indicated that the first shaft critical speed is 71,700 RPM for a rigid bearing support system; however, it is considered impractical to achieve a sufficiently rigid system to insure a first critical above design speed (50,700 RPM). Consequently, the thrust bearing is shown flexibly mounted and dampened by an oil film. Both a three-bearing arrangement and a two-bearing arrangement, which operate between first and second critical, were considered in the study. The latter alternative was selected as the most desirable solution to the critical speed problem. The spring rate of the bearing mount structure can be so selected that the first critical occurs below idle speed ( $<$ 40 percent), while the second critical is above the maximum operating speed of the shaft system.

The axial stage rotor wheel is a precision casting in 17-4PH in which the supersonic blading is integral with the disc. Integral blading results in low cost and simplicity, factors so vital in this size machine.

The centrifugal wheel is a scaled version of the RF-1 design. The wheel tip speed of the scaled version is lower than that of the existing design because of the lower pressure ratio requirement. On the other hand, the higher pressure level demanded will require close control of the axial clearance of the impeller. The thrust bearing has been located at the centrifugal wheel to minimize the potential axial movement, therefore minimizing the permissible clearance.

## ADVANCED GAS GENERATOR

The preliminary design study of the gas generator of an advanced small gas turbine engine has been conducted. The engine includes the two-spool version of the 16:1 compressor discussed in the previous section. A two-spool gas generator with a 2500°F turbine inlet temperature, a free-power turbine, and variable-power turbine stators was selected for this design. This engine configuration provides the lowest specific fuel consumption of compressor configurations 4, 5, and 5a, as indicated in the results of the gas generator performance studies.

### Engine and Component Performance

The design point component performance data for the engine is given in Table V; Figures 17, 18, and 19 present the overall performance.

TABLE V. ENGINE CONFIGURATION AND COMPONENT PERFORMANCE DATA

| | LP Compressor | HP Compressor | Overall Compressor | Burner | HP Turbine | LP Turbine | Power Turbine |
|---|---|---|---|---|---|---|---|
| Designation | SSC (2.8) | RF-1 | 4 | | | | |
| No. of stages | 1 | 1 | 2 | | 1 | 1 | 2 |
| Type | axial | centrifugal | | | axial | axial | axial |
| Pressure ratio | 2.8 | 5.71 | 16 | 0.97 | 2.7 | 1.485 | 3.78 |
| Flow rate (lb/sec) | 4.0 | 4.0 | 4.0 | 3.37 | 3.73 | 4.00 | 4.06 |
| Inlet stators | fixed | none | | | fixed | fixed | variable |
| Adiabatic Eff. (%) | 79 | - | 77.5 | | 90 | 89 | 87 |
| Exit stators | fixed | fixed | | | - | - | - |
| Inlet O.D. (in.) | 6.29 | 4.35 | | | 6.47 | 6.62 | 7.6 |
| Inlet I.D. (in.) | 4.33 | 2.62 | | | 5.79 | 5.79 | 5.79 |
| Exit O.D. (in.) | 4.35 | 18.0 | | | 6.62 | 7.0 | 8.38 |
| Exit I.D. (in.) | 2.62 | - | | | 5.79 | 5.79 | 5.79 |
| Axial length (in.) | 8.2 | 4.4 | 12.6 | 9.0 | 2.5 | 2.8 | 5.5 |
| Design speed (RPM) | 50,700 | 50,700 | | | 50,700 (Rotor) | 50,700 (Rotor) | 36,000 (Rotor) |
| Inlet total temp (°R) | 519 | 735 | | 1329 | 2830 | 2251 | 2063 |
| Exit total temp (°R) | 735 | 1329 | | 2960 | 2314 | 2073 | 2063 |
| Stator cooling air (lb/sec) | | | | | 0.25 | | |
| Rotor cooling air (lb/sec) | | | | | 0.27 | 0.06 | 0.05 |

## Engine Flow Path

A layout of the turboshaft engine arrangement embodying the basic gas generator is shown in Figure 27. A description of the engine flow path will best serve to illustrate the arrangement of components.

The air is taken in axially through the six-spoke inlet housing that serves as the front main bearing support and also contains the inlet guide vanes and the inlet bullet. Energy is added to the air in the rotor of the first-stage axial supersonic compressor((SSC 2.8). An outlet stator and an interconnecting transition duct turn the air to axial, decrease the Mach number, and direct it to the inlet of the single-stage centrifugal impeller (RF-1). A radial, vaned diffuser decreases the Mach number and whirl of the air exiting from the impeller prior to entering the scroll. Final diffusion is accomplished in the scroll prior to combustion. A four-can-annular combustor utilizing a vaporizing fuel system adds fuel to the air, and combustion takes place. A transition from the cans to an annulus occurs within the combustion chamber. From the combustor, the hot gases pass through the axial high-pressure turbine and axial low-pressure turbine. The low-pressure turbine drives the first-stage compressor. The hot gases pass through the two stages of variable-area power turbines before entering the exhaust collector scroll, where they exhaust to the atmosphere.

## Mechanical Design Considerations

The basic gas generator is a two-spool unit. The compressor of this gas generator consists of the supersonic axial (SSC 2.8) first stage and the centrifugal (RF-1) second stage from the advanced 16:1 compressor discussed in the previous section. The centrifugal compressor is driven by a single-stage high-pressure turbine. The supersonic axial stage is driven by a single-stage low-pressure turbine. The two-stage power turbine is a free-spool design driving an end-mounted reduction gearbox. Two versions of the output gearbox are illustrated. One has the output shaft concentric with the engine center line, while the other has a double output shaft offset from the engine center line.

The low-pressure spool of the gas generator is straddle mounted on rolling element bearings with the single row ball thrust bearing at the compressor end. The thrust bearing is flexibly mounted and oil film dampened. Preliminary calculations indicate that it is impractical for a two-bearing arrangement of this spool to have a critical speed above the maximum operating speed. The alternatives are a three-bearing arrangement and a two-bearing arrangement which operate between first and second critical. The latter alternative was selected as the most desirable solution to the critical speed problem. The spring rates of the bearing mount structures are so selected that the first critical occurs below idle speed, while the second critical is above the maximum operating speed of the rotor system.

The supersonic axial compressor rotor is a precision casting in 17-4PH steel. The blades are cast integrally with the disc, resulting

in a durable, low-cost unit with excellent environment resistance. The inlet guide vanes as well as the exit stator assembly are precision cast.

The high-pressure spool of the gas generator is supported by a pair of bearings, with a rotor overhung at both ends. The bearing span of this rotor system is relatively short and consequently has a first critical speed above the maximum operating speed. The high-pressure spool thrust bearing is located at the centrifugal rotor in order to retain close control of the compressor tip clearances. The centrifugal compressor casing is reinforced to take both gas pressure loads and applied loads without adversely affecting the compressor running clearances.

The accessory drive gearbox is driven from the high-pressure spool by a spur gear located just aft of the thrust bearing. A splined quill shaft passing through the thick section of one of the diffuser vanes transfers the drive to the forward side of the vaned diffuser. The accessory gearbox is within the envelope of the vaned diffuser. Spur gearing is used throughout the box, with all shaft gears positioned by their mounting.

The four-can-annular combustor design has a film-cooled liner with a vaporizing fuel injection system. This design concept has the advantage of only four fuel injection points, thereby lessening the possibility of clogging of small metering orifices. One of the factors involved in the selection of a vaporizing fuel injection system was the demonstrated ability of this system to produce a minimum of smoke under all operating conditions, using a variety of fuels.

The turbine section consists of two stages of transpiration cooled gas generator turbines and a two-stage free-power turbine. The gas generator turbine wheels are Inconel 718, with welded blades. The blade airfoil sections are made of porous material that is electron-beam-welded to the blade struts. The high-pressure nozzle vanes are also transpiration cooled and are individual units composed of cast struts with the porous material airfoils electron-beam-welded to the struts. The individual vane assemblies are retained and sealed between supporting rings. The inner rings form a box section which also functions as an air manifold, a seal runner, and a combustor liner support. A boost impeller attached to the front face of the high-pressure turbine raises the cooling air pressure sufficiently to overcome the pressure drop of the porous skin of the stator vanes.

The two-stage power turbine is straddle mounted with the thrust bearing located at the input pinion end. The first critical speed of this rotor system would be well above the operating speed range. The two turbine wheels are coupled together through an intermediate curvic coupling labyrinth seal piece and a single central tie bolt. The variable stators of both power turbine stages are operated through separate unison rings. The variable stator actuation hardware is all external to the engine; therefore, a number of design problems are minimized.

The gearbox is contained within a cast Ni-Resist housing located aft of the power turbine. A two-stage reduction with all spur gearing was selected on the basis of design simplicity and small number of parts. Two

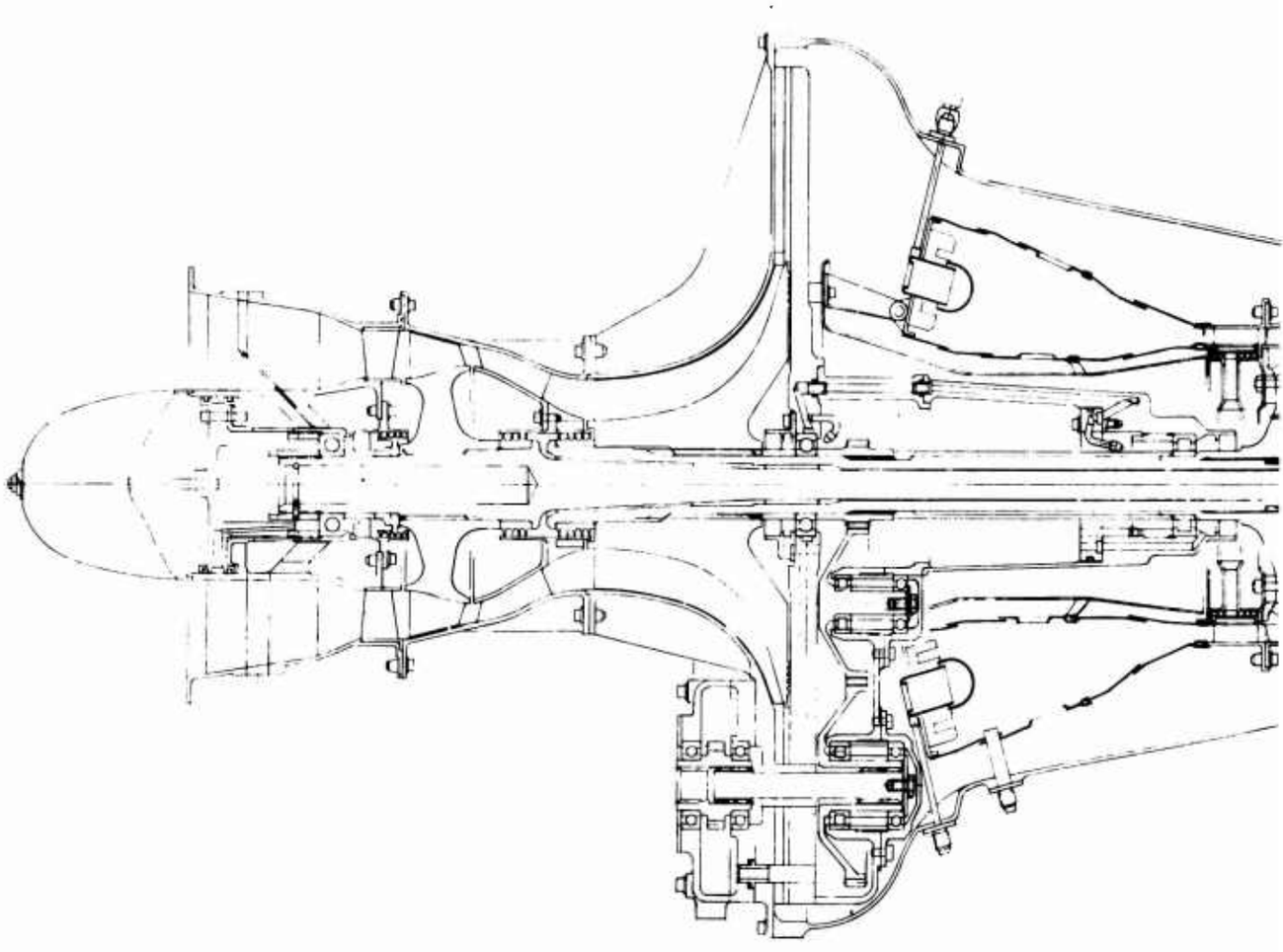

Figure 27. Advanced Gas Generator With Advanced 16:1 Compressor, Preliminary Design.

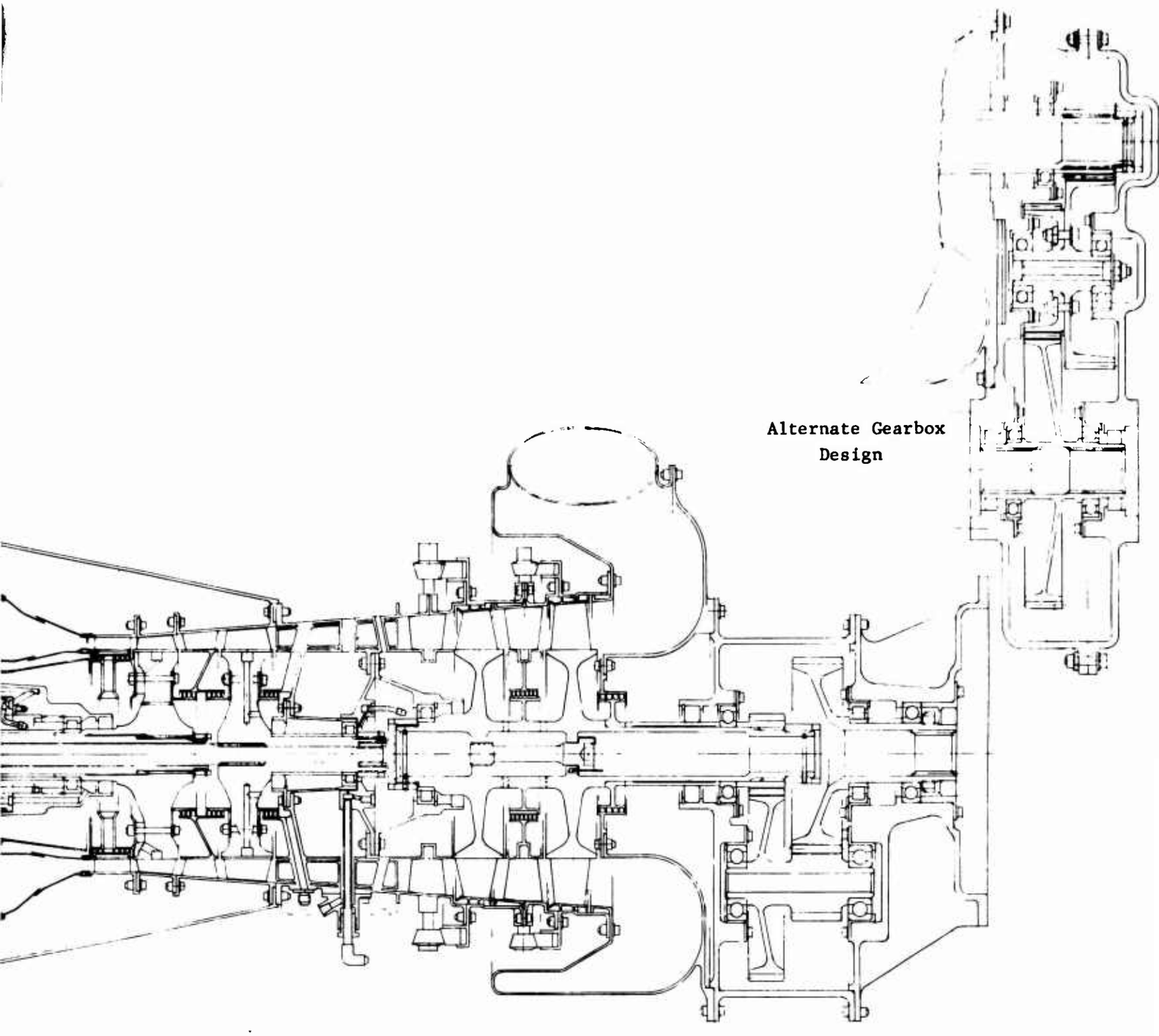

Alternate Gearbox
Design

designs of reduction gearboxes are shown. The final choice of design would be dictated by the installation requirements.

## VARIABLE-GEOMETRY COMPRESSOR ROTOR

Small turboshaft engines are required to have good performance at part-power. The part-speed characteristics of high-performance compressor designs, however, present two problems. First, their pressure ratio capability decreases rapidly with rotor speed. Second, a high degree of mismatching occurs between stages on a single shaft as speed is decreased. Consequently, some form of variability such as variable guide vanes, interstage bleed, or two spooling, has often been employed to improve the part-power, matching and performance.

Another concept which offers considerable promise for improving part-power performance is a variable-geometry compressor rotor. In this approach, the compressor rotor design airfoil geometry can be varied at part-speed operation so as to increase the pressure ratio capability, improve the efficiency, and vary the airflow. A linear surge line characteristic between the design speed and idle is a goal of this scheme.

A preliminary design study of the variable-geometry rotor has been performed, including an aerodynamic performance evaluation and an investigation of practical mechanical schemes. The 2.8:1 axial supersonic compressor design has been used as the basis of this study.

### Aerodynamic Performance Evaluation

A one-dimensional vector diagram analysis was conducted at 70 percent speed. It has been assumed in this analysis that at the part-speed setting, the air enters the rotor with a relative angle parallel to the leading edge suction surface of the rotor blade and that the design deviation angle at the rotor exit remains constant. This has been demonstrated to be essentially true for supersonic compressors. Consequently, there was no incidence loss, and the curve of pressure recovery versus relative inlet Mach number, Figure 33, established the rotor loss. The exit stator total pressure recovery was assumed to remain constant at 97 percent. Although this assumption is known to introduce some degree of error since the stator loss will vary with the incidence angle, it was considered to be acceptable for this preliminary study. The calculation procedure is the same as that used for the design point.

Figure 28 presents axial stage pressure ratio versus airflow corrected to exit conditions (inlet corrected flow for the centrifugal stage of the 16:1 compressor) as a function of rotor inlet and exit relative air angles for 70 percent speed. Efficiency lines and diffusion factors are also included. The diffusion factor is a measure of the degree of diffusion and air turning associated with the rotor geometry. The results indicate that a variable-geometry rotor has the potential for a considerable improvement in pressure ratio and efficiency at 70 percent speed. In addition, the rotor airflow can be varied substantially. For the angle variations investigated (inlet 5 degrees and exit 9 degrees from design), a 17 percent

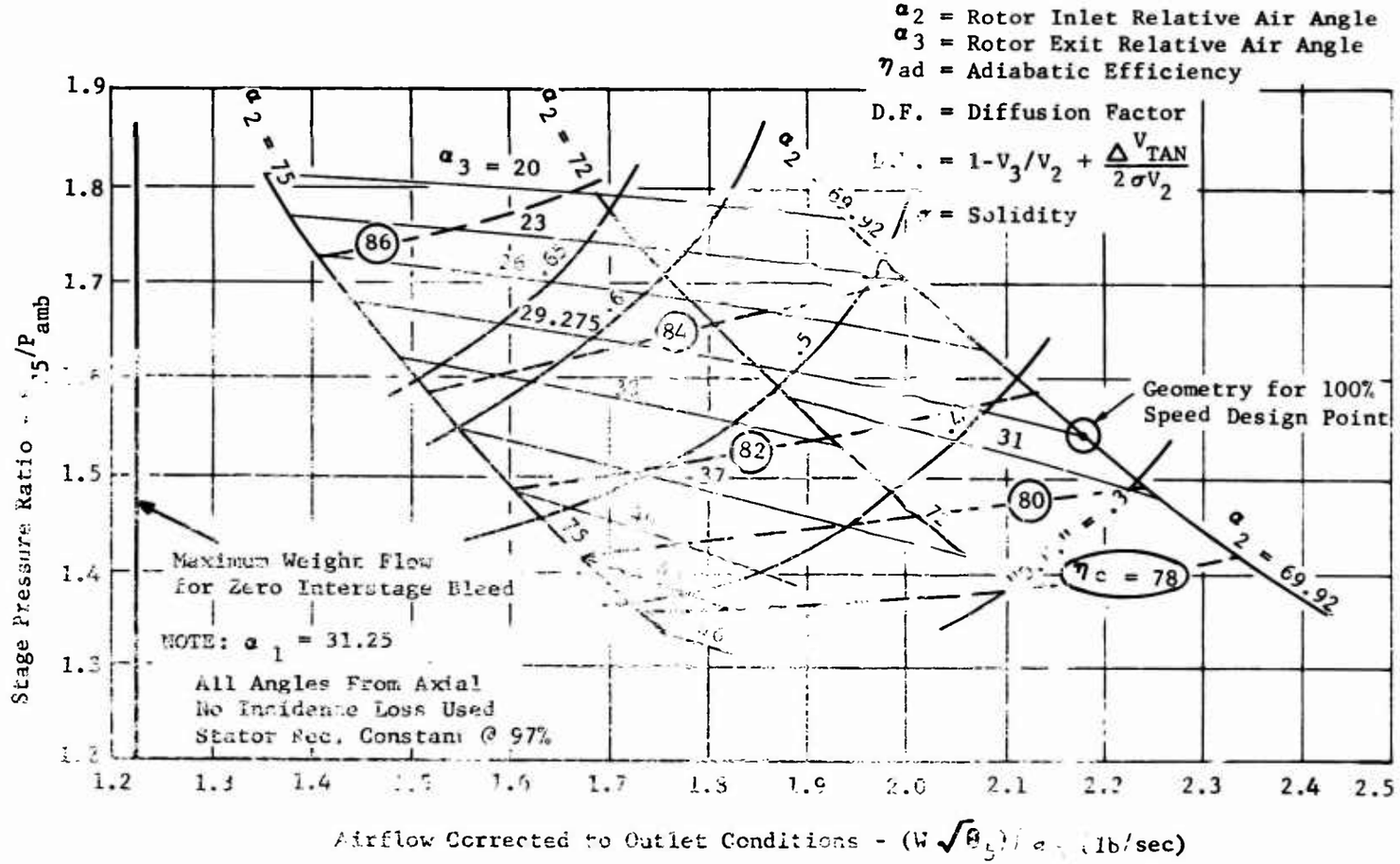


Figure 28. 2.8:1 Supersonic Compressor Variable Rotor Parametric Study for 70 Percent of Design RPM.

increase in pressure ratio, a 5 point increase in efficiency, and a 30 percent decrease in airflow resulted. The mechanical studies indicated that a greater inlet angle variation may be feasible, and therefore the results do not necessarily represent the limiting values. The pressure ratio and efficiency can be increased by either a decrease in exit angle or an increase in leading edge angle or a combination of both of these angle changes. These same angle changes also result in a decrease in the airflow corrected to exit conditions; however, a given degree of leading edge angle increase results in between 5 and 6 times the airflow reduction compared to the same degree of exit angle decrease. In cases where the airflow mismatch is substantial between stages of a single-shaft compressor, such as the axial/centrifugal 16:1 compressor studied in this program, the most beneficial geometric change is toward the maximum reduction in airflow. Increasing the leading edge angle while holding the exit angle constant increases pressure ratio as well as reduces the airflow but rapidly approaches diffusion factors well beyond 0.7. Operation in this range involves air turning angles and diffusion far beyond the ranges currently in use or under experimental investigation. Total pressure recoveries and surge prediction criteria are not defined for this range of geometries. Consequently, in choosing the setting for evaluation in the gas generator performance studies, the airfoil geometry was limited to that which is consistent with current experimental programs. On this basis, a setting with an increased exit angle was chosen to permit a greater reduction in airflow without encountering a high degree of turning and diffusion. The geometry and performance for this point are as follows:

| | |
|---|---|
| rotor inlet air angle | 75 degrees |
| rotor exit air angle | 33 degrees |
| pressure ratio | 1.62:1 |
| corrected airflow (exit) | 1.485 pounds per second |
| adiabatic efficiency | 85.4 percent |

Mechanical Schemes

A number of mechanical schemes and new concepts were reviewed as an initial step in the preliminary design study. Of these, only two were considered to have enough merit to carry into the preliminary design stage.

Studies of these two designs were made to determine the range of geometric variation possible, actuation means required, and structural considerations. The rotor in the first scheme consists of a series of laminations which are staggered to effect a geometry change. The concept of the second scheme is a non-radial flexible leading and trailing edge portion which responds to the effects of centrifugal force. This latter concept makes the geometric variation a direct function of speed.

A layout of the laminated scheme is presented in Figure 29. The typical airfoil sections depict the two extremes of the laminate orientations. The left-hand section represents the off-design setting, while the right-hand section is the design. At an off-design setting, the locus of the protruding corners from the staggered segments defines the effective geometric surfaces. The relative inlet air angle is controlled by the

effective expansion surface angle near the blade leading edge. The layout shows a 50 percent overlap at the segment interfaces for the off-design setting. The effective angle variations plotted on the layout are consistent with this overlap. Crossflow leakage, from the pressure surface through the splitline at the segment interfaces to the suction surface, is the consideration which will determine the minimum overlap that can be tolerated. The acceptable leakage and the overlap limit can be established only through experimentation. The practical variation of effective geometric angle for the leading edge is estimated to be between 2 and 5 degrees. The irregular surface along the expansion side, at the part-speed setting, offers an additional angle effect through increased boundary layer; this is estimated to be from 2 to 4 degrees, resulting in a total variation from design setting of 4 to 9 degrees. The exit angle change capability is estimated to be less than 8 degrees. The boundary layer effect on angle change variation at the exit is expected to be negligible at off-design, but the irregular surface in the design setting may result in some minor loss in design efficiency. The effect on secondary flow of the radial channels formed by the irregular surface has to be experimentally determined.

A two-position actuation arrangement is shown for this scheme. It has not been concluded that a fully variable approach is impractical, but the mechanical considerations for the two-position approach appeared more straightforward within this study. A mechanical scheme for accomplishing the desired geometric variation with the wheel rotating is depicted in the lower portion of Figure 29. Two internal plate clutches are utilized to drive the rotor. The engagement of one or the other clutch determines from which end the rotor is driven. With the rotor being driven from the rear, a series of pins in each laminate drives the adjacent laminate by engagement of the pin with one side of a slot. When the rotor is being driven from the front, the opposite sides of the slots drive the pins in the adjacent laminates. This mechanical arrangement results in two discrete positions of the laminates. The laminates are in one position or the other and not continuously variable between the two extremes. The slender airfoil elements of the laminates do not impose a serious stress problem inasmuch as this particular rotor configuration was designed with all the blade elements radial. The slight bending load imposed by the gas load is partially offset by the restoring moment due to the centrifugal effect. One question which arises is whether or not the laminate segments will be very susceptible to flutter problems. The question can be answered only by test, but one consideration is that the rubbing of the interfaces will offer some mechanical damping. Another disadvantage of this approach is the increased growth at the blade tips which results from the increased growth of the hollow disc. This may require part-speed operation at increased tip clearances relative to a fixed-geometry rotor. A rotor which simulates the part-speed setting geometry of the variable-geometry scheme but which is designed in a fixed position for the purpose of experimental performance evaluation is also shown on the layout. In the scheme on the layout, the laminates are fastened to two stub shafts by means of a common bolt circle. The laminates are equipped with two sets of holes. Each set of holes represents one of the blade camber angle

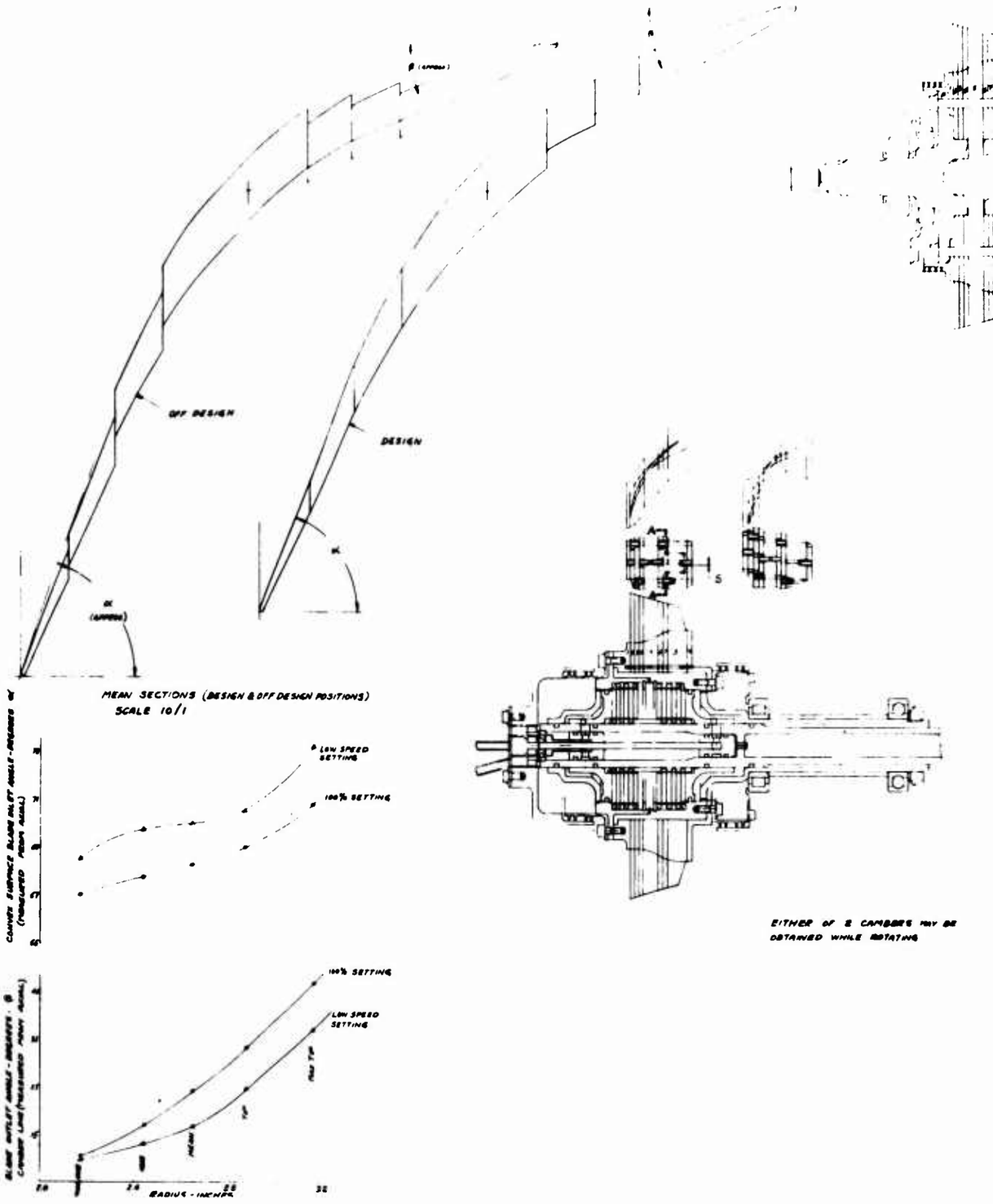


Figure 29. Variable-Geometry Compressor Rotor Scheme With Laminated Disc, Preliminary Design.

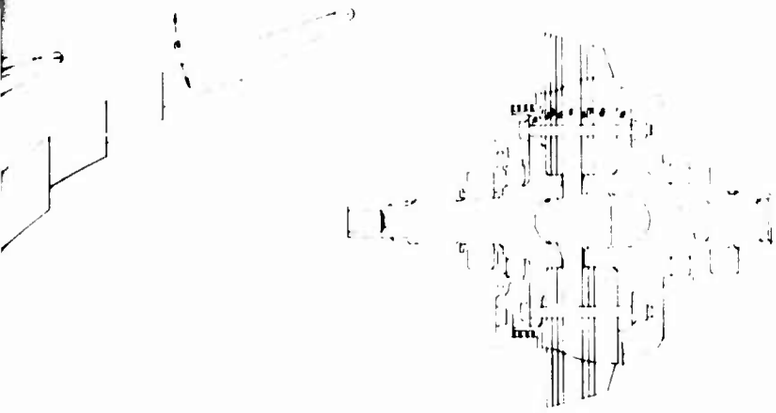

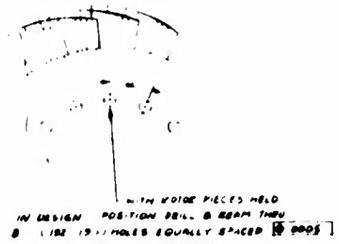


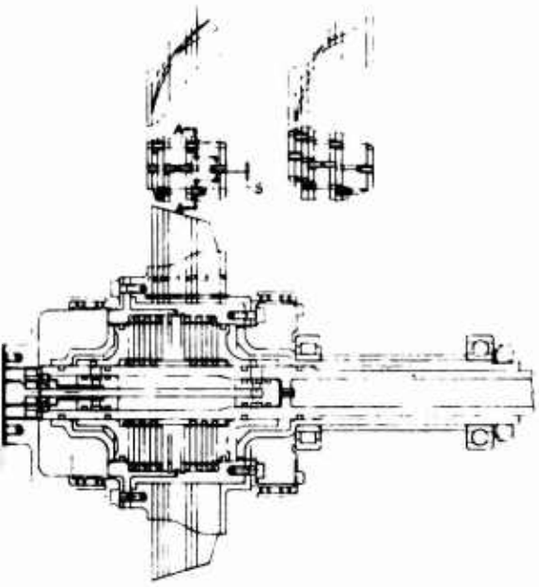

EITHER OF 2 CAMBERS MAY BE OBTAINED WHILE ROTATING

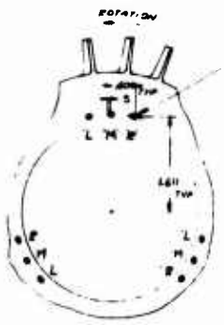


WITH ROTOR PIECES HELD IN
DESIGN POSITION DRILL & REAM THRU 3 SETS OF
3-(.661-.668) HOLES EQUALLY SPACED
9 HOLES TOTAL
HOLES TO BE ELONGATED TO 3 DIMENSIONS SHOULD BE
OPENED TO (.0635-.0645) DIA
NO RELATIONSHIP BETWEEN HOLES & BLADES

r Scheme With Laminated Disc,



2

settings. To change from one setting to the other simply requires a disassembly and reassembly of the rotor.

Figure 30 shows the concept of the second scheme. The leading edge and trailing edge portions of the airfoil are separated from the main airfoil. Each of these two separated sections is supported from its own flexible ribbon. The ribbon and its respective airfoil section are stacked non-radially. The degree of tilt from radial is a maximum at the extreme leading edge of the leading edge section and the extreme trailing edge of the trailing edge section and in each case decreased smoothly to radial at the interface with the main airfoil section. A variation of rotor speed from zero to design speed causes the leading and trailing edges to deflect and approach a radial condition. The degree of geometric variation possible with this scheme is difficult to assess accurately on a preliminary basis because of the large number of factors involved (ribbon length, ribbon cross section, initial curvature of beam, etc.). The solution of a curved beam in a centrifugal field requires an iteration process which is beyond the scope of this preliminary effort. An approximation based on some simplifying assumptions indicates a potential angle variation in the same range as for the laminated scheme (leading edge 4 - 9 degrees, trailing edge less than 8 degrees). This scheme requires no mechanical actuation.

Conclusions

The results of this preliminary study indicate that:

1. The variable-geometry compressor rotor offers significant improvement in the part-speed performance of single-spool high-pressure-ratio compressors.

2. The full extent of the performance benefit cannot be assessed until the performance of rotor turning angles and diffusion far beyond the levels currently under investigation is established.

3. Both the laminated and non-radial element schemes are promising mechanical concepts for a variable-geometry rotor.

4. Both schemes offer the same effective geometric variation potential.

5. The non-radial elements provide a far simpler mechanical scheme, which is fully variable but is limited to the variation schedule dictated by the speed.

6. The problem of establishing the true operating geometry of the non-radial scheme under the dynamic forces of rotation may hamper the development of a predictable design technique.

7. The geometric configuration of the laminated construction is predictable, and the variation can be accomplished at any desired speed. Some slight penalty in design point performance may be associated with this scheme, and the leakage and flutter characteristics have to be established.

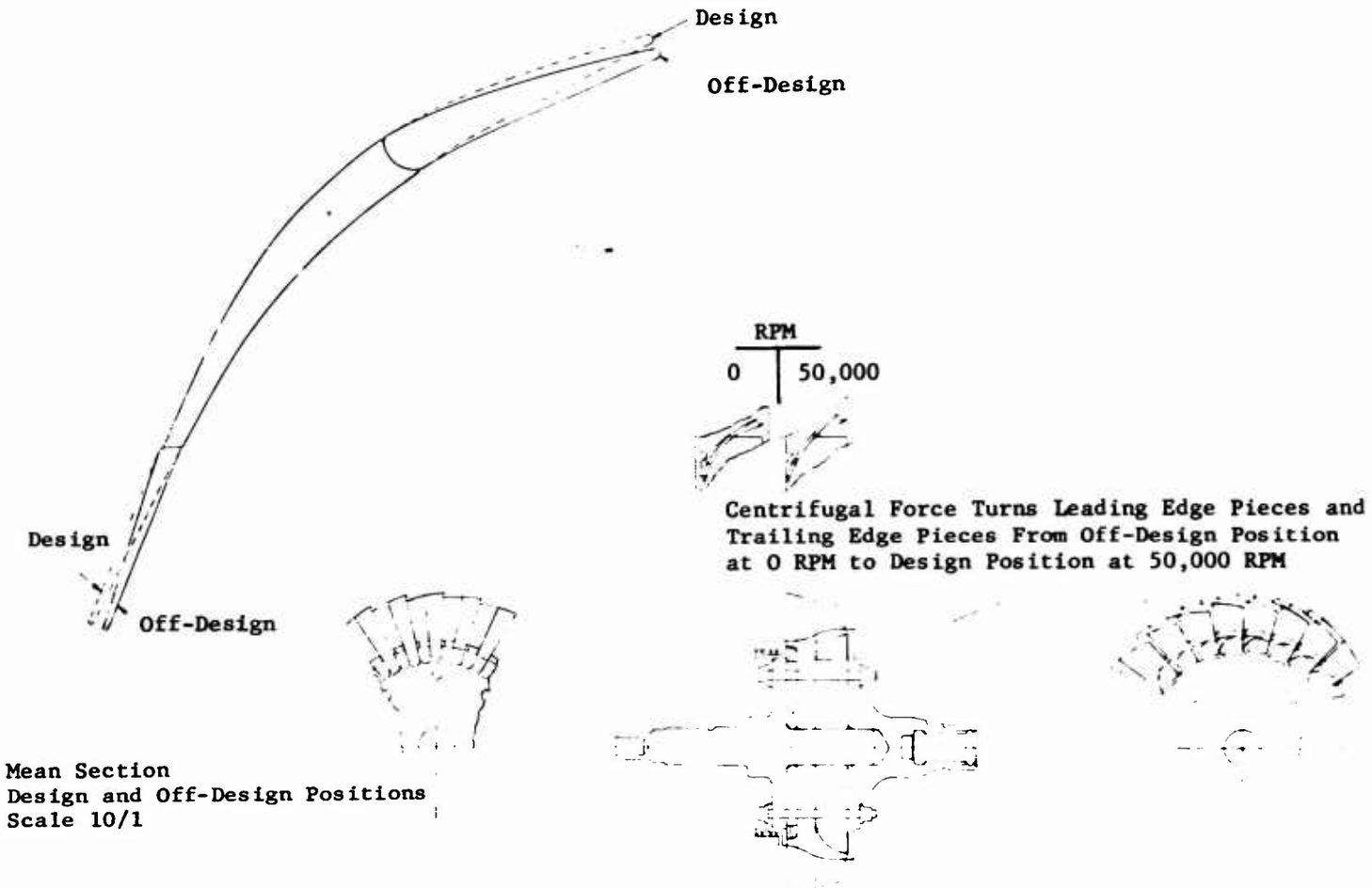


Figure 30. Variable-Geometry Compressor Rotor Scheme With Non-Radial Blade Elements, Preliminary Design.

## (C) SUPERSONIC AXIAL COMPRESSOR (U)

(U) The compressor component to be advanced under this program is a single-stage axial supersonic compressor. The data and results for two designs are discussed in this report.

(U) A 2.8:1 pressure ratio supersonic (SSC 2.8) compressor has been designed during Phase I of this contract and is discussed in this section. The detailed design of the inlet guide vanes and compressor rotor has been completed, and procurement is in progress for experimental evaluation of these components under Phase II. A preliminary design of the exit stator and interconnecting duct has been completed, and detailed design of this component is scheduled for Phase III of the program.

(U) A company-funded program involving a 2:1 pressure ratio supersonic compressor design is in the rotor development and experimental evaluation phase. The data from this program are discussed in Appendix I.

### (U) DESCRIPTION AND SELECTION OF SUPERSONIC TYPE COMPRESSOR

(U) The mechanical energy addition to air in a compressor is a function of the rotor airfoil section speed. The desire to increase the pressure ratio per stage and the mass flow per frontal area has led designers to pursue designs with higher rotational speeds and therefore higher section speeds. Thus, the next step beyond the conventional subsonic compressors was the investigation of the transonic compressors and, following that, the supersonic compressors.

(U) The successful transonic compressor stages display several common attributes that distinguish them from their subsonic counterparts. First, the airfoil sections have relatively sharp leading edges and small wedges. Second, their cascades utilize higher solidities (chord/pitch ratios), and the flow process clearly departs from isolated airfoil behavior to passage flow. The third, and probably the most significant, departure from subsonic designs is the requirement for a large spread in operational relative Mach number between cascade hub and tip. (A typical spread is from .8 to 1.3.) It is this quality which permits radial redistribution of flow to provide ample choking margins and good off-design characteristics. The section speeds compatible with the blade relative Mach numbers and the flow deceleration possibilities limit the stage pressure ratio to a maximum of about 2:1. The supersonic compressors possess the section speeds necessary to achieve stage pressure ratios in excess of 2:1.

(U) Various types of supersonic stages have been proposed and investigated as described in the literature. However, when closely reviewed, these designs can be categorized into two fundamental rotor types: the impulse rotor, and the passage-contained shock-down process rotor (shock-in-rotor). In the impulse rotor, the air enters at relatively high supersonic Mach numbers, undergoes little deceleration, and exits at high supersonic Mach numbers for both relative and absolute vectors. The shock-in-rotor type differs in that the shock process in the rotor passage results in a subsonic Mach number which may be diffused further so as to exit at even lower subsonic

Mach numbers. Thus the exit stator in the latter type is not faced with diffusion from supersonic to subsonic Mach numbers. Of the two, the impulse type offered the higher potential pressure ratios and therefore was given primary attention in investigations conducted through the middle and late 1950's. The addition of kinetic energy to the air was accomplished very effectively by impulse rotors at highly desirable efficiencies. When the cycle demanded deceleration of this flow to low subsonic values, the efficiencies of the downstream stators and diffusers proved to be tragically poor. Rotor total pressure ratios of 4, 6, 8, and higher were experimentally achieved. In several instances, the diffusing stator row permitted recovery of only about half of the rotor pressure ratio.

(U) The shock-down rotor, which is limited to pressure ratios near 4:1 as a maximum, has not enjoyed the intense interest of the compressor community by virtue of this limitation. Early efforts in the late 1940's and early 1950's indicated that much had to be learned before desirable rotor efficiencies could be achieved.

(U) The early work in diffusing supersonic rotors applied cascade parameters that have since been shown to be entirely unsatisfactory. References 5, 6, and 10 are typical of stationary cascade work contributing to this assessment. Specifically, three areas of departure from past design are suggested in the following:

1. The utilization of higher solidity values and higher passage length/width values.

2. Accomplishment of flow deceleration with more nearly constant area passage. This implies substantially lower divergence than used in earlier designs.

3. Utilization of body forces to aid in the control of pressure gradients. This implies hub and tip curvature as well as blade lean and sweep.

(U) Although the losses expected in the supersonic compressor rotor may be several times those of a conventional subsonic stage, the overall efficiency of the supersonic rotor can still be high if it is a highly loaded high-pressure-ratio stage.

(U) Investigation of the shock-in-rotor type of supersonic compressor, therefore, has been far too inadequate to assess its true performance potential. It is believed that good efficiencies and high pressures can be achieved with proper advancement of this type of design. The relatively good efficiency that it offers together with its rugged airfoils and capability of producing a pressure ratio well in excess of 2:1 in only one stage makes it particularly attractive as a boost stage for small gas turbine engines. On this basis, the single-stage axial supersonic shock-in-rotor type of compressor has been selected as the component to be advanced and demonstrated under this program.

(C) DESIGN PROCEDURES AND ANALYSIS (U)

(C) Aerodynamic Design (U)

(C) The aerodynamic design procedure is initiated by conducting a one-dimensional vector diagram analysis to arrive at a preliminary configuration which satisfies the performance goals. The final design is established by performing an analysis of three streamtubes (tip, mean, and hub) using the one-dimensional results as a guide. In each case, the calculation proceeds from station to station while satisfying continuity, energy, and radial equilibrium. A sample streamtube calculation is presented at the end of the following discussion.

(C) Inlet Guide Vanes - A 1.5 percent total pressure loss was assumed to occur through the compressor inlet and guide vanes. Figures 31 and 32 present the plotted characteristics for the guide vanes. The radial distribution of the tangential velocity at the blade exit was varied to satisfy a free vortex flow. The exit axial velocity variation was computed taking into account the curvature of the flow path. A very nearly symmetrical convergence of the annulus between the inlet guide vanes (IGV) and the first rotor was established by assigning similar radii of curvature at the outer diameter (O.D.) and the inner diameter (I.D.). The radius of curvature for the flow was assumed to be equal at both extremes of the path and was determined as the average between the effective radii of curvature at the hub and the tip contours. The variation of axial velocity across the flow path was based on a straight-line variation of the radius of curvature from the average value computed at the extremity to $\infty$ at the mean diameter. This variation was computed according to the method described in Reference 19. The mean turning of the inlet guide vanes was held to approximately 30 degrees to provide a configuration within practical fabrication limits. The inlet guide vanes represent an accelerating flow passage. Turbine test results have established zero incidence as the optimum design level; hence, this value was used for the IGV cascade. Deviation was computed using Carter's Rule (Reference 15) for circular arc mean-line airfoils. Previous experience has shown this to be a reasonable approach for IGV design. The solidity for the cascade was determined as the one which would produce the minimum profile pressure loss (British Report Reference 1).

(C) Rotor - The passage total pressure recovery assigned to the rotor blade row is based on the recovery curves in Figure 33. The curves are based on a compilation of experimental data from supersonic and subsonic cascade tests. In the three-dimensional design, the tip tube aerodynamic recovery of the rotors is multiplied by a correction factor, called a streamtube factor, of 0.99 to account for tip clearance losses. In the hub region of rotors, experimental evidence has indicated that boundary layer is centrifuged toward the tip. To account for this effect, the aerodynamic recovery of the hub streamtube in each rotor is multiplied by a streamtube factor of 1.01. The mean streamtube recovery is considered unaffected (factor of 1.0).

(C) The calculations for the rotor include adjustment of the relative total temperatures and pressures for the energy change associated with a change in

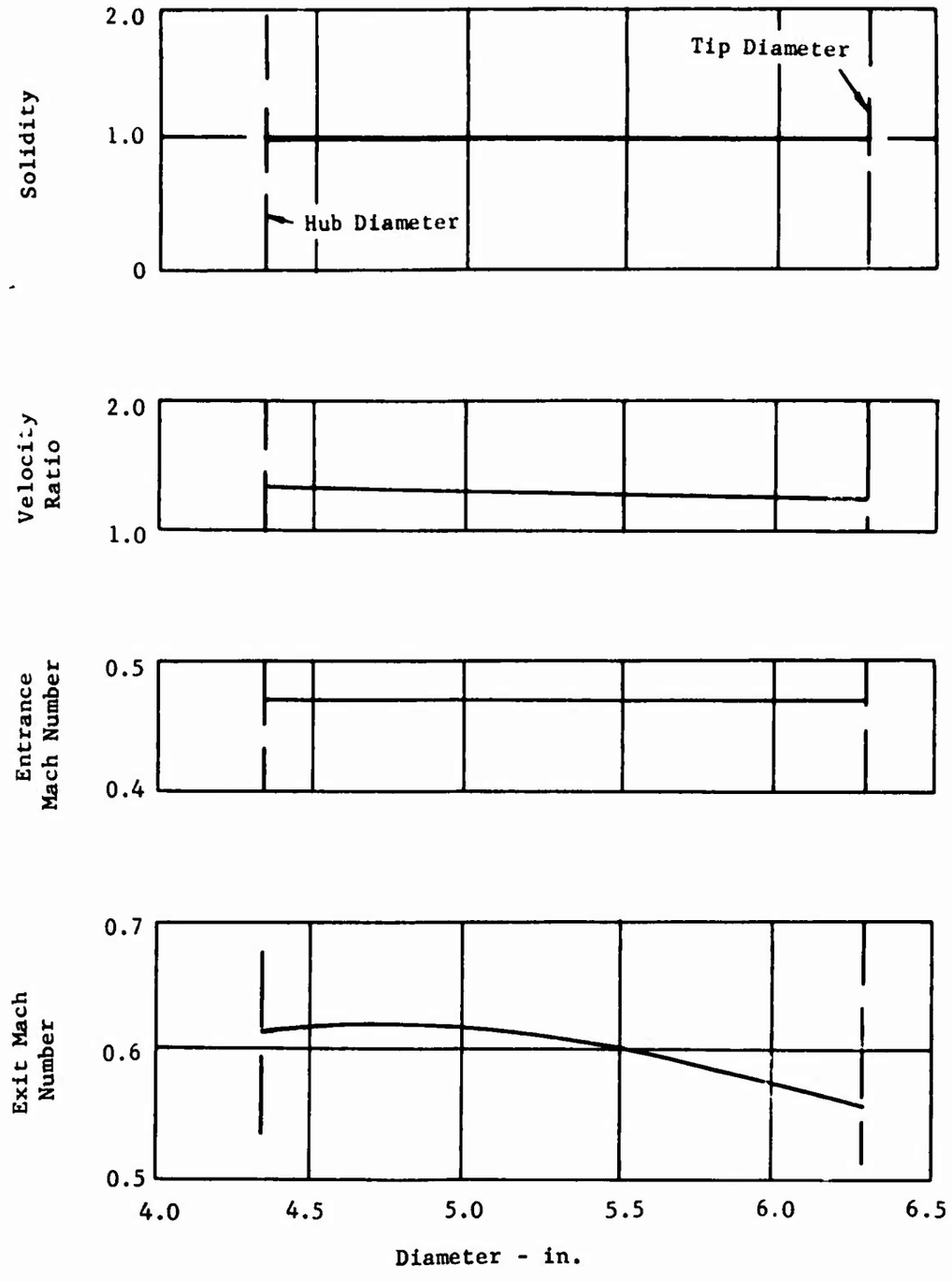


Figure 31. (U) 2.8:1 Supersonic Compressor Inlet Guide Vane Design Data.

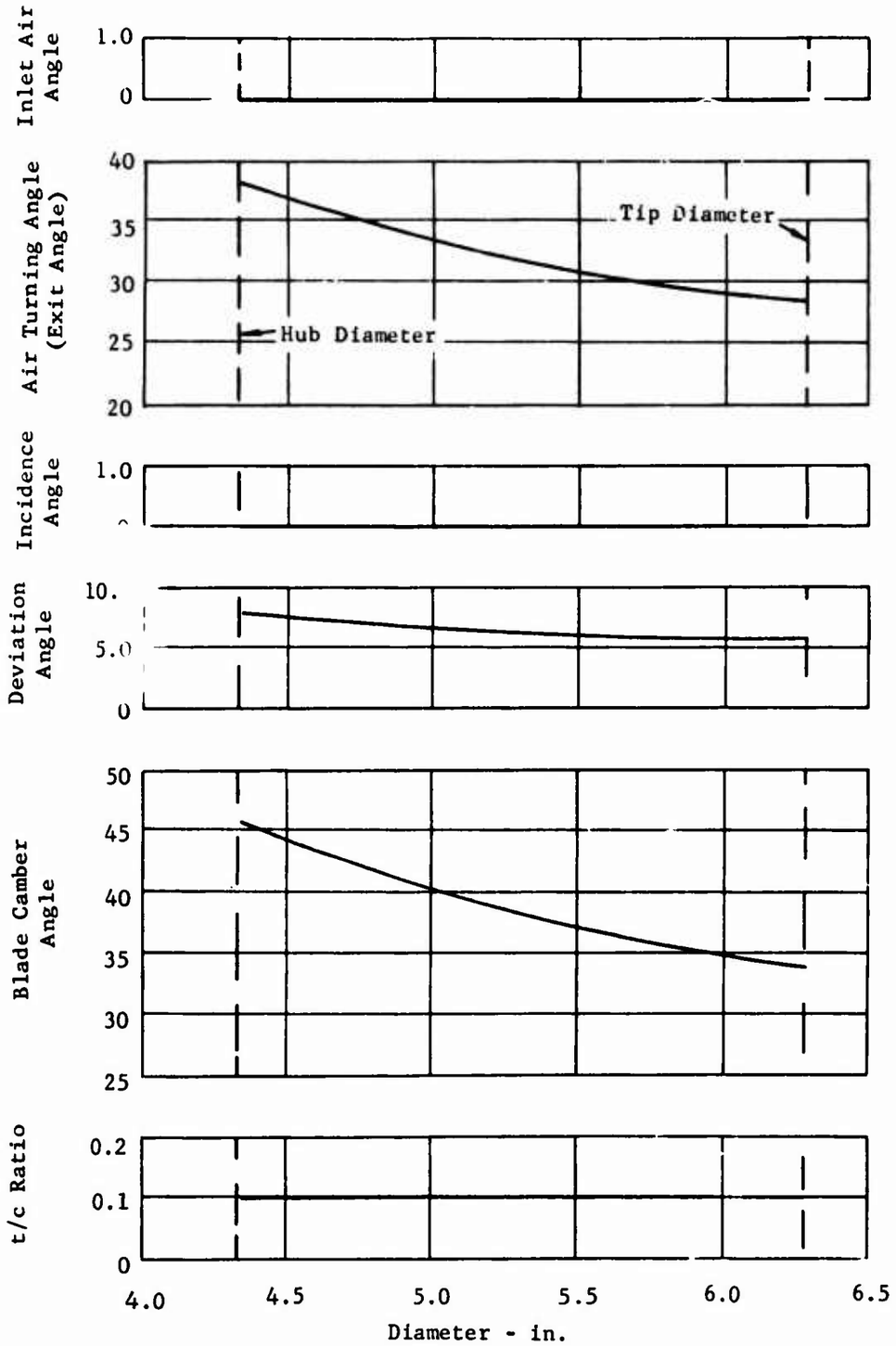


Figure 32. (U) 2.8:1 Supersonic Compressor Inlet Guide Vane Design Data.

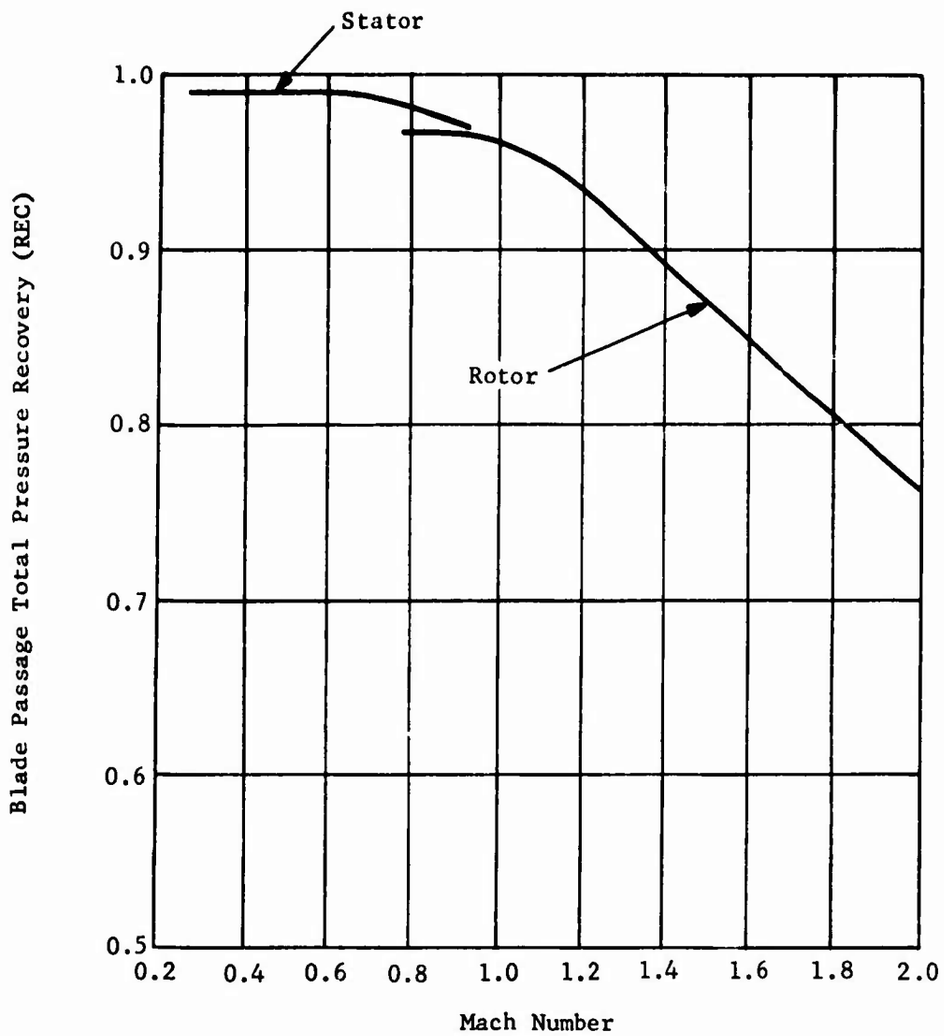


Figure 33. (U) Blade Passage Recovery Curve.

the streamline radial location from the inlet to the exit according to the equations

$$T_{T_3}/T_{T_2} = 1 + \left(\frac{\gamma-1}{2}\right)\left(\frac{U_3}{a_{T_2}}\right)\left[1 - \left(\frac{D_2}{D_3}\right)^2\right]$$

$$P_{T_3}/P_{T_2} = \left(T_3/T_2\right)^{\gamma/\gamma-1}$$

(C) The hub contour in the meridional plane of the downstream half of each rotor has a curvature which turns the flow back toward the machine axis. This curvature contributed an outward radial force which was evaluated in satisfying radial equilibrium at the rotor exit. This force was added to the radial force resulting from the rotational or tangential component velocity. The radius of curvature was assumed to vary linearly from the computed hub value to $\infty$ at the tip. As a result of the hub curvature effect, the hub streamtube experienced the highest flow turning but the least diffusion of the three streamtubes analyzed in each rotor.

(C) The Reynolds number for the rotors is above $1.0 \times 10^6$ and laminar separation cannot occur, especially since the oblique shocks at the inlet should trip any laminar boundary layers which tend to exist.

(C) The flow induction process of a rotating blade row having supersonic relative entrance velocities has been described and subsequently experimentally verified in numerous engineering efforts (References 13 and 17). In summary, it can be concluded that when the cascade is unchoked and flow deflections are limited to values permitting attachment of oblique shock waves, the blades will generate the appropriate shock or expansion waves to cause the approach flow to enter the cascade in a direction parallel to the suction surface of the blades at the leading edge. Many of the NACA supersonic compressor studies indicated that if one can attribute approximately one degree additonal blade thickness to boundary layer growth, the stated entrance flow theory is quite valid. Therefore, the incidence values for the first- and second-stage rotors were selected to have the blade suction surface in the vicinity of the leading edge at an angle one degree smaller than the design flow direction along the entire span.

(C) The operating Mach numbers, at design speed, of the first- and second-stage rotors are between 1.30 and 1.60. This is a region which permits very little passage contraction if the problems of "supersonic starting" are to be avoided. Simultaneously, very little flow deflection through an oblique shock is possible without flow detachment and its associated losses. For this reason, a leading-edge wedge angle of 4 degrees was selected in the design. It provides adequate structural rigidity while requiring relatively small deflections of the cascade entrance flow.

(C) Two subtle requirements were implied by the gas dynamics solution of the stages. Radial equilibrium was satisfied for a given hub contour radius of curvature. Obviously, the hub geometry had to conform with the specified curvature to validate the vector solutions. This was a strict

requirement in the rotor because of the magnitude of forces resulting from the curvature. The other requirement, which was not quite so apparent, was that the radial body forces, which might be applied by blade cant, be negligible in magnitude at the rear of the blade row. Since no such forces were assumed to exist in the solution of the state conditions, it was necessary to generate blades having nearly radial elements in the region of the trailing edge.

(C) The sharpest practical leading edge is desired for these designs. The design leading-edge radius for the SSC (2.0) rotor was .0075 inch, but this was reduced to .0035 inch for the SSC (2.8).

(C) Considerable experimental evidence indicates that supersonic compressor rotors will tend to discharge flow parallel to the exit pressure surface. The criterion was used to establish the deviation angle at approximately half the exit wedge angles. Small adjustments from strict adherence to this criterion were allowed to compromise with the passage area schedule.

(C) Designers of contemporary turbomachinery components frequently apply a "blockage factor" to account for flow passage area reductions resulting from boundary layers. An estimate is made of the displacement thickness of the boundary layers along all the walls of the flow passages, and the cross-sectional area is increased by some factor (one percent or more, depending on the boundary layer estimate) to provide an effective area compatible with aerodynamic state conditions.

(C) The design of the subject compressor did not include a "blockage factor" superimposed on the computed areas. The total pressure recovery of the passage flow combined with the careful selection of area ratios and passage area distribution provided a comparable relationship between areas and state conditions. Use of the recovery curve, which includes boundary losses, should provide a more realistic set of state conditions than offered by only area adjustment.

(C) Experimental cascade tests at supersonic entrance Mach numbers have indicated that some configurations experience a form of local choking within the blade passage despite the fact that the flow area increases continuously. This local choking tends to limit the maximum airflow which the passage will pass. Some correlation has been established between the experimental local choking and the flow conditions indicated by two-dimensional supersonic flow net analysis for which an incremental wedge angle along the compression surface of the blade is too high for local supersonic flow attachment. Based on this information, local detachment within the blade passage, indicated by a supersonic passage flow analysis, was utilized as the criterion for choking within supersonic blade rows.

(C) Two blade sections were initially generated along cylinders having radii near the tip and near the hub, but within the flow passage. Two adjacent blades were always drawn to insure that they formed a two-dimensional

passage having no contraction. Turning and thickness distribution was allowed to vary to satisfy the passage area requirements (to avoid choking) and the needed radial distribution in blade section areas (structural). When the two sections for a particular rotor completely satisfied all stated requirements, three additional sections were generated on cylindrical surfaces at radii representing the extreme hub, some mid-section and beyond the tip. The two initial sections were stacked on their centers of gravity, and the other sections were graphically determined. Straight-line elements defined the additional three sections where possible in the rotor. However, straight-line elements aided in generating only the middle 80 percent of the chord of the rotor. Leading and trailing edge regions had to be modified to satisfy the non-linear distribution of the mean camber line.

(C) Upon completion of the five sections of a blade row, views were taken through the resulting three-dimensional passage (normal to the flow direction) to determine the area distribution. Since the compressor outer case was to be conical, the hub contour provided the only means by which adjustment of the area distribution could be made within the blade passage. A smooth, continuous curve could be generated along the hub without violating area distribution requirements. It should be noted that the chord of the rotor increases toward the tip, and the resulting trailing edge lines were less than 10 degrees from a radial line. This was considered to be sufficiently small that no radial body forces would result.

(C) A two-dimensional flow net was computed for the hub area of the first-stage rotor, as this area appeared to be most critical. This analysis indicated that the expansion waves from the preceding blade tend to accelerate the flow which initially strikes the leading edge of the blade. At the leading edge, the flow is computed to pass through a detached shock and to exit parallel to the compression surface at a slightly reduced Mach number (method described in Reference 22). For this configuration, the flow local to the compression surface is influenced by a second substantial expansion from the preceding blade prior to impinging on the first incremental wedge of the compression surface. As a result, the first effective incremental wedge is 0.4 degree and the upstream Mach number is 1.49. The detachment angle for 1.49 Mach number is 11.9 degrees; therefore, the flow is safe from detachment by a considerable margin. As the flow analysis proceeds in a downstream direction, the expansions from the preceding blade have an even greater influence, and the detachment margin for the flow along the compression surface increases.

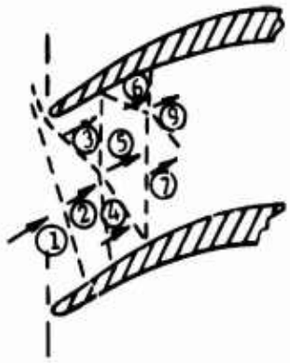


| Region | Mach No. | Flow Direction Relative to Compression Surface (Wedge Angle) |
|---|---|---|
| 1 | 1.42 | |
| 2 | 1.47 | |
| 3 | 1.38 | |
| 4 | 1.57 | |
| 5 | 1.49 | 0.4 degree |
| 6 | 1.47 | |
| 7 | 1.55 | |
| 8 | 1.54 | 1.5 degrees |

(C) The hub contour through the first rotor has a curvature in the meridional plane which tends to impose a compression in the first half of the passage. As this effect is a function of a subsonic meridional Mach number, a potential flow analysis would have to be superimposed on the two-dimensional supersonic analysis to determine the three-dimensional picture. Such an analysis would be rather complex and is considered to be unwarranted. The detachment margin indicated by the two-dimensional analysis is considered to be safe enough that the compression from the hub contour does not present a risky condition.

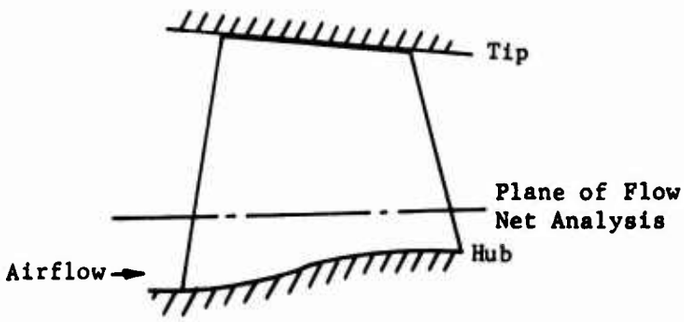


(C) The leading edge of the SSC (2.0) was designed with a sweep. A review of this approach during the design of the SSC (2.8) indicated that with a conical shroud this sweep reduced the leading edge span for the rotor, and this presented a possible source of loss in airflow induction. Consequently, the SSC (2.8) was designed with a radial leading edge. In an attempt to reduce the tip clearance of the SSC (2.8) relative to the SSC (2.0), an abradable shroud was introduced.

(C) Blade spacing between the trailing edge of the inlet guide vane and the leading edge of the compressor rotor was assigned so as to satisfy a criterion based on unpublished turbine data existing at Curtiss-Wright. These data indicated that a minimum axial spacing of 13 percent of the upstream blade chord is required, below which the performance deteriorates.

(C) Exit Stator and Interconnecting Duct - The preliminary design of the exit stator and interconnecting duct has been made for SSC (2.8). The exit stator has been integrated in the interconnecting duct which is required to meet the inlet geometry of the centrifugal stage for the 16:1 compressor. The stator turns the flow to an axial direction and decelerates it to an axial Mach number of 0.32 to match the required centrifugal stage inlet conditions. Due to the high subsonic Mach numbers entering the stator, developed airfoils are generated for this blade row also. A zero incidence was assigned at the design conditions. The air turning schedule, the thickness distribution, and the hub and shroud contours have all been carefully matched to provide an area schedule which continually diverges and presents no local choking regions. The rates of contour turning have been evaluated with respect to excessive local diffusion rates which might induce separation. A diffusion factor of 0.557 has been computed for the stator. The deviation at the exit is zero since an axial direction is established. The flow path and blade sections are presented in Figure 34. The area and Mach number schedules are presented in Figure 35. A total pressure recovery of 0.97 was estimated for the stator and interconnecting duct. Data from a transonic compressor tested at Curtiss-Wright (Figure 36) indicate that this is a reasonable recovery for the range of inlet Mach numbers from 0.78 to 0.92.

(C) Sample Calculation - The calculation procedure is illustrated by the calculation for the mean streamtube. The assumed ambient conditions are

$$P_{T_{amb}} = 29.92 \text{ inches of mercury absolute (in. Hg abs.)}$$

$$T_{T_{amb}} = 519^\circ R$$

(C) The airflow (W) of the mean streamtube is approximately one-third of the total flow, or 1.353 pounds per second. A 1 percent total pressure loss is estimated from the inlet to station zero just upstream of the inlet guide vanes (IGV).

$$P_{T_o} = 29.92 \times .99 = 29.621 \text{ (in. Hg)}$$

(C) A uniform Mach number of 0.47 is assumed for this station, and the isentropic area ratio A/A* is determined to be 1.4018 (tables for air $\gamma = 1.4$). The flow is axial at this station, and the streamtube flow area is computed from the continuity equation:

$$A_{flow_o} = \frac{W\ (A/A^*)_o \sqrt{T_{T_o}}}{K\ P_{T_o}} = \frac{1.353\ (1.4018)\ 519}{.2605\ (29.62)} = 5.599 \text{ square inches}$$

Figure 34. (U) 2.8:1 Supersonic Compressor - Exit Stator and Interconnecting Duct Schematic.

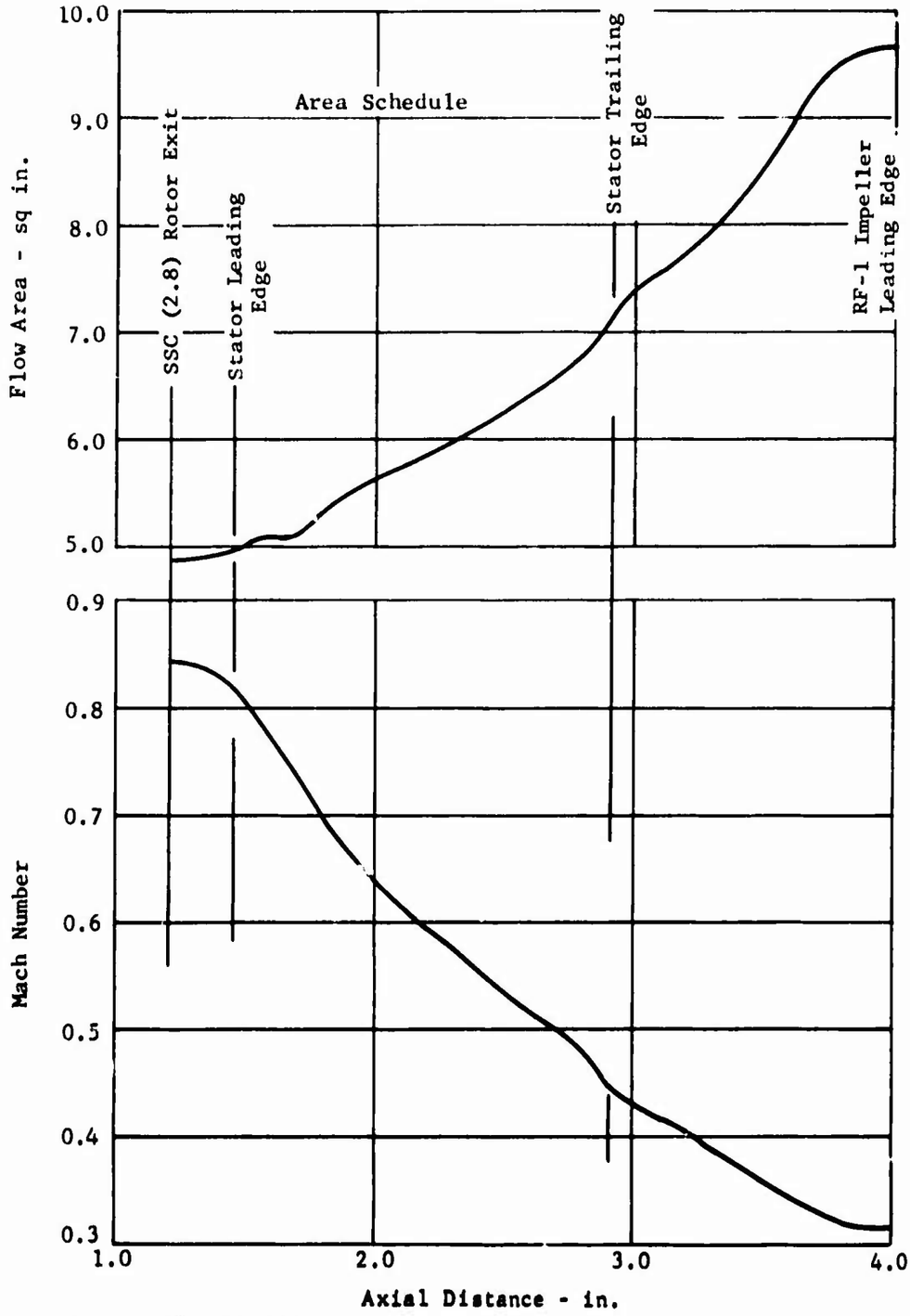


Figure 35. (U) 2.8:1 Supersonic Compressor Area Schedule and Mach Number for Exit Stator and Interconnecting Duct.

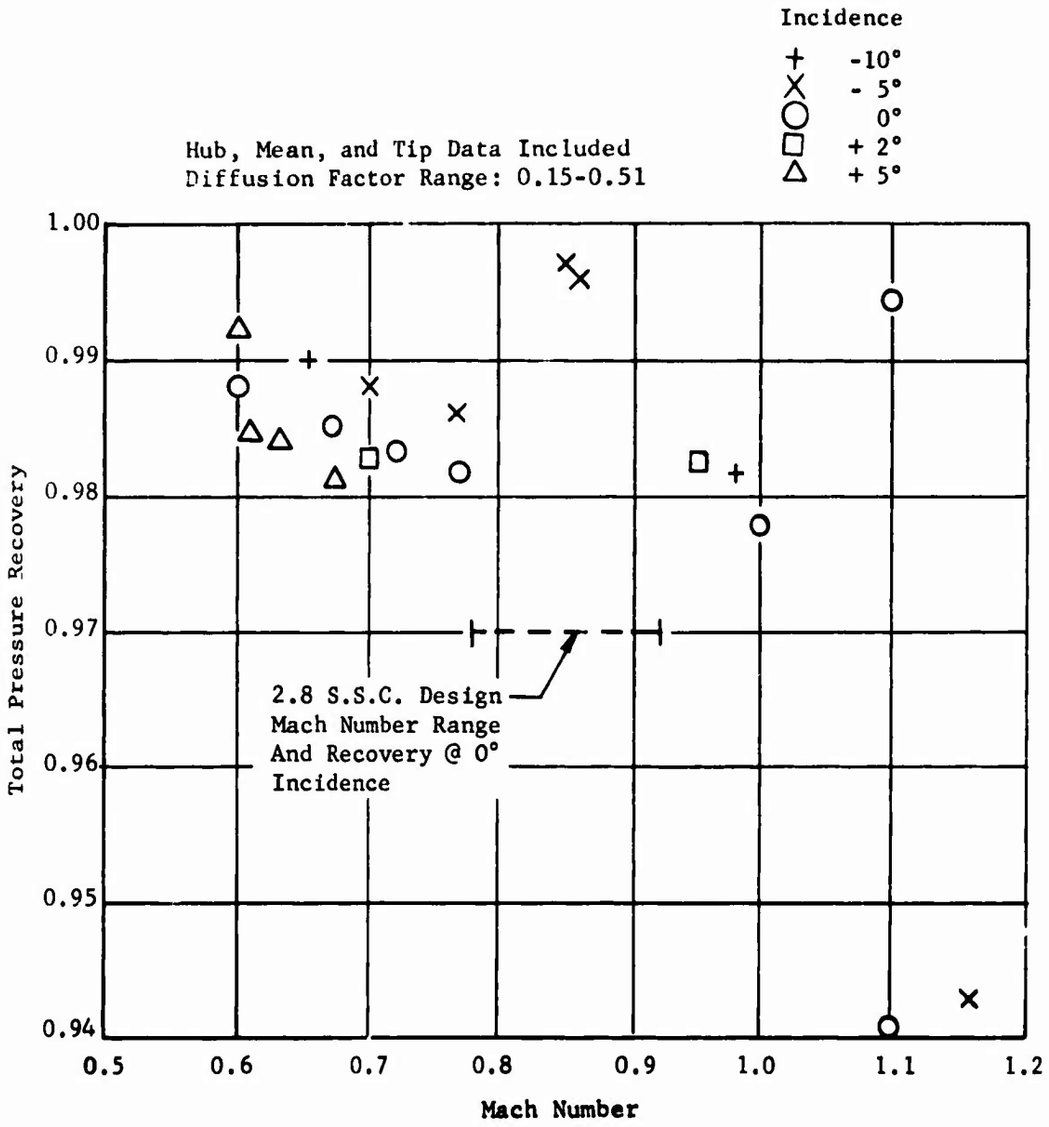


Figure 36. (U) Exit Stator Performance Data From Curtiss-Wright Transonic Compressor Tests - Double Circular Arc Blades.

(C) At this station, the streamtube annulus area is equal to the flow area due to the axial flow direction ( $\alpha = 0$). At any station, the total annulus area is determined by the summation of the annulus area computed for each of the three respective streamtubes (hub, mean, and tip). The diameter of the streamtube at which the state conditions and vector triangles exist is assumed to be the one which divides the streamtube annulus area into two equal areas. This diameter is computed by first selecting the shroud diameter and computing the tip streamtube annulus area. The inside diameter of the tip streamtube is computed and thus establishes the outside diameter of the mean streamtube. The mean diameter of the mean streamtube is computed by the formula

$$D_m = \sqrt{(O.D.)^2 - \frac{4}{\pi}\left(A_{ann_{mo}}\right)}$$

(C) The hub and shroud of the passage are chosen to be cylindrical from the entrance to the exit of the IGV. The turning through the inlet guide vanes is varied to provide a free vortex tangential velocity distribution as the exit. ($V_{tan} = \frac{K}{r}$). The axial velocity is varied to satisfy the meridional curvature of the hub and shroud from the IGV exit into the rotor. ($\int_1^2 dV_z = \int_1^2 \left[ Ar + B \right] dr$.) A turning angle which provides a 1.4 to 1.6 relative Mach number to the rotor blades is desired. An iteration process is necessary to satisfy all of these conditions and radial equilibrium at the exit of the inlet guide vanes.

$$(dp_s/dr) = \left( \frac{\rho \overrightarrow{V}_{tan}^2}{gr} + \frac{\rho \overrightarrow{V}_{ax}^2}{gR} \right)$$

(C) The total pressure recovery through the guide vanes is estimated to be 0.994, and the mean streamtube conditions which result from the iteration process at the IGV exit are

tangential angle $\alpha_1 = 31.25$

total temperature $T_{T_1} = 519°R$

total pressure $P_{T_1} = 29.62 \times 0.994 - 29.45$ (in. Hg abs.)

annulus area $A_{ann_1} = 5.531$

flow area $A_{flow_1} = 5.531 \times \cos 31.25 = 4.729$

isentropic area ratio $(A/A^*)_1 = \frac{K P_T A_{flow}}{W \sqrt{T_T}} = \frac{.2605(29.45)\ 4.729}{1.353\sqrt{519}} = 1.177$

static to total pressure ratio $Ps/P_{T_2} = .778$ (from table of isentropic functions)

static to total temperature ratio $(Ts/T_T)1 = .931$

Mach number $M_1 = .6096$

Therefore,

$$P_{s_1} = .778 \times 29.45 = 22.91 \text{ in. Hg abs.}$$

$$T_{s_1} = .931 \times 519 = 483°R$$

acoustic velocity $a_1 = \sqrt{\gamma\, gRT_s} = \sqrt{1.4 \times 32.2 \times 53.3 \times 483} = 1079$

velocity $V_1 = M_1 \times a_1 = 657.2$ ft/sec

axial component $V_{ax_1} = V_1 \times \cos 31.25° = 561.9$ ft/sec

tangential component $V_{tan_1} = V_1 \times \sin 31.25° = 341$ ft/sec

mean diameter $D_{m_1} = 5.418$ inches $= D_{m_2}$

wheel section speed for 50,700 RPM

$$U_2 = \frac{D_{m_2} \quad N \quad \pi}{720} = 1{,}196 \text{ ft/sec}$$

(C) The relative conditions to the rotor inlet are then determined.

relative tangential and axial velocity components:

$$V_{tan_2} = V_{tan_1} + U_1 = 341 + 1196 = 1{,}537 \text{ ft/sec}$$

$$V_{axial_2} = V_{ax_1}$$

relative velocity $= V_2 = \sqrt{V_{tan_2}^2 + V_{ax_2}^2} = 1{,}636$ ft/sec

acoustic velocity $= a_1 = a_2 = 1{,}079$ ft/sec

relative Mach number $= M_2 = \frac{V_2}{a_2} = 1.518$

corresponding isentropic parameters: $A/A^*_2 = 1.189$

$P_s/P_{T_2} = .265$

$T_s/T_{T_2} = .684$

(C) The static conditions remain the same.

$$P_{s_2} = P_{s_1} \quad \text{and} \quad T_{s_2} = T_{s_1}$$

(C) Therefore, the relative conditions to the rotor blades are computed as follows

relative total pressure $$P_{T_2} = \frac{P_{s_2}}{P_{s_{1/P_{T_2}}}} = 86.33 \text{ in. Hg abs.}$$

relative total temperature $$T_{T_2} = \frac{T_{s_2}}{\left(T_{s/T_T}\right)_2} = 705.6°R$$

relative angle $$2 = \tan^{-1} \frac{V_{ax_2}}{V_{tan_2}} = 69.92°$$

annulus area $$A_{ann_2} = A_{ann_1} = 5.531 \text{ sq in.}$$

flow area $$A_{flow_2} = A_{ann_2} \times \cos \alpha_2 = 1.899 \text{ sq in.}$$

(C) The total pressure loss in the rotor blade passage is accounted for by utilizing the recovery curve (Figure 33) and a streamtube factor (1.0 for the mean streamtube):

$$\text{Recovery} = 0.87 \text{ (at } M_2 = 1.518) \times 1.0 = 0.87$$

(C) As in the case of the solution at the station upstream of the rotor, the solution for the conditions at the exit station of the rotor is an iteration process. Continuity, radial equilibrium, energy, and desired pressure ratio must all be satisfied. The mean diameter for the streamtube is a function of the solution. The resultant diameter is 5.418 inches and enters into establishing the wheel section speed and the energy change due to radial displacement within the rotor for the streamtube.

$$U_3 = \frac{D_{m3} \quad N}{720} = 1,170 \text{ ft/sec}$$

(C) The relative total temperature change in the rotor is computed by

$$\Delta T_T = \frac{U_3^2 - U_2^2}{2gJ\ Cp} = -5.1°R$$

and $$T_{T_3} = T_{T_2} + \Delta T_T = 705.6 - 5.1 = 700.5°R$$

The relative total pressure at the rotor exit is computed by

$$P_{T_3} = P_{T_2} \times \text{Recovery} \left(\frac{T_{T3}}{T_{T2}}\right)^{\gamma/\gamma-1} = 86.33 \times .87 \times \left(\frac{700.5}{705.6}\right)^{3.5}$$

$$= 73.23 \text{ in. Hg abs.}$$

(C) The rotor exit flow area is established by assuming values in the iteration process. $A_{flow_3}$ = 2.11 square inches.

By continuity $$A/A^*_3 = \frac{K\, P_{T_3}\, A_{flow_3}}{W\sqrt{T_{T_3}}} = 1.124$$

(C) The static pressure is assumed to be high enough that this represents a subsonic A/A*, and the corresponding parameters are

$$M_3 = .662$$

$$\left(P_s/P_T\right)_3 = .745$$

$$\left(T_s/T_T\right)_3 = .919$$

(C) Therefore, $$P_{s_3} = P_{T_3}\left(P_s/P_T\right)_3 = 54.55 \text{ in. Hg abs.}$$

$$T_{s_3} = T_{T_3}\left(T_s/T_T\right)_3 = 644\ ^\circ R$$

$$a_3 = \sqrt{\gamma g R t_{s_3}} = 1{,}242 \text{ ft/sec}$$

$$V_3 = M_3 \times a_3 = 824.6 \text{ ft/sec}$$

(C) The relative exit tangential air angle is also established by the iteration process. When the streamtube slopes conically at an angle to the machine axis ($\epsilon$), the relationship between the annulus area and flow area is

$$A_{flow} = A_{ann} \cos \alpha \cos \epsilon$$

(C) For the mean streamtube, the cos $\epsilon$ is small enough to neglect.

$$\cos \alpha_3 = \frac{A_{flow_3}}{A_{ann_3}} = \frac{2.11}{2.42}$$

$$\alpha_3 = 29.27$$

(C) The relative tangential and axial component velocities at the rotor exit are

$$V_{tan_3} = V_3 \cos \alpha_3 = 719.3 \text{ ft/sec}$$

$$V_{ax_3} = V_3 \sin \alpha_3 = 403.2 \text{ ft/sec}$$

(C) The absolute rotor exit conditions are calculated by first computing the absolute tangential velocity component:

$$V_{tan_4} = U_3 - V_{tan_3} = 766.8 \text{ ft/sec}$$

$$V_{ax_4} = V_{ax_3} = 403.2 \text{ ft/sec}$$

(C) The absolute velocity at the rotor exit is

$$V_4 = \sqrt{V^2_{ax_4} + V^2_{tan_4}} = 1051.3 \text{ ft/sec}$$

(C) The acoustic velocity is $a_4 = a_3 = 1,242$ ft/sec

(C) The absolute Mach number is $M_4 = \frac{V_4}{a_4} = 0.845$

(C) The corresponding parameters are

$$\left(A/A^*\right)_4 = 1.022$$

$$\left(P_s/P_T\right)_4 = 0.627$$

$$\left(T_s/T_T\right)_4 = 0.875$$

$$P_{s_4} = P_{s_3} = 54.55 \text{ in. Hg abs.} \qquad T_{s_4} = T_{s_3} = 644°R$$

(C) The exit absolute total pressure and temperature are therefore

$$T_{T_4} = \frac{T_{s_4}}{T_{s_4}/T_{T_4}} = 735.9°R$$

$$P_{T_4} = \frac{P_{s_4}}{P_{s_4}/P_{T_4}} = 87.00 \text{ in. Hg abs.}$$

(C) The absolute tangential angle at the rotor exit is

$$\alpha_4 = \tan^{-1}\frac{V_{tan_4}}{V_{ax_4}} = 46.83°$$

(C) A 3 percent total pressure loss is estimated through the exit stators and interconnecting duct, and the total pressure at the axial stage exit (entrance to the centrifugal stage) is

$$P_{T_5} = P_{T_4} \times 0.97 = 84.39 \text{ in. Hg abs.}$$

(C) The total temperature at the axial stage exit (entrance to the centrifugal stage) is

$$T_{T_5} = T_{T_4} = 735.9°R$$

(C) The stage streamtube pressure ratio is

$$\frac{P_{T_5}}{P_{T_{amb}}} = \frac{84.39}{29.92} = 2.82:1$$

(C) The stage streamtube adiabatic efficiency is

$$\eta = \frac{T_{T_o}\left(1 + \frac{P_{T_5}}{P_{T_{amb}}}\right)}{T_{T_5} - T_{T_o}} \times 100 = 82.2 \text{ percent}$$

(C) Mechanical Design (U)

The mechanical design of the compressor components, including inlet guide vanes, compressor rotor, exit guide vanes, and interconnecting duct, is discussed in the following section.

Inlet Guide Vanes - The inlet guide vanes have been designed for an NACA 65 series airfoil thickness distribution with a circular arc mean camber line. The airfoils are stacked with the center of gravity along a radial line. A cantilever support from the O.D. is used which is adjustable for blade angle. AMS 5655 is the material specified for these blades.

Rotor - The rotor blade airfoil sections are generated rather than using one of the standard NACA series. The following method is used to generate the airfoils. The aerodynamic considerations define the mean camber angles and wedge angles for the leading and trailing edges, a reference solidity, the number of blades, and the leading and trailing edge thicknesses (Table VI). With these inputs, a preliminary choice of blade chord length and number of blades is made. A first-order estimate of the root section pure tensile load per unit area (P/A) stress is then performed to determine feasibility. If the stress appears reasonable, the design can then proceed. A single section near the hub is selected for the starting section. The inlet and

TABLE VI. (C) AERODYNAMIC DESIGN DATA FOR 2.8:1 SUPERSONIC COMPRESSOR (U)

| | HUB | MEAN | TIP | OVERALL |
|---|---|---|---|---|
| $\alpha_o$ | 0° | 0° | 0° | |
| $\alpha_1$ | 35.32° | 31.25° | 29.02° | |
| $\delta_1$ | 7.0° | 6.0° | 5.7° | |
| $\alpha_2$ | 68.95° | 69.92° | 71.38° | |
| $i_2$ | 3.12° | 2.95° | 3.20° | |
| $\alpha_3$ | 23.55° | 29.28° | 35.88° | |
| $\delta_3$ | 4.75° | 5.8° | 6.0° | |
| $\alpha_4$ | 43.32° | 46.83° | 48.88° | |
| $\alpha_5$ | 0° | 0° | 0° | |
| $A_{ann_1}$ in.$^2$ | 5.4387 | 5.5313 | 5.5789 | 16.549 |
| $O.D._1$ in. | 5.0828 | 5.7339 | 6.3182 | 6.3182 |
| $I.D._1$ in. | 4.3350 | 5.0828 | 5.7339 | 4.3350 |
| $D_{m_1}$ in. | 4.7237 | 5.4180 | 6.0331 | |
| $O.D._3$ in. | 5.1518 | 5.4447 | 5.7428 | 5.7428 |
| $I.D._3$ in. | 4.8715 | 5.1518 | 5.4447 | 4.8715 |
| $D_{m_3}$ in. | 5.0136 | 5.3003 | 5.5958 | 5.3003 |
| $A_{ann_3}$ in.$^2$ | 2.2069 | 2.4374 | 2.6195 | 7.2638 |

$\beta$ = mean camber angle = average metal angle

$\beta_2 = \alpha_2 - i_2$

$\beta_3 = \alpha_3 - \delta_3$

$\beta_1 = \alpha_1 + \delta_1$

$\beta_o = 0°$

$\beta_4 = \alpha_4$

$\beta_5 = \alpha_5 = 0°$

Minimum length of 4° wedge @ rotor leading edge = .25"
.0035" maximum leading edge radius - rotor
.010" maximum trailing edge radius - rotor
Use 10° trailing edge wedge angle
Number of blades - 26
Tip solidity - 2.5

outlet of the line are drawn such that they intersect near mid-chord. A circle equal to the desired maximum thickness of the section is drawn at this mid-chord point. A 4-degree wedge about the inlet mean camber line is constructed, while a 10-degree wedge is used at the outlet. A smooth curve is constructed tangent to the inlet wedge, the outlet wedge, and the maximum thickness circle. This construction is shown in Figure 37, Section C. An end view (parallel to compressor axis) of the mean camber line of this section is then drawn. This will appear as an arc of a circle, since these generating sections lie on cylinders by definition. The section center of gravity is located on this arc, and a normal line to the tangent at this point provides the radial direction. The radial distance of this section is laid off on this line to locate the compressor axis. A series of radial lines is then drawn for use in generating mean camber lines at various radii. These mean camber lines now represent true radial elements about the rotor axis. Figure 40 shows these radial element camber lines. Cylindrical airfoil sections at each selected radius can now be generated. The inlet and outlet mean camber angle from the aerodynamic input is now matched with the radial element camber line. An exact match can always be obtained but may not always be desirable. An exact match could result in extremes of leading or trailing edge sweep or too short a chord. A compromise is often in order. Sections D and E of Figure 37 are typical of the degree of compromise accepted. Coordinate dimensions of these cylindrical airfoil sections are then used as inputs to a computer program which transposes these sections into so-called manufacturing sections. These manufacturing sections are in planes parallel to the rotor centerline. The computer program also determines the section properties. Figure 41 is a typical output of the computer for one section.

(C) The section properties along with the blade loading are combined to establish the stresses. Figure 42 is a plot of the combined blade stresses for design point loading. The maximum stress is slightly over 48,000 pounds per square inch (psi) for the SSC (2.8). A modified Goodman diagram, Figure 43, shows an allowable vibratory stress of 50,000 psi. Since an allowable vibratory margin of 30,000 psi is considered to be satisfactory, the blade stresses are acceptable.

(C) A frequency analysis of the blade element was conducted, with the results as shown in Figure 44. This analysis includes the fundamental bending and torsional natural frequencies of the blade as a function of speed. The frequencies which are associated with most significant excitation forces are also shown as a function of speed. These are 1st and 2nd engine order (EO) frequencies, the 6th engine order frequency corresponding to the six inlet struts and the 28th engine order corresponding to the 28 inlet guide vanes. The blade is acceptable for steady-state operation at any speed except for the interference at or near 28,000 RPM and 39,000 RPM. Interferences of the 28th engine order excitation occur with the blade torsional first mode frequency at 28,000 RPM and the first mode bending frequency at 39,000 RPM. These excitation forces are relatively small, and there has been no evidence of blade flutter in the testing of the SSC (2.0). However, caution will be exercised during initial testing, and prolonged operation at these speeds will be avoided.

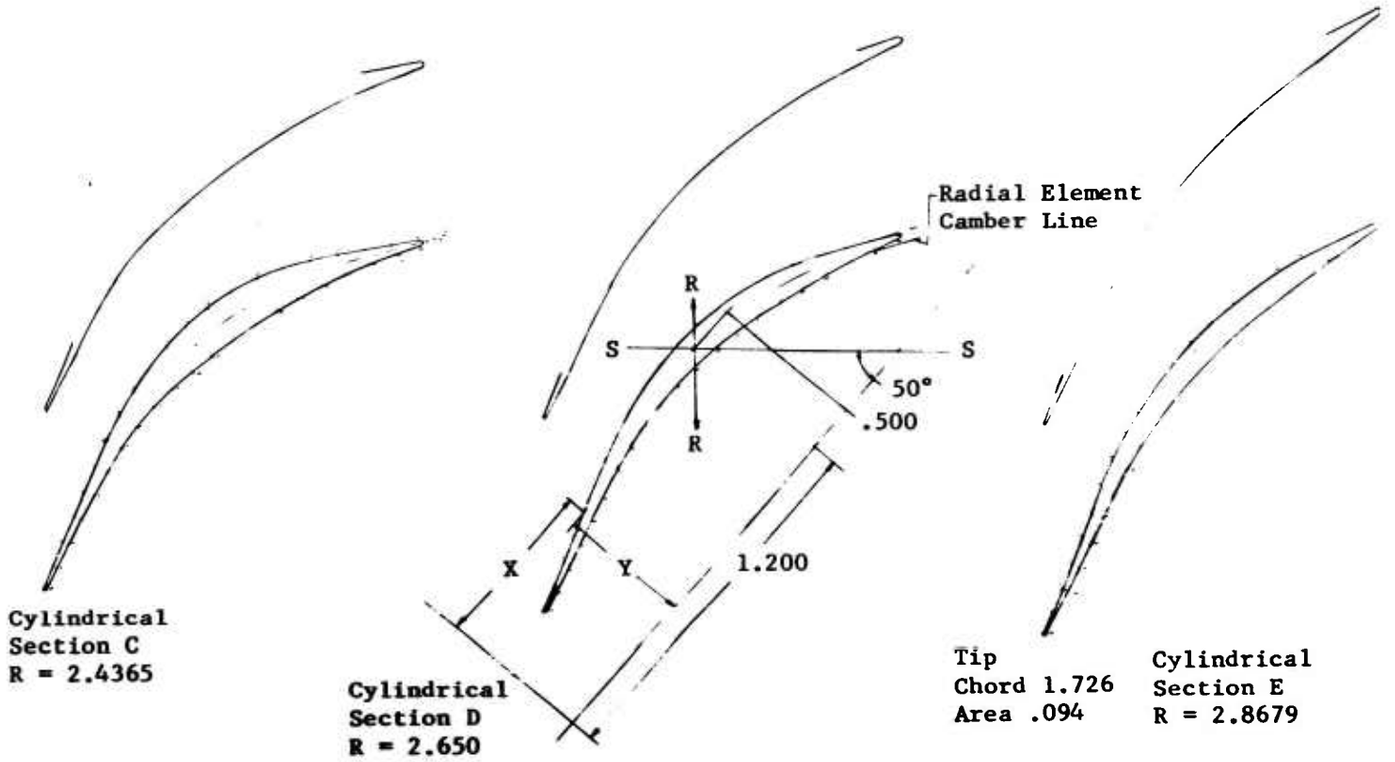


**Figure 37. (U) Airfoil Sections 2.8:1 Supersonic Compressor Rotor.**

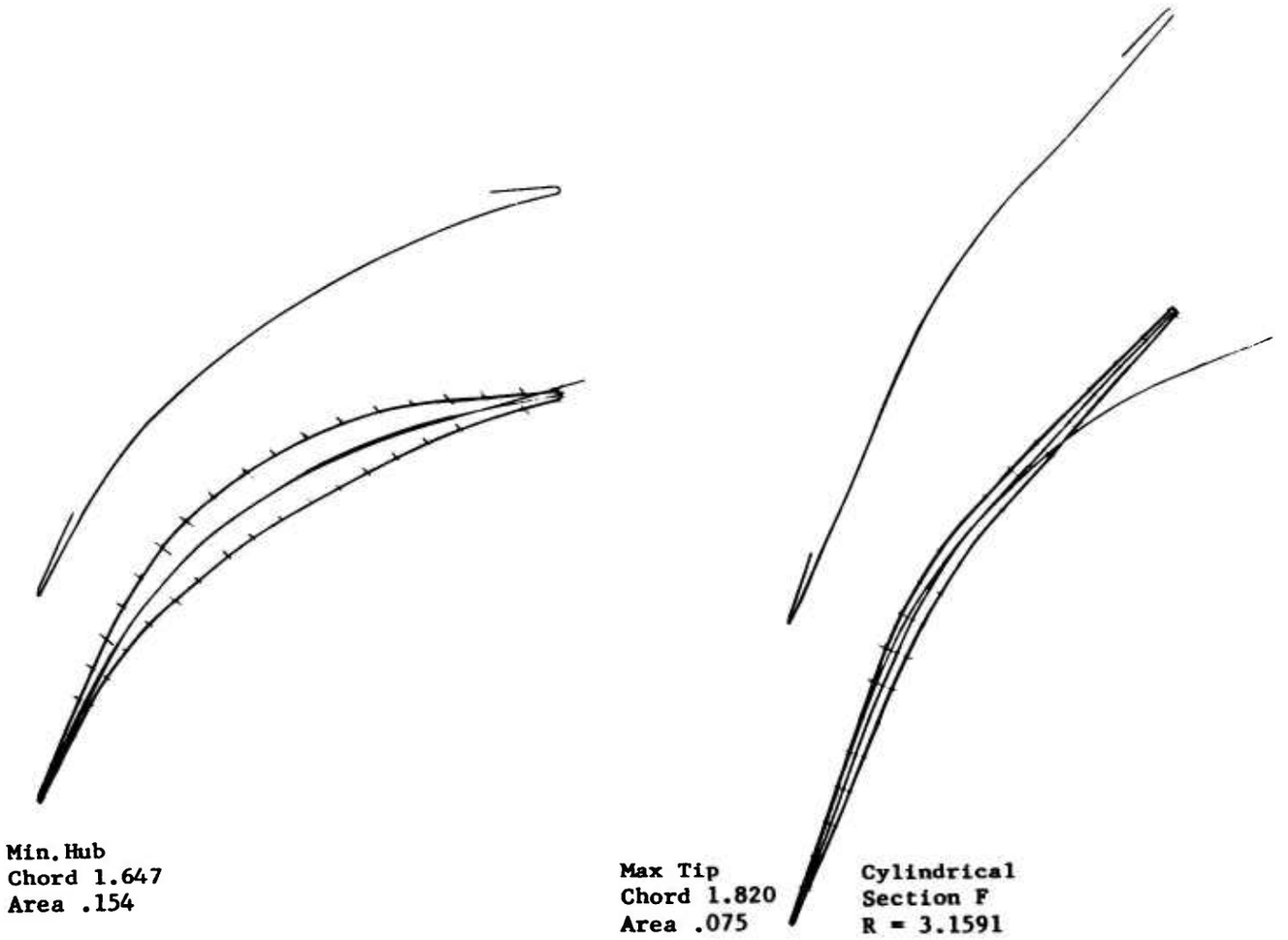


Figure 38. (U) Airfoil Sections 2.8:1 Supersonic Compressor R[illegible]

Figure 39. (U) Airfoil Sections 2.8:1 Supersonic Compressor Rotor.

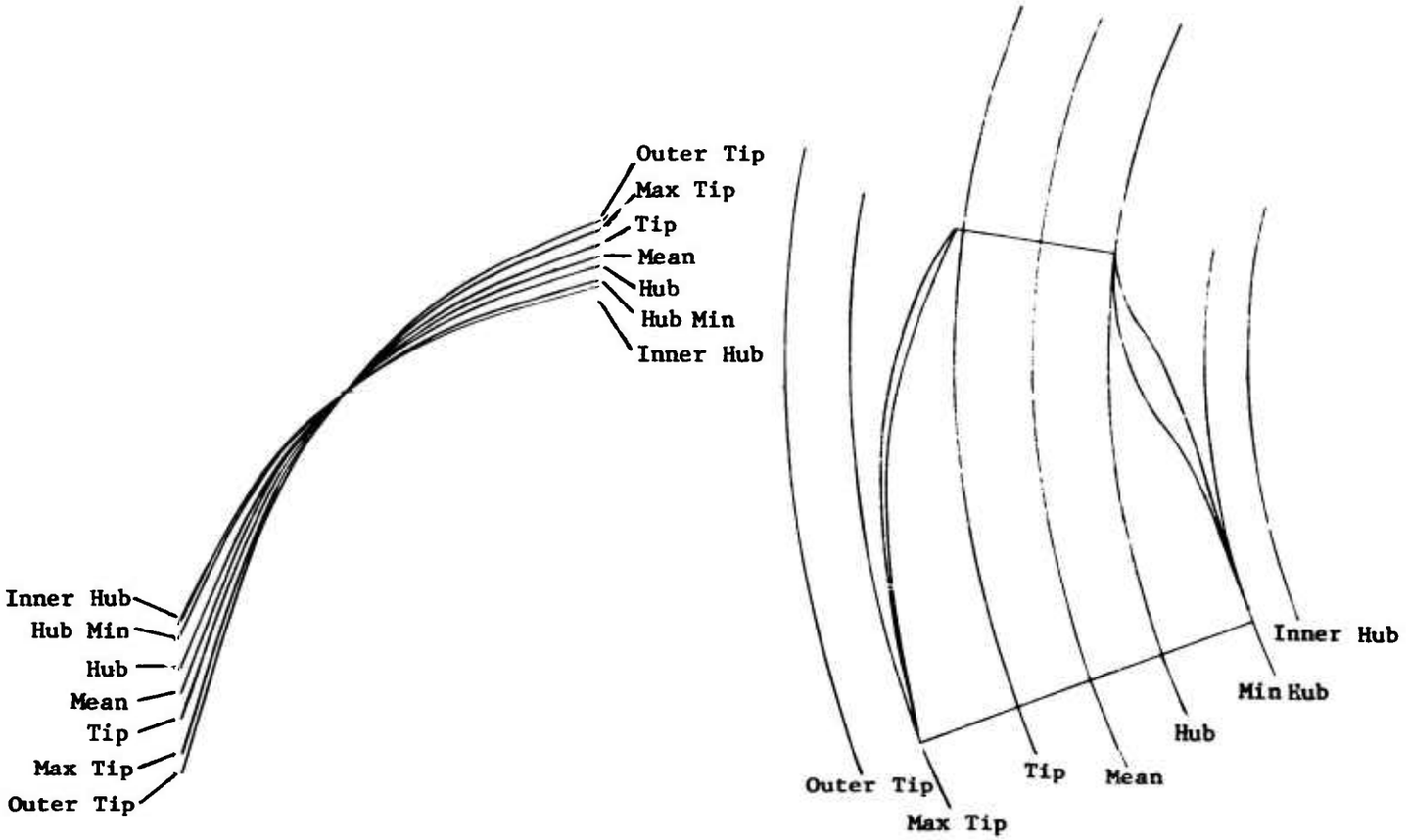


Figure 40. (U) Radial Element Camber Lines 2.8:1 Supersonic Compressor Rotor.

Output Data Outer Tip Section — Radius Equals 3.3421

| X Bar | Y Bar | Theta | I Max | I Min | Area |
|---|---|---|---|---|---|
| 0.115732E 01 | 0.492100E-00 | 0.274249E 03 | 0.810364E-02 | -0.119579E-03 | 0.723802E-01 |
| X | Y | C wk | C str | | |
| -0.154594E-01 | 0.487865E-01 | -0.120240E 01 | 0.355209E-00 | | |
| 0.161065E-01 | 0.395115E-01 | -0.117161E 01 | 0.366797E-00 | | |
| -0.119192E-00 | 0.573258E-01 | -0.130921E 01 | 0.339008E-00 | | |
| 0.327023E-01 | 0.139589E-00 | -0.114764E 01 | 0.268224E-00 | | |
| 0.186594E-00 | 0.221679E-00 | -0.988092E 00 | 0.197761E-00 | | |
| 0.313174E-00 | 0.281197E-00 | -0.857451E 00 | 0.147784E-00 | | |
| 0.442096E-00 | 0.335455E-00 | -0.724863E 00 | 0.103227E-00 | | |
| 0.545172E 00 | 0.382521E-00 | -0.618583E 00 | 0.639259E-01 | | |
| 0.648854E 00 | 0.423110E-00 | -0.512180E 00 | 0.311306E-01 | | |
| 0.749303E 00 | 0.452774E-00 | -0.409809E-00 | 0.899003E-02 | | |
| 0.848554E 00 | 0.479378E-00 | -0.308860E-00 | -0.101885E-01 | | |
| 0.945735E 00 | 0.502552E 00 | -0.210230E-00 | -0.260990E-01 | | |
| 0.104112E 01 | 0.520359E 00 | -0.113783E-00 | -0.367899E-01 | | |
| 0.114000E 01 | 0.534032E 00 | -0.141641E-01 | -0.430998E-01 | | |
| 0.123489E 01 | 0.542920E 00 | 0.811238E-01 | -0.449338E-01 | | |
| 0.133033E 01 | 0.546946E 00 | 0.176600E-00 | -0.418772E-01 | | |
| 0.142570E 01 | 0.552219E 00 | 0.272092E-00 | -0.400714E-01 | | |
| 0.152163E 01 | 0.558502E 00 | 0.368226E-00 | -0.392294E-01 | | |
| 0.161747E 01 | 0.564386E 00 | 0.464241E-00 | -0.379964E-01 | | |
| 0.171387E 01 | 0.575259E 00 | 0.561184E 00 | -0.416973E-01 | | |
| 0.181568E 01 | 0.587349E 00 | 0.663604E 00 | -0.462119E-01 | | |
| 0.191018E 01 | 0.598559E 00 | 0.758678E 00 | -0.503896E-01 | | |
| 0.192258E 01 | 0.590993E 00 | 0.770482E 00 | -0.419262E-01 | | |
| 0.192258E 01 | 0.590993E 00 | 0.770482E 00 | -0.419262E-01 | | |
| 0.190927E 01 | 0.572254E 00 | 0.755825E 00 | -0.242246E-01 | | |
| 0.181260E 01 | 0.550828E 00 | 0.657834E 00 | -0.100193E-01 | | |
| 0.171504E 01 | 0.535225E 00 | 0.559379E 00 | -0.168717E-02 | | |
| 0.161919E 01 | 0.523765E 00 | 0.462948E-00 | 0.264050E-02 | | |
| 0.152472E 01 | 0.512621E 00 | 0.367906E-00 | 0.675432E-02 | | |
| 0.143051E 01 | 0.504441E 00 | 0.273354E-00 | 0.793299E-02 | | |
| 0.133357E 01 | 0.497068E-00 | 0.176130E-00 | 0.810257E-02 | | |
| 0.123897E 01 | 0.488094E-00 | 0.811315E-01 | 0.100448E-01 | | |
| 0.114475E 01 | 0.480719E-00 | -0.133792E-01 | 0.104184E-01 | | |
| 0.105018E 01 | 0.466736E-00 | -0.108729E-00 | 0.173565E-01 | | |
| 0.955688E 00 | 0.450276E-00 | -0.204177E-00 | 0.267712E-01 | | |
| 0.858905E 00 | 0.427174E-00 | -0.302405E-00 | 0.426392E-01 | | |
| 0.759736E 00 | 0.398916E-00 | -0.403395E-00 | 0.634721E-01 | | |
| 0.659189E 00 | 0.367222E-00 | -0.506014E 00 | 0.876307E-01 | | |
| 0.556680E 00 | 0.335324E-00 | -0.610604E 00 | 0.111846E-00 | | |
| 0.450399E-00 | 0.297786E-00 | -0.719374E 00 | 0.141407E-00 | | |
| 0.324520E-00 | 0.253598E-00 | -0.848181E 00 | 0.176148E-00 | | |
| 0.178315E-00 | 0.230881E-00 | -0.995667E 00 | 0.187971E-00 | | |
| 0.130724E-01 | 0.149025E-00 | -0.116652E 01 | 0.257360E-00 | | |
| -0.163493E-00 | 0.909417E-01 | -0.134690E 01 | 0.302202E-00 | | |
| 0.830196E-02 | 0.5022503-01 | -0.117860E 01 | 0.355535E-00 | | |
| -0.154594E-01 | 0.487865E-01 | -0.120240E 01 | 0.355209E-00 | | |

Figure 41. (U) Sample Computer Data - Blade Coordinates and Section Properties.

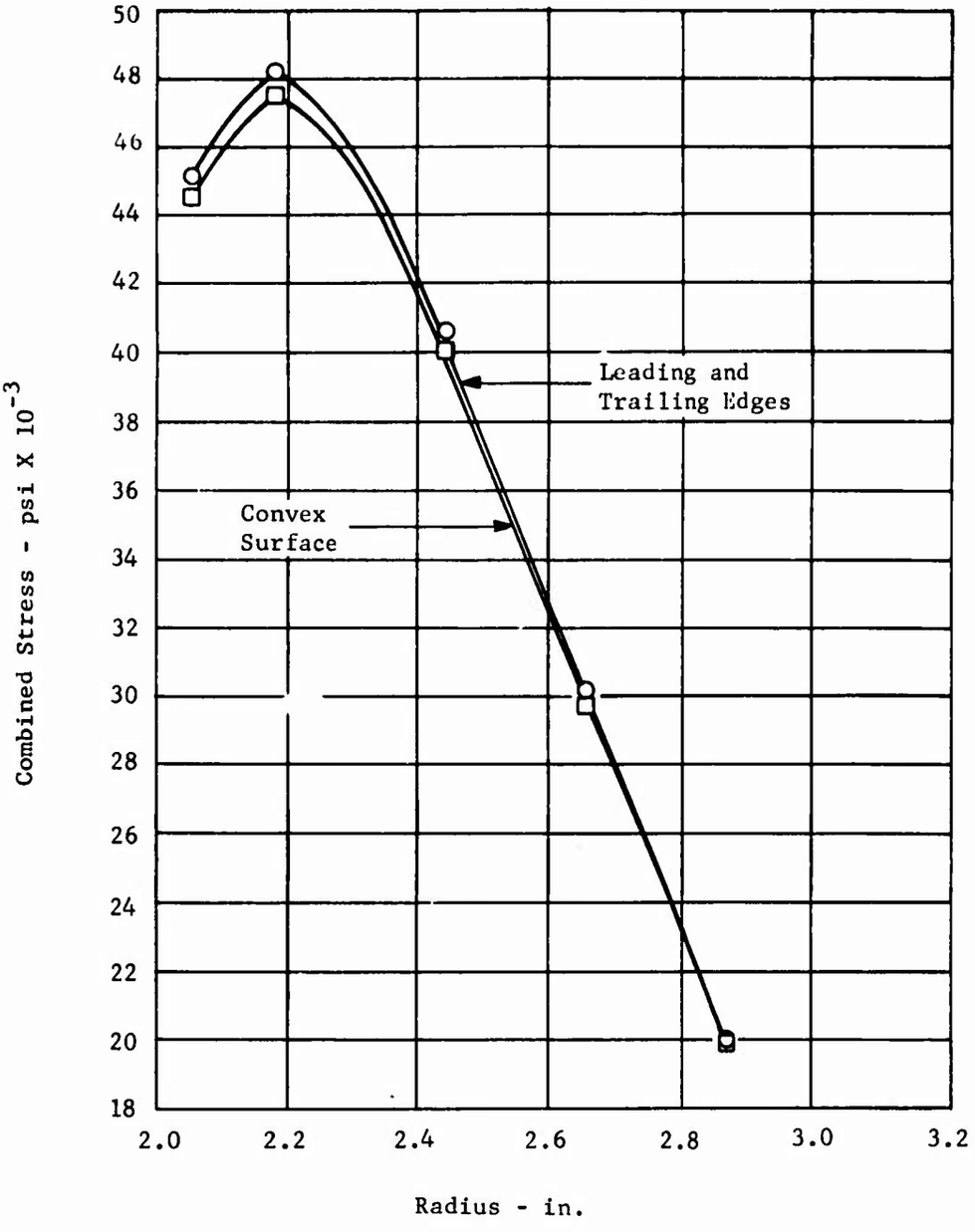


Figure 42. (U) 2.8:1 Supersonic Compressor - Rotor Blade Stresses.

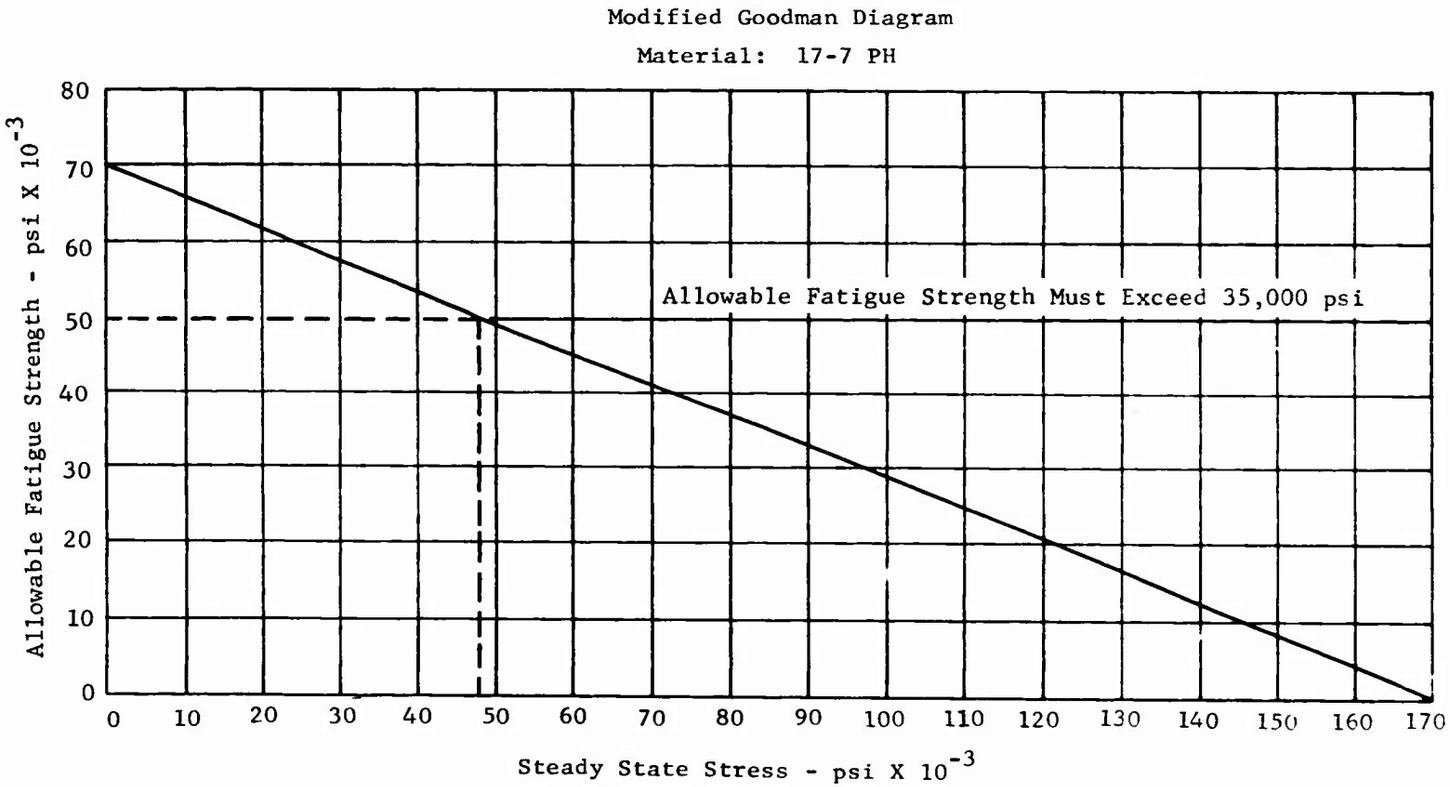


Figure 43. (U) 2.8:1 Supersonic Compressor Rig - Rotor Blade Fatigue Strength Analysis.

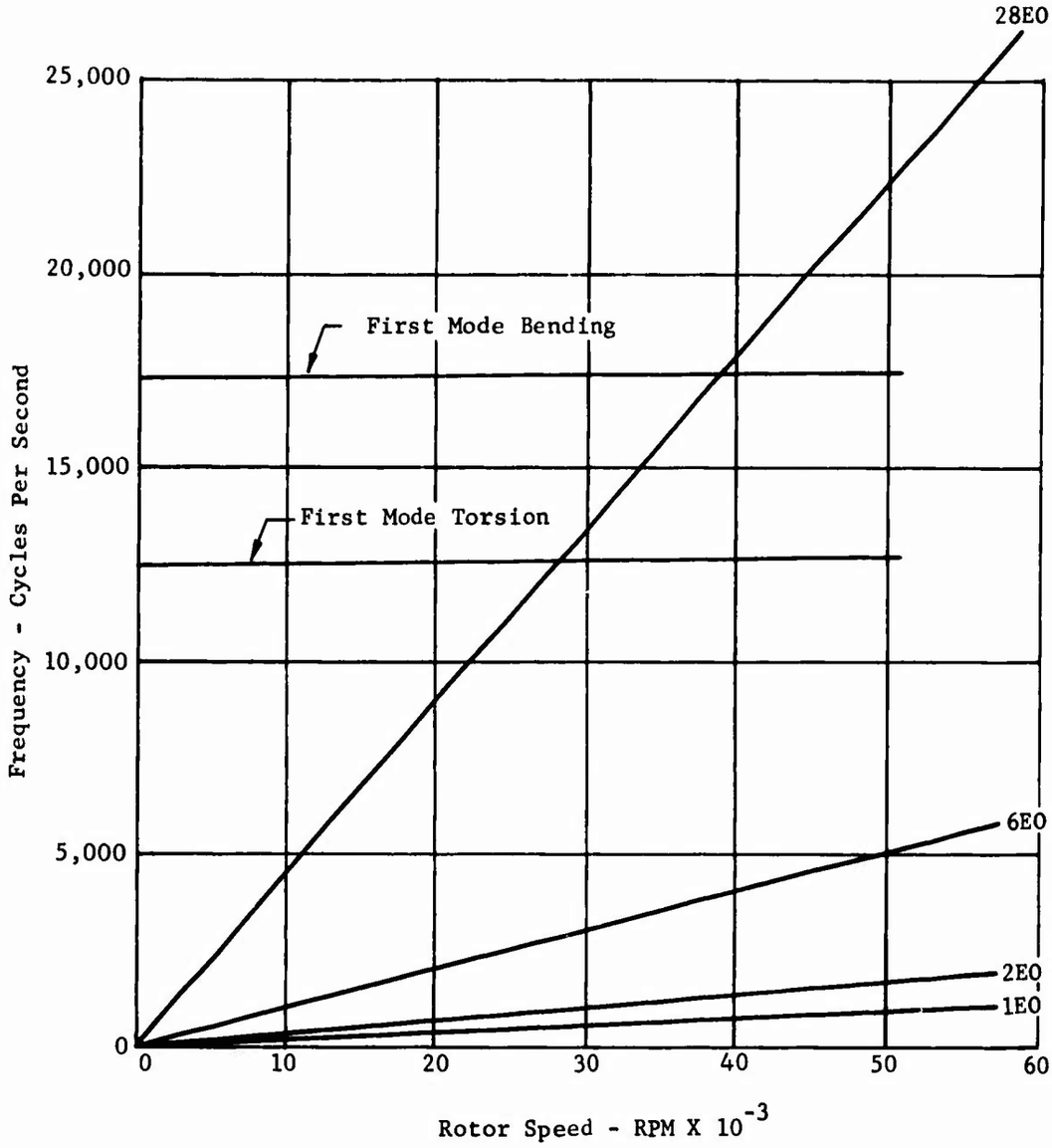


Figure 44. (U) 2.8:1 Supersonic Compressor Rotor Blade - Interference Diagram.

(C) A stress analysis of the rotor disc was conducted with the results as shown in Figure 45. A maximum stress of 104,000 psi occurs at the bore with a conservative estimate of the radial rim stress. This value is well within the limits of the material, which has a yield strength of 140,000 psi.

(C) Exit Stator and Interconnecting Duct - A preliminary design of the exit stator and interconnecting passage of the compressor is shown on Figure 46. It is the arrangement depicted above the center line. With some rework, this configuration is interchangeable with the scheme shown below the center line. The stator vanes of this design are integral with an inner shroud ring and will be fully machined from a solid section. A single-piece outer shroud ring will be machined to match the contour of the O.D. of the stator vanes with only a few thousandths of an inch radial gap. The stator vanes will then be brazed to this outer ring. Brazing of the stator vanes to the outer shroud ring accomplishes two things. First, it precludes stator tip losses; second, it restores stiffness to the rear bearing mount lost by having to remove material from the inner member of the plenum chamber. This bearing mount stiffness is of major concern, since it affects the critical speed of the rotor. The finalized design may entail the addition of structure to tie the inner member to the outer member. This additional structure, however, would be placed downstream of the interconnecting duct.

(C) DESIGN PERFORMANCE (U)

(C) The design conditions and vector diagrams for the 2.8:1 supersonic compressor rotor are presented in Figures 47 through 50. The design performance goals are:

| | IGV & Rotor | IGV & Rotor & Exit Stator |
|---|---|---|
| pressure ratio | 2.89:1 | 2.80 |
| adiabatic efficiency | 87.2 percent | 82.2 percent |
| airflow | 4.0 pounds per second | 4.0 pounds per second |
| design | 50,700 RPM | 50,700 RPM |

(C) The predicted compressor map for this stage is presented in Figure 3.

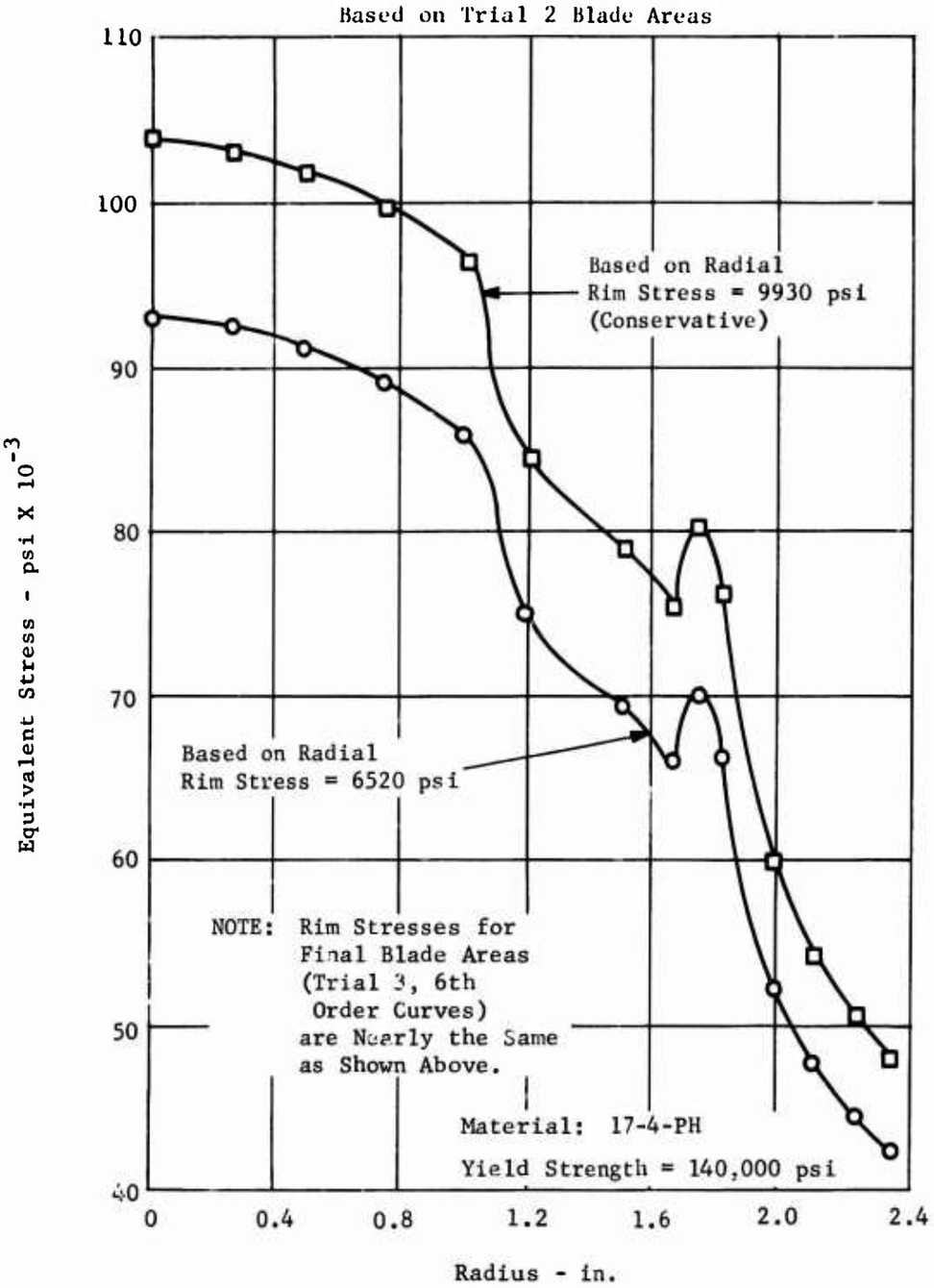


Figure 45. (U) 2.8:1 Supersonic Compressor - Rotor Disc Stresses.

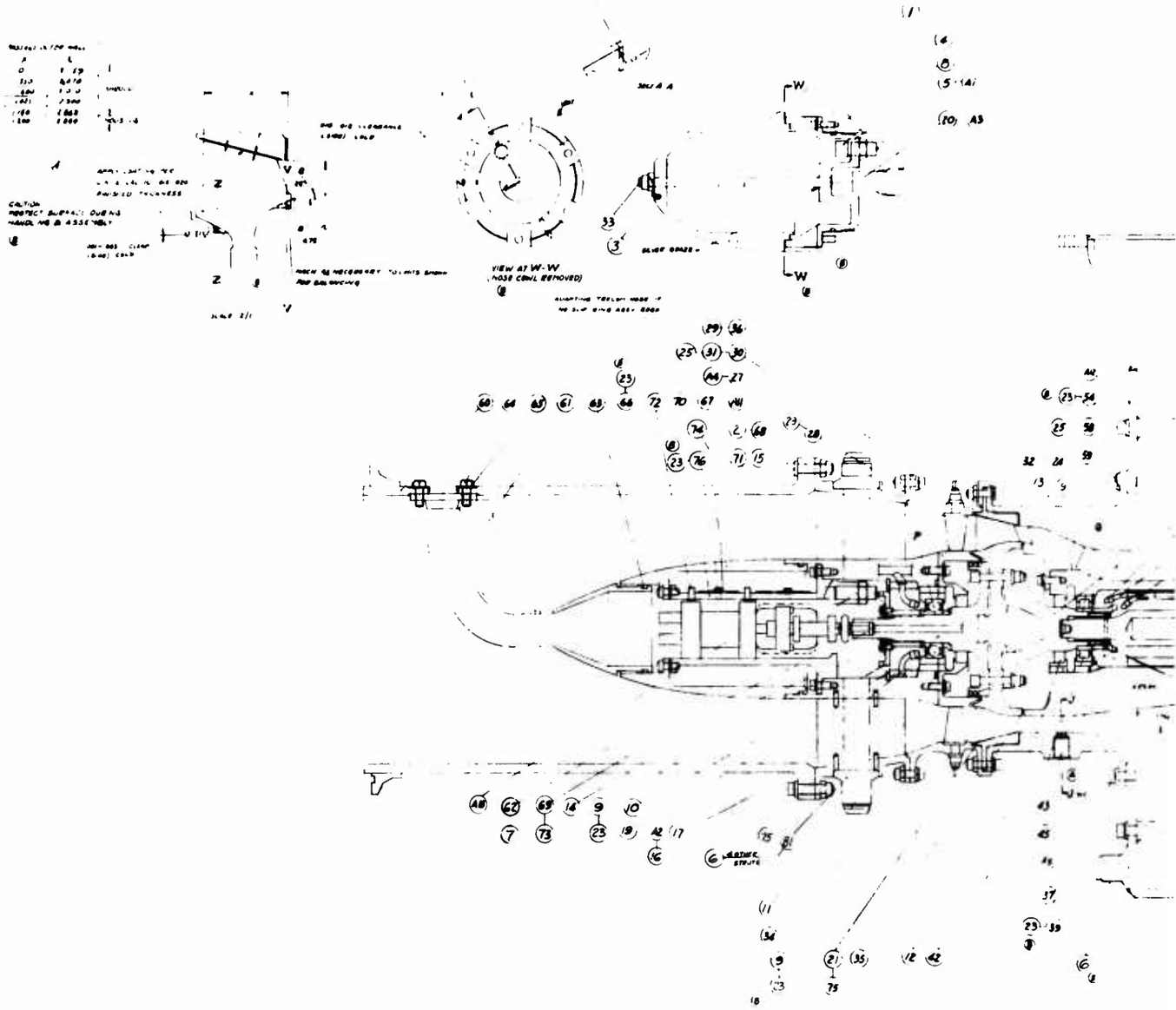

Figure 46. (U) Layout of 2.8:1 Supersonic Compressor and Test Ri

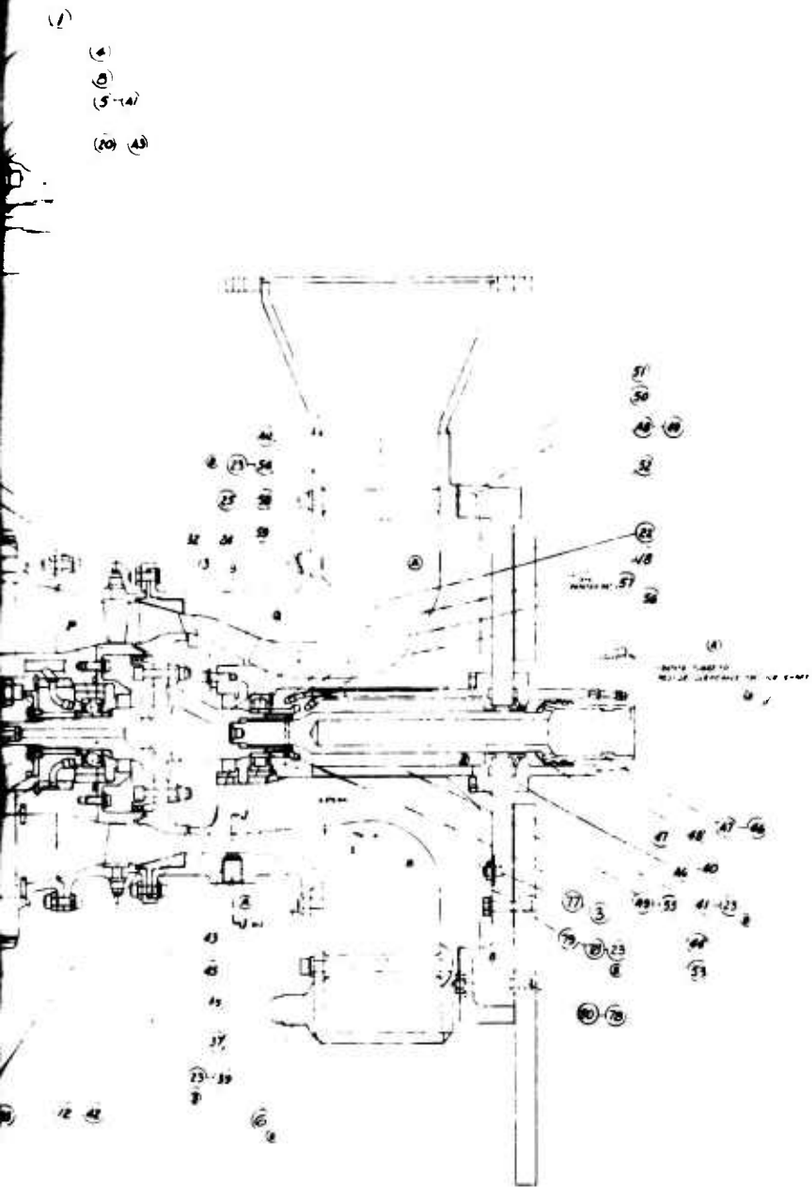

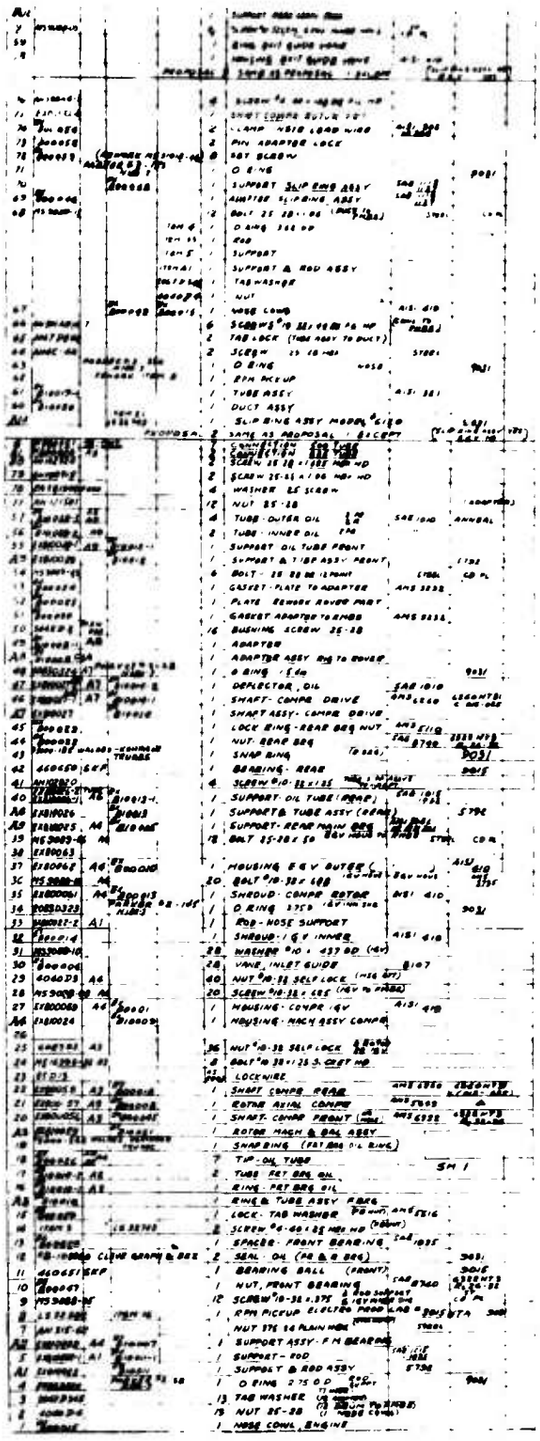

49 Pages

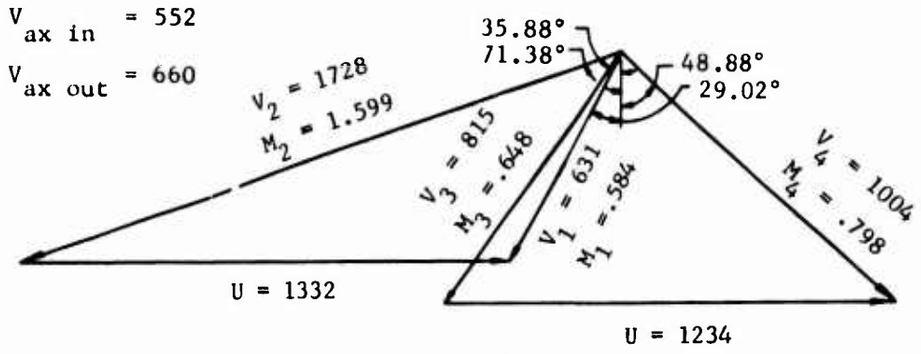


Tip Streamtube

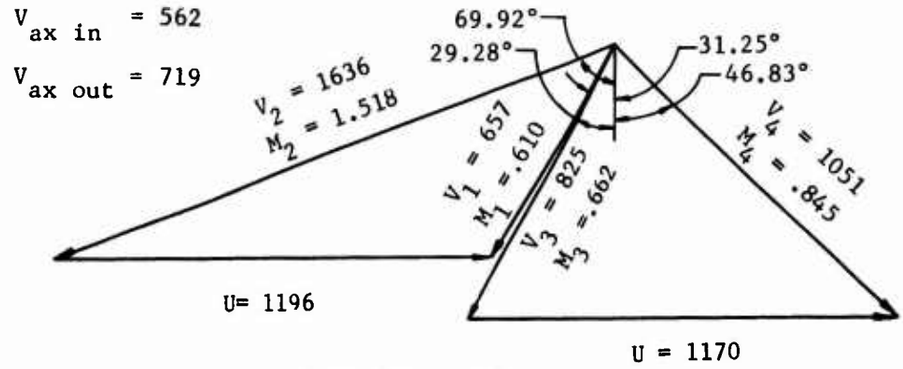


Mean Streamtube

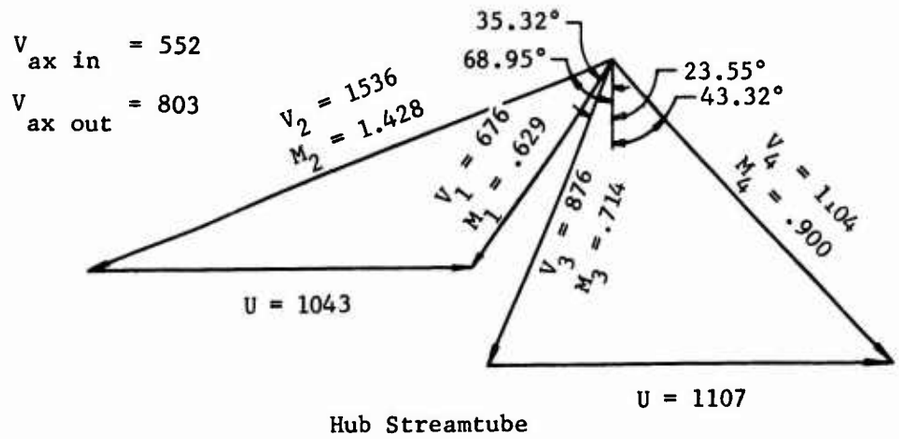


Hub Streamtube

Figure 47. (U) 2.8:1 Supersonic Compressor - Design Point Vector Diagram.

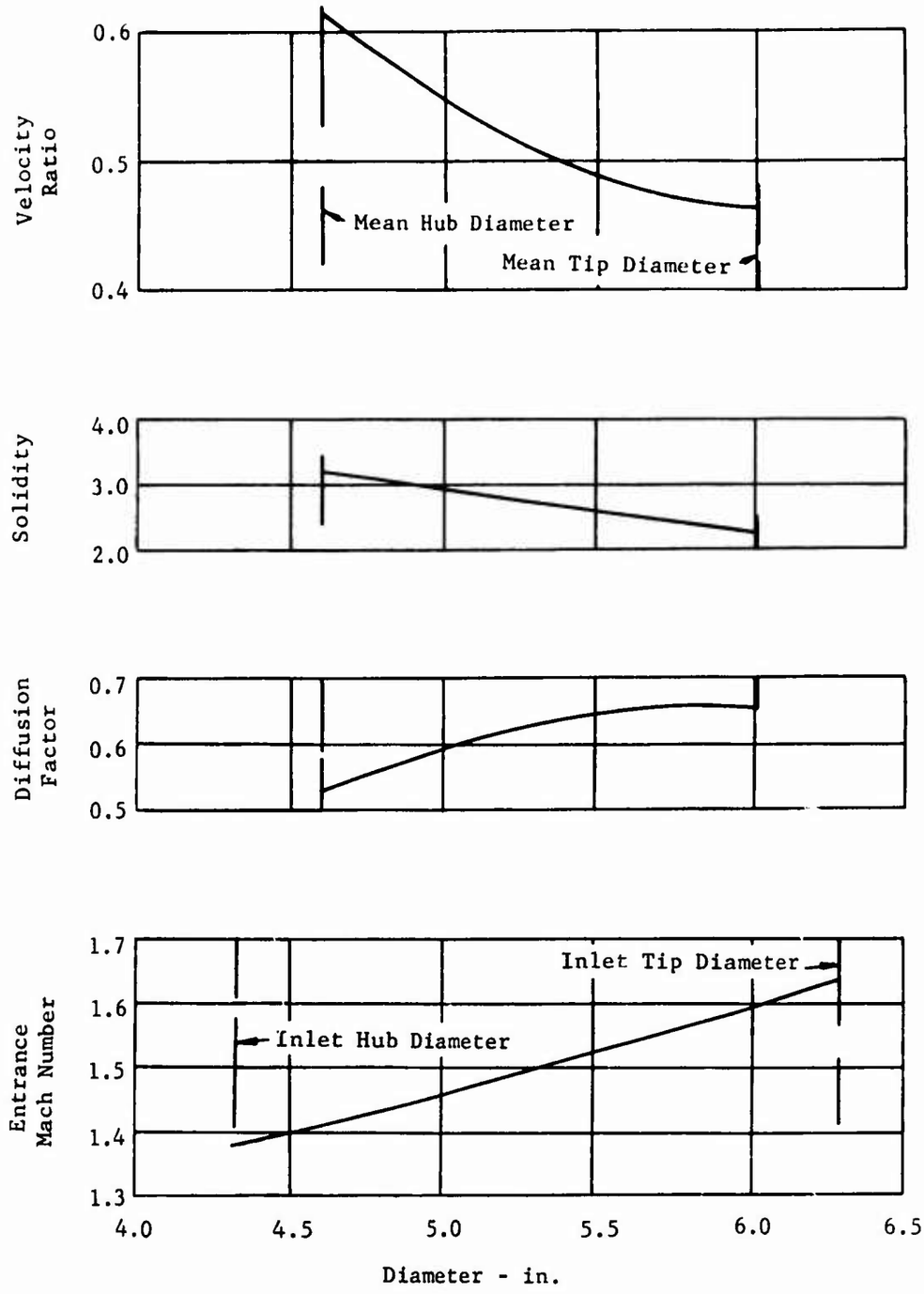


Figure 48. (U) 2.8:1 Supersonic Compressor Rotor Design Data.

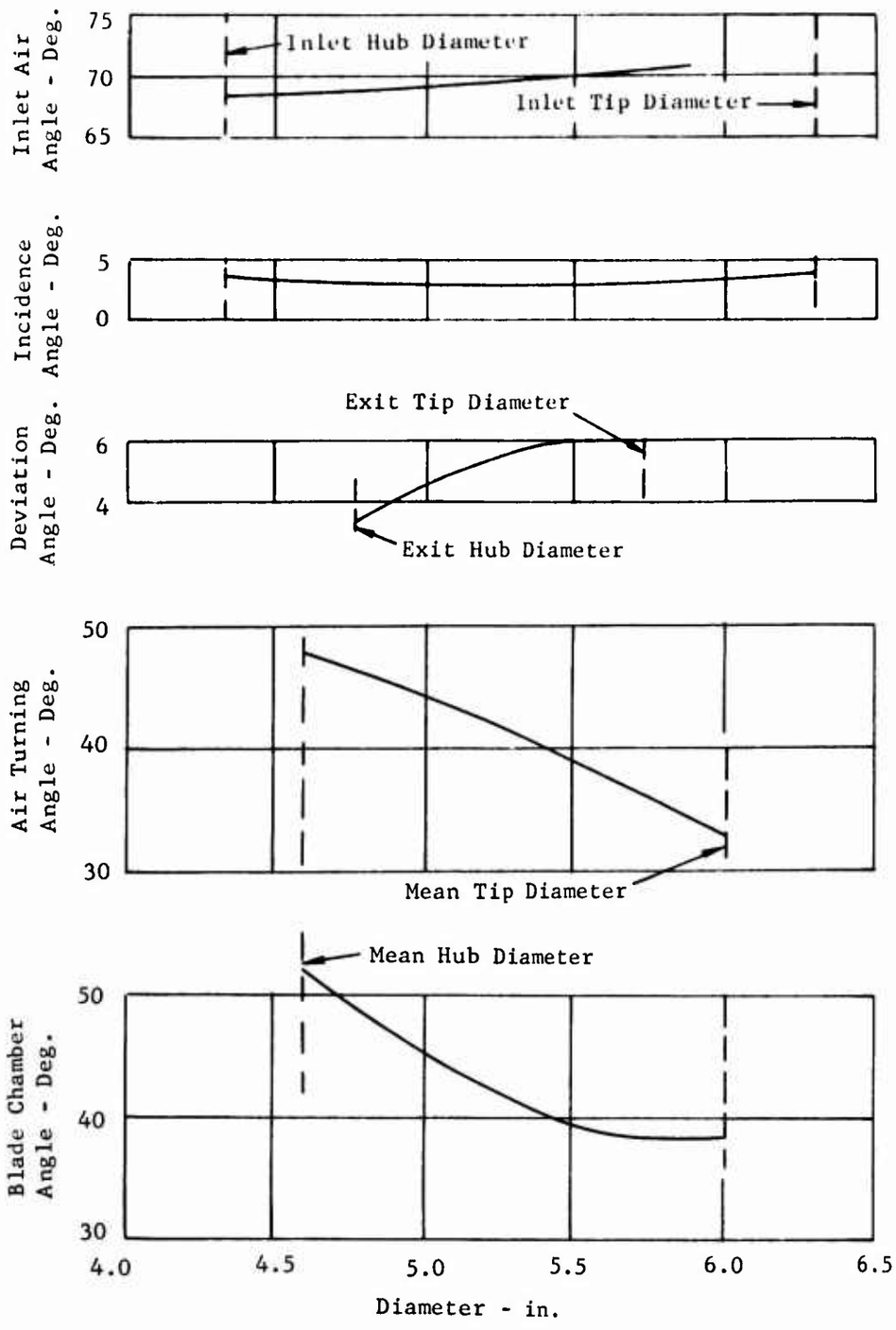


Figure 49. (U) 2.8:1 Supersonic Compressor Rotor Design Data.

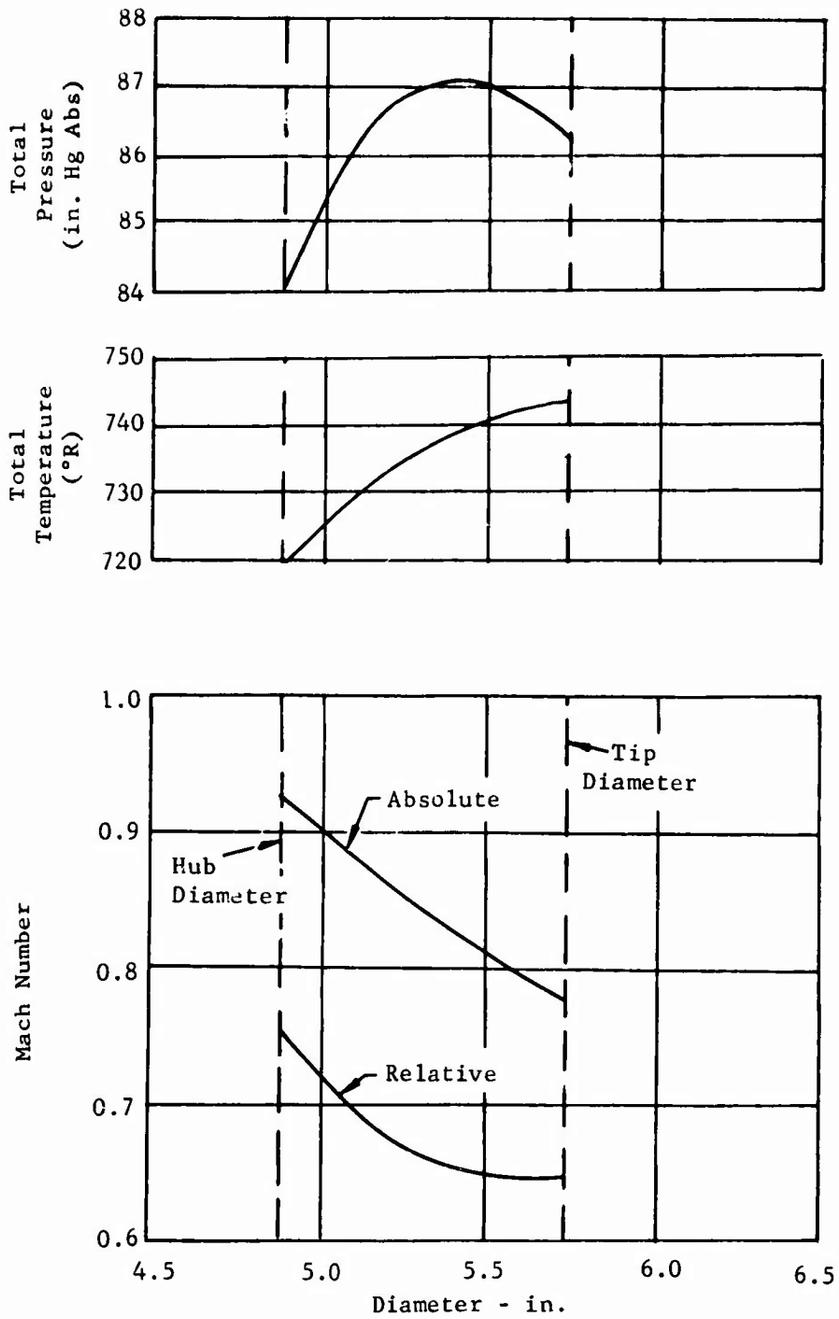


Figure 50. (U) 2.8:1 Supersonic Compressor Design Rotor Exit Conditions.

## (U) COMPRESSOR TEST RIG

The compressor test rig is composed of two major elements: the compressor unit and a steam driving turbine. The compressor unit section and the prime mover are completely independent assembly packages for maximum test efficiency and flexibility. The turbine drives the test compressor through a splined quill shaft.

### COMPRESSOR UNIT

The layout of the compressor unit of the test rig is shown on Figure 46. The test section is a self-contained unit. The compressor rotor is straddle mounted on rolling element bearings with the single-row ball thrust bearing at the front end. The axial stage rotor blades are machined integral with the disc from an AMS 5643 forging. This material can also be precision cast with essentially the same physical properties. An integrally cast rotor is envisioned for the production item, since low cost and simplicity are part of the desired goals. The front and rear stub shafts are bolted to the rotor disc by means of a common bolting joint. The shafts were not made integral with the disc to minimize hardware costs for the number of rotors to be evaluated. For weight considerations, an engine design would have integral shafting.

The thrust bearing is located in a six-strut fabricated inlet housing. The six struts of the housing are doweled to the inner and outer housings and brazed. Pressure and scavenge oil for the front bearing pass through the struts. One strut is used to vent the bearing scavenging cavity, and the remaining three struts supply pressure air to the bearing oil seal. The thrust bearing is lubricated by two separate jets 180 degrees apart. Bearing cavities are provided on both sides of the bearing for proper oil scavenging. Lubrication and scavenging are provided from separate test stand oil systems. Thermocouples for monitoring bearing oil temperatures are included in the oil system. The thrust bearing oil seal, which normally would be subjected to the suction pressure ahead of the rotor, is slightly pressurized by means of an external air supply. A pre-grooved, rub-tolerant, labyrinth seal limits the flow of this external air into the compressor main stream. A conservative estimate of the L10 life of the thrust bearing was calculated to be 115 hours. This life is based on design point loading. The inner race retaining nut of the thrust bearing incorporates a face spline at the upstream end. The spline teeth provide a variable gap for a magnetic pickup and rotor speed determination. At this time, strain gages are not anticipated for stress monitoring. However, provisions in the inlet housing have been made to mount and drive a high-speed, water-cooled, slip ring assembly should strain gaging become necessary.

An analysis was conducted on the rig shafting in order to establish its critical speeds. The shaft was mathematically represented by the 21 point lumped parameter system shown in Figure 51. To simulate the spline connection between the compressor rotor and quill shaft, a hinge was introduced at Station 9. The fictitious values for $\Delta$ L and I introduced at this

point maintain a continuous shear and deflection while permitting a discontinuity in the moment and slope. The critical speeds of this system were predicted by computer LOG 115, which uses Prohl's Method. The critical speed is a function of the spring rates of both the front and rear bearing supports. During the final review of the test rig critical speed analysis, it was decided to increase the spring rate of the rear bearing support from $1.2 \times 10^6$ to $10^7$ pounds per inch. Although the calculations indicated a critical speed beyond the operating range, the results were considered to be too sensitive to a variation in the spring rate at its original level. The new spring rate approaches that of the rear bearing support in the currently operational supersonic compressor (SSC 2.0) test rig and thus approaches the same overall confidence level. The spring rate of the front bearing support is essentially the same as that of the SSC (2.0), which has encountered no evidence of critical speed problems in operation through 100 percent speed. The critical speed as a function of the total front support spring rate ($k_1$) is shown in Figure 52. The results indicate that by varying the thrust on the front bearing, the spring rate can be increased to a point such that the rig is operating well up on the flat plateau region of the critical speed curve.

An important feature of the compressor rig is the incorporation of adjustability for the inlet guide vanes. The method of construction permits manual resetting of blade angles during shutdown with disassembling the compressor. The blades are cantilever mounted in a separate housing, with blade orientation being established by machined flats on the external stems of the vanes. External nuts are utilized to secure the vanes in position in the casing.

The rotor radial tip clearance at design speed has been dimensionally set at .001 - .003 inch. This requires a cold setting clearance of .010 - .012 inch. This close running clearance is made possible as a result of the following factors:

1. All housings are assembled with interference fits at the pilots.
2. The bearing bores are machined with all the housings assembled.
3. The rotor is axially positioned to obtain the .010 - .012 inch cold clearance by means of a selective spacer.
4. A separate rotor shroud is lined with an abradable aluminum graphite matrix.

The rear bearing support is a fabricated structure and serves as the collector housing for the compressor discharge air. Figure 46 shows two arrangements of this housing. The arrangement above the center line depicts the "S" duct and exit stator vanes that normally would precede a second-stage centrifugal compressor. The arrangement below the center line illustrates the configuration that will initially be tested. In the latter

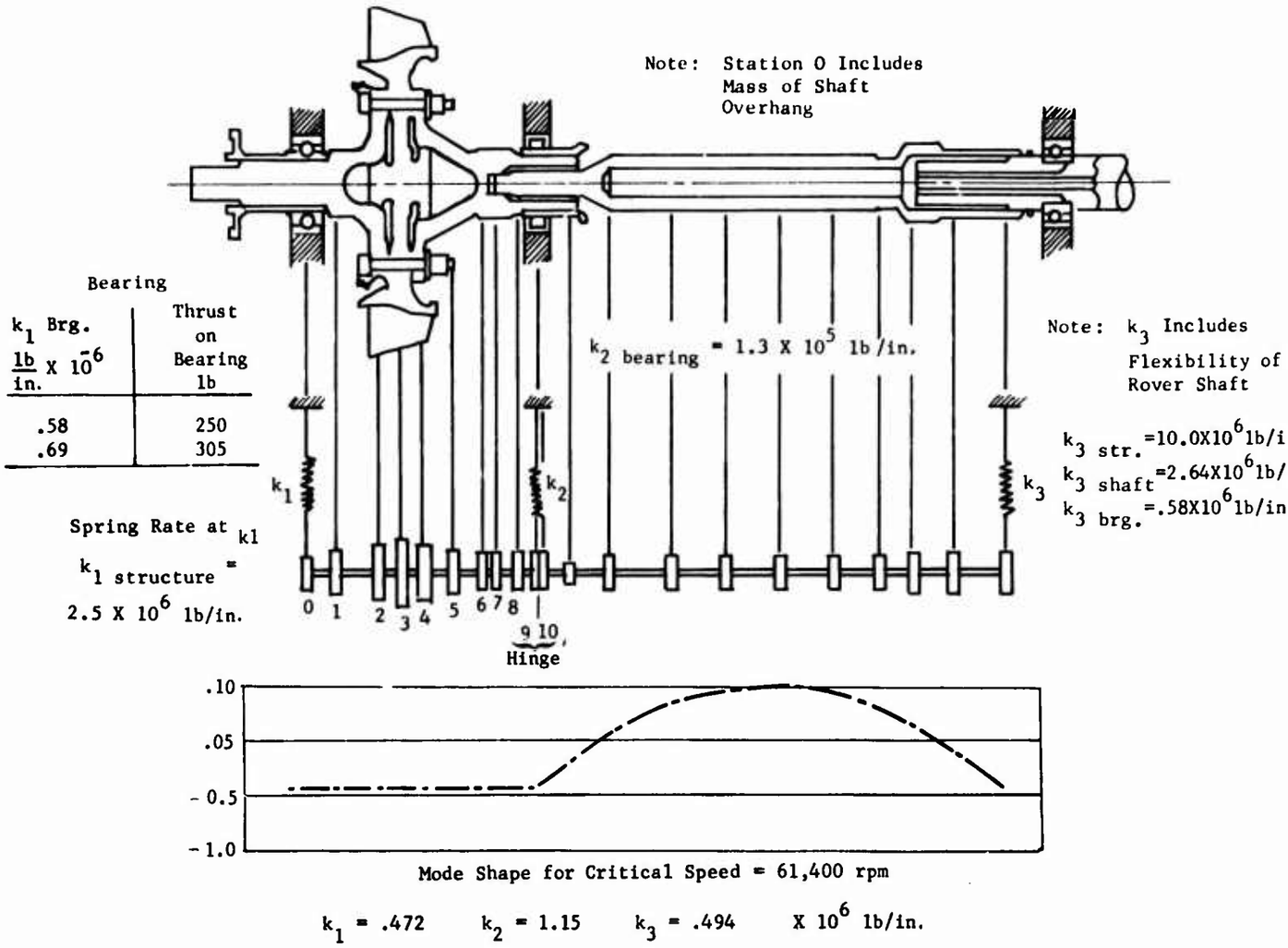


Figure 51. 2.8:1 Supersonic Compressor Rig - Critical Speed Analysis.

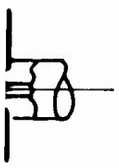

te: $k_3$ Includes Flexibility of Rover Shaft

$t_{3\ str.} = 10.0 \times 10^6$ lb/in.

$t_{3\ shaft} = 2.64 \times 10^6$ lb/in.

$t_{3\ brg.} = .58 \times 10^6$ lb/in.

| Station No. | M Mass lb/sec$^2$/in. | $I_P$ Polar Moment of Inertia lb/in/sec$^2$ | $I_D$ Diam. Moment of Inertia lb/in/sec$^2$ | L Length in. | I Moment of Inertia in$^4$ | A Area in.$^2$ | |
|---|---|---|---|---|---|---|---|
| 0 | .0016 | .0004169 | .0002084 | .580 | .01908 | .4902 | Bearing |
| 1 | .0004223 | .00008195 | .00004098 | .790 | .09880 | .7421 | |
| 2 | .002182 | .003117 | .001559 | .325 | 4.485 | 4.785 | |
| 3 | .009772 | .03949 | .019795 | .310 | 4.6125 | 5.6703 | Eccentricity |
| 4 | .001407 | .001992 | .000996 | .580 | .624 | 1.948 | |
| 5 | .001234 | .0005895 | .0002948 | .720 | .275 | 1.521 | |
| 6 | .0002876 | .00005617 | .00002809 | .285 | .1168 | 1.0509 | |
| 7 | .0002106 | .00004390 | .00002195 | .225 | .07706 | .6721 | |
| 8 | .0001411 | .00002351 | .00001176 | .400 | .03975 | .4902 | |
| 9 | .0001206 | .00008046 | .00004023 | $1 \times 10^{-4}$ | $1 \times 10^{-21}$ | .3848 | Bearing-Hinge |
| 10 | .000022 | .000001170 | .000000585 | .630 | .01178 | .3848 | |
| 11 | .0002161 | .00008735 | .00004368 | .630 | .00555 | .2642 | |
| 12 | .0003714 | .00004733 | .00002367 | 1.20 | .04353 | .5212 | |
| 13 | .0003816 | .00006375 | .00003188 | 1.00 | .04353 | .5212 | |
| 14 | .0003816 | .00006375 | .00003188 | 1.00 | .04353 | .5212 | |
| 15 | .0003816 | .00006375 | .00003188 | 1.00 | .04353 | .5212 | Eccentricity |
| 16 | .0003816 | .00006375 | .00003188 | 1.00 | .04353 | .5212 | |
| 17 | .0002519 | .00003852 | .00001946 | .575 | .03276 | .4298 | |
| 18 | .0004029 | .0001274 | .0000637 | .980 | .06319 | .3299 | |
| 19 | .0003882 | .00006207 | .00003103 | .980 | .06319 | .3299 | |
| 20 | .0007026 | .0001199 | .00005995 | .000 | - | - | Bearing |

Mathematical Representation and Mode Shape of 2.8:1 Supersonic Compressor Rig Speed Analysis

ges

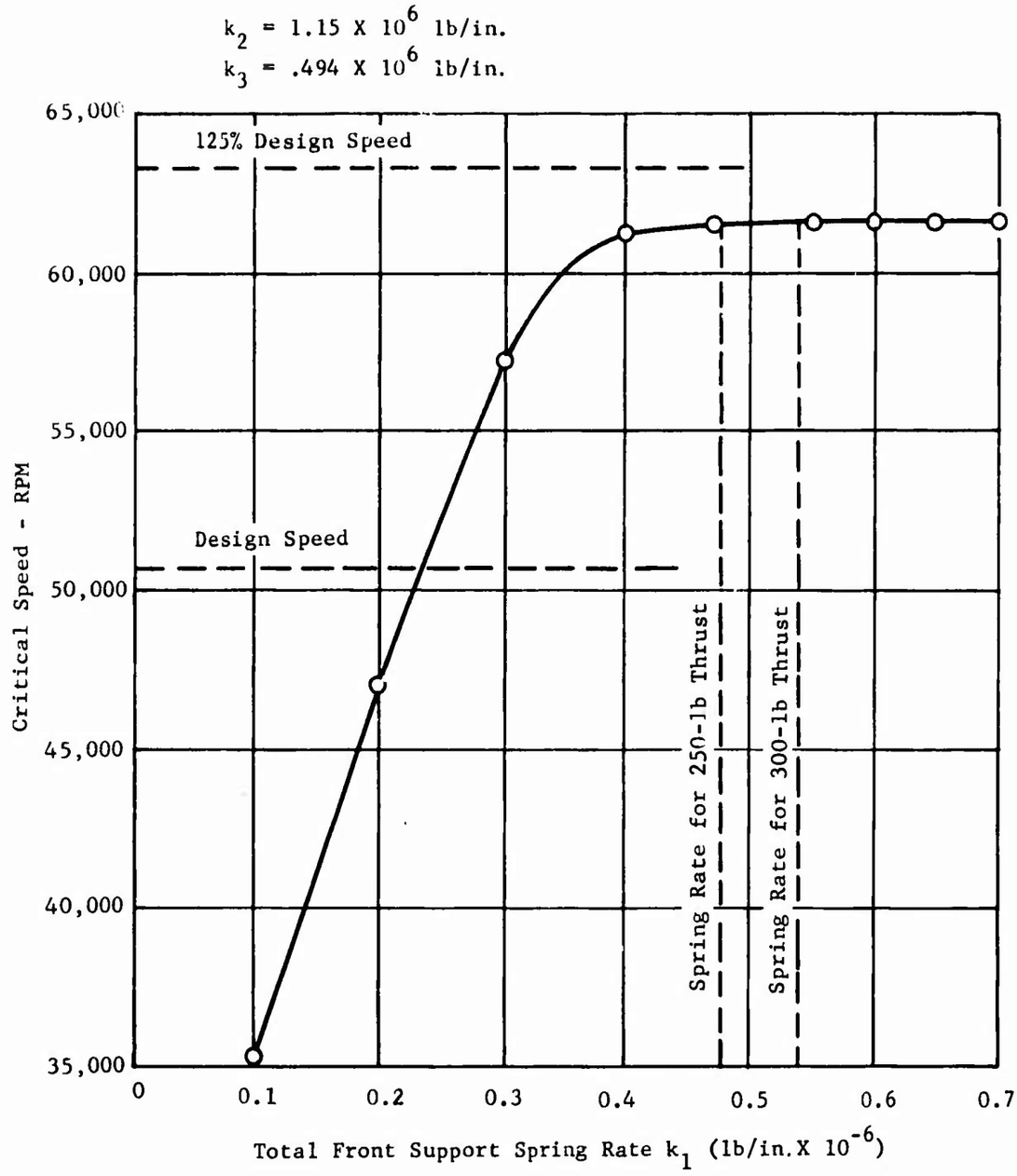


Figure 52. 2.8:1 Supersonic Compressor Rig - Critical Speed vs Front Support Spring Rate.

arrangement, the compressor rotor is followed by a straight-sided annular passage. An annular diffuser slows the air down from this passage before dumping it into the collector plenum chamber. The large drilled and tapped holes at the aft end of the straight-sided annular passage are for instrumentation. It can be seen that the inner portion of the bearing support is quite substantial. A rigid bearing support was required in order for the critical speed of the compressor to be above the design operating speed. The critical speed data are fully covered in the beginning of this section. The rear roller bearing is lubricated by two separate oil jets 180 degrees apart. Bearing cavities are provided on both sides of the bearing for proper oil scavenging. The scavenge oil from this bearing drains into the turbine section through appropriate drain holes and then into the test stand oil system. The rear bearing oil seal is pressurized by the discharge air from the rotor.

The collector housing terminates in a single outlet of approximately 5-1/2 inches diameter. The test stand back-pressure valve attaches to the flange of this outlet.

DRIVE TURBINE

The prime mover for the test rig is a converted small gas turbine (Rover Model 15/60) capable of operating at the required speed and power. The centrifugal compressor of the gas turbine has been replaced with a disc having the same mass moment and center of gravity location. The substitute disc also serves as a balancing piston for counteracting the thrust of the turbine. Steam is supplied to the turbine by a steam jacket which replaces the burner can. A test stand oil system provides oil to the bearings and scavenging of the bearing drains. As previously mentioned, the turbine is connected to the compressor rig through a splined quill shaft. These splines are oil lubricated to minimize spline wear caused by misalignment. This prime mover has been operating for approximately six months, driving the SSC (2.0) with relatively minor difficulties.

## (U) PHASE II TEST PLAN

A test plan has been prepared for the 2.8:1 supersonic compressor experimental rotor development program to be conducted in Phase II of this contract. The testing procedures, instrumentation, test equipment, and methods of data reduction and analysis are discussed in this plan. The test plan is presented in Appendix II of this report.

## (U) LITERATURE CITED


1. Ainley, D. G., and Nathieson, G. C., A Method of Performance Estimation for Axial-Flow Turbines, N.G.T.E. R 111, December 1951.

2. Bienkowski, George, Turbine Design Methods, Mean Camber Line Turbine Blade Section Layout Procedure, Wright Aeronautical Division, Curtiss-Wright Corporation, Project No. XD-715, Report No. 3, August 1958.

3. Brennan, Donald F., Test Performance of a Highly Loaded Short Span Single Stage Axial Compressor, Wright Aeronautical Division, Curtiss-Wright Corporation, Project No. XC-739, Report No. 38, November 1960.

4. Brown, Larry E., Deer, Carmine A., and Farley, Edward, Performance of the 1.755 $C_L$ High Pressure 0.7 Diameter Ratio Single Stage Axial Compressor, Wright Aeronautical Division, Curtiss-Wright Corporation, Project No. XC-739, Report No. 6, November 1954.

5. Fejer, Andrew A., Heath, George L., and Driftmyer, Richard T., An Investigation of Constant Area Supersonic Flow Diffusion, ARL 64-81, May 1964.

6. Fejer, Andrew A., and Heath, George L., Supersonic Cascade Studies, Part 1 - Passage Studies, ARL 125, Part 1, December 1961.

7. Goldberg, Theodore J., Experimental Investigation of an Axial-Flow Supersonic Compressor Having Sharp Leading-Edge Blades with an 8 Percent Mean Thickness - Chord Ratio, NACA RM L54K16, February 1955.

8. Goldberg, Theodore J., Boxer, Emanuel, and Bernot, Peter T., Experimental Investigation of an Axial-Flow Supersonic Compressor Having Rounded Leading-Edge Blades with an 8 Percent Mean Thickness - Chord Ratio, NACA RM L53G16, December 1953.

9. Gottschalk, James, The Effect of Area Ratio on Performance in a Plane Cascade of High Solidity, Straight-Back Turbine Blades, Wright Aeronautical Division, Curtiss-Wright Corporation, Project No. XC-741, Report No. 14, August 1957.

10. Heath, George L., An Investigation of Diffusion of Supersonic Flows in Curved Constant Area Passages, ARL 65-179, September 1965.

11. Jahnsen, Lawrence J., and Hartmann, Melvin J., Investigation of Supersonic Compressor Rotors Designed with External Compression, NACA RM E54G27a, September 1954.

12. Johnson, Elmer G., Ohain, Han Von, Lawson, Maurice O., and Crames, Kenneth R., A Blunt Trailing Edge Supersonic Compressor Blading, WADC TN-59-269, August 1959.

13. Kantrowitz, A., The Supersonic Axial-Flow Compressor, NACA A.C.R. No. L6D02, April 1946.

14. Klapproth, John F., Jacklitch, John J., Jr., and Tysl, Edward R., Design and Performance of a 1400 Foot per Second Tip Speed Supersonic Compressor Rotor, NACA RM E55A27, April 1955.

15. Lewis Research Center, Cleveland, Ohio, Aerodynamic Design of Axial-Flow Compressors, NASA SP-36, 1965.

16. Lieblein, Seymour, Schwenk, Francis C., and Broderick, Robert L., Diffusion Factor for Estimating Losses and Limiting Blade Loadings in Axial-Flow Compressor Blade Elements, NACA RM E53D01, June 1951.

17. Loeb, W. A., A Study of the Supersonic Axial-Flow Compressor, Journal of Applied Mechanics, Vol. 16, March 1949, pp. 19-26.

18. Page, Russell,J., The Study and Design of a Research Inlet Stage Transonic Compressor, WADC Technical Report No. 55-8, 1955.

19. Provenzale, Dr. Gaetano, The Effects of Hub and Tip Curvature, and Aspect Ratio on the Radial Distribution of Axial Velocity in Axial-Flow Turbomachinery Free-Vortex Design, Wright Aeronautical Division, Curtiss-Wright Corporation, Project No. XD-711, Report No. 1, April 1958.

20. Provenzale, Dr. Gaetano, Compressibility and Three-Dimensional Effects of the Minimum Loss Angles of Incidence and Deviation in Axial-Flow Double Circular Arc Compressor Rotors, Wright Aeronautical Division, Curtiss-Wright Corporation, Project No. XD-711, Report No. 2, April 1959.

21. Robb, Wayne L., Polson, Bruce C., Smith, William I., and Groh, Fred G., Supersonic Compressor Investigation, Curtiss-Wright Research Report No. 300-109, December 1959.

22. Shapiro, Ascher H., The Dynamics and Thermodynamics of Compressible Fluid Flow, Volume II, First Edition, Ronald Press Co., New York, New York, 1954.

23. Young, Woodrow H., The Experimental Investigation of a Research Transonic Inlet Stage Compressor, WADC Technical Report 57-207, May 1957.

## (U) APPENDIX I
## 2:1 SUPERSONIC COMPRESSOR

The Wright Aeronautical Division of the Curtiss-Wright Corporation is conducting a program for the design and development of a single-stage axial supersonic compressor with a design pressure ratio of 2.08:1. The technology developed under this program is closely related to that of the 2.8:1 supersonic compressor; therefore, the results obtained to date are presented in this appendix.

The design of the inlet guide vanes and compressor rotor for the 2:1 compressor has been completed. Experimental evaluation of the inlet guide vanes has also been completed, and the rotor development phase which involves the experimental evaluation and modification of the rotor with inlet guide vanes is in progress.

### DESIGN PERFORMANCE

The design conditions and vector diagrams for the 2:1 supersonic compressor rotor are presented in Figures 53 through 56. The design performance goals are:

| | IGV & Rotor | IGV & Rotor & Exit Stator |
|---|---|---|
| pressure ratio | 2.13 | 2.08 |
| adiabatic efficiency | 81.2 percent | 79.0 percent |
| airflow | 4.0 pounds per second | 4.0 pounds per second |
| design | 50,700 RPM | 50,700 RPM |

The predicted compressor map is presented in Figure 1.

### EXPERIMENTAL DATA

#### Inlet Guide Vane Flow Test

The first phase of the experimental program for the 2:1 supersonic compressor involved a flow test of the inlet guide vanes without the compressor rotor present. This test was performed to evaluate the performance of this blade row relative to the design values and to establish the off-design performance. It was not possible to measure this performance during rotor testing, since the axial spacing between the inlet guide vanes (IGV) and the rotor is too small to allow adequate instrumentation without jeopardizing the safety of the rotor. Although it is recognized that the conditions at the IGV exit, when the rotor is inducing the flow, are not duplicated in the flow test, it was considered that these data would serve as a reasonable approximation of the performance of this blade row. In this test the inlet ducting, inlet housing, and IGV housing from the compressor rig were attached to an air supply capable of flowing in excess of 4.0 pounds per second. The air exiting from the IGV discharged to ambient conditions. A traversing yaw probe was installed at the exit plane, and the total pressure profiles and air angles were determined. A total pressure rake located at the inlet duct of the compressor rig, which is the same rake used in the compressor testing, was used to establish the

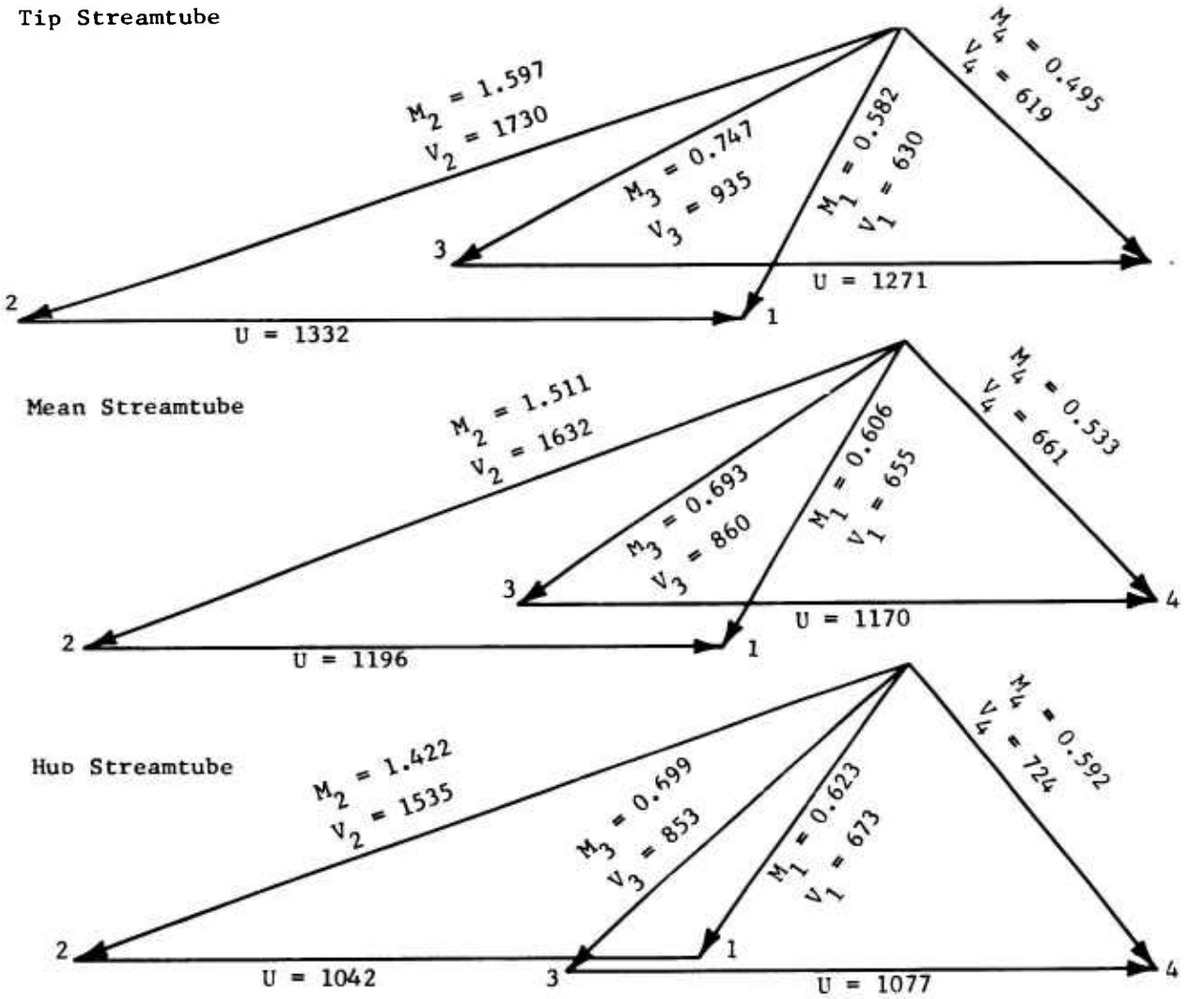


Figure 53. 2:1 Supersonic Compressor Design Vector Diagrams

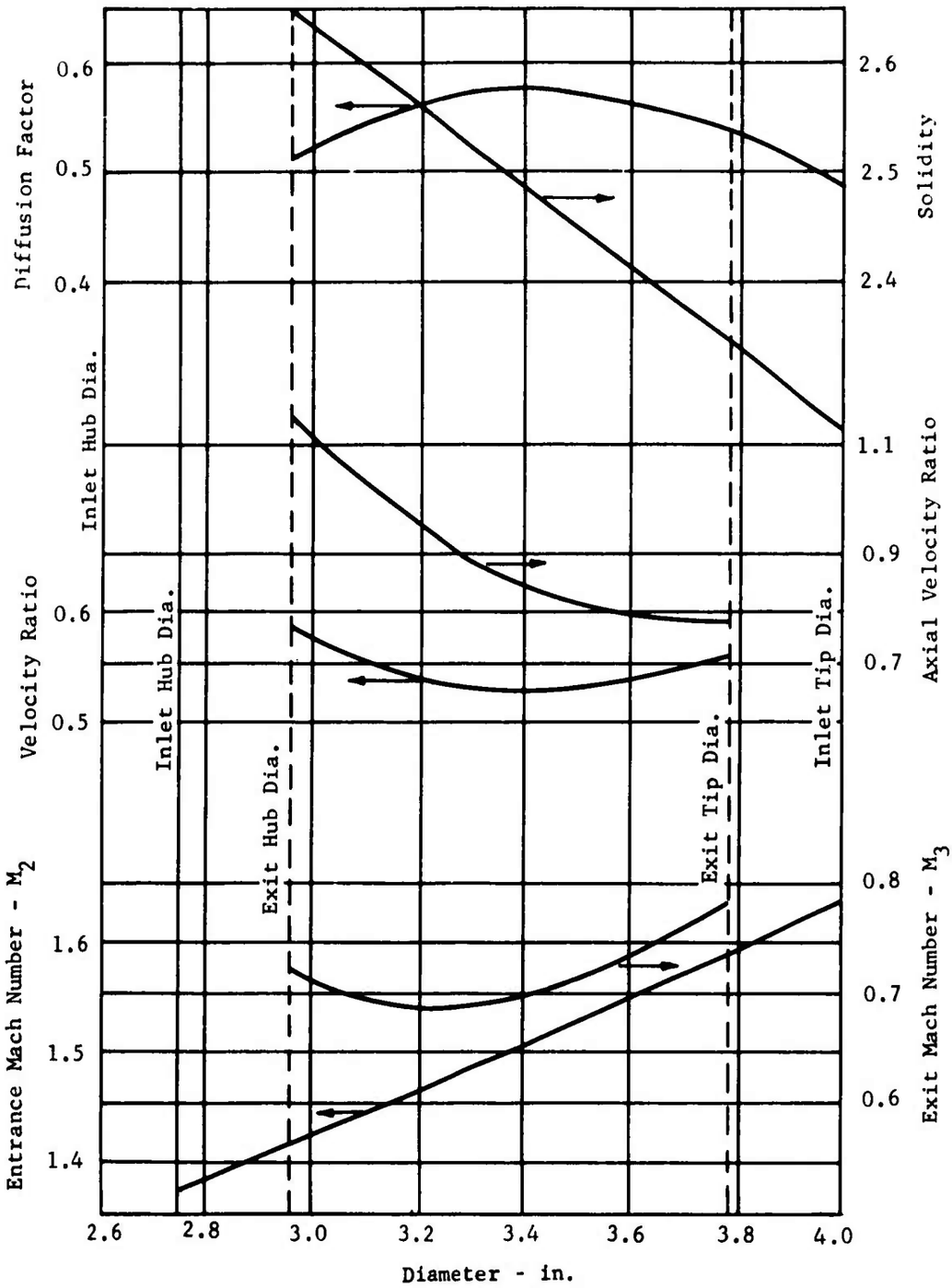


Figure 54. 2:1 Supersonic Compressor - Rotor Design Data.

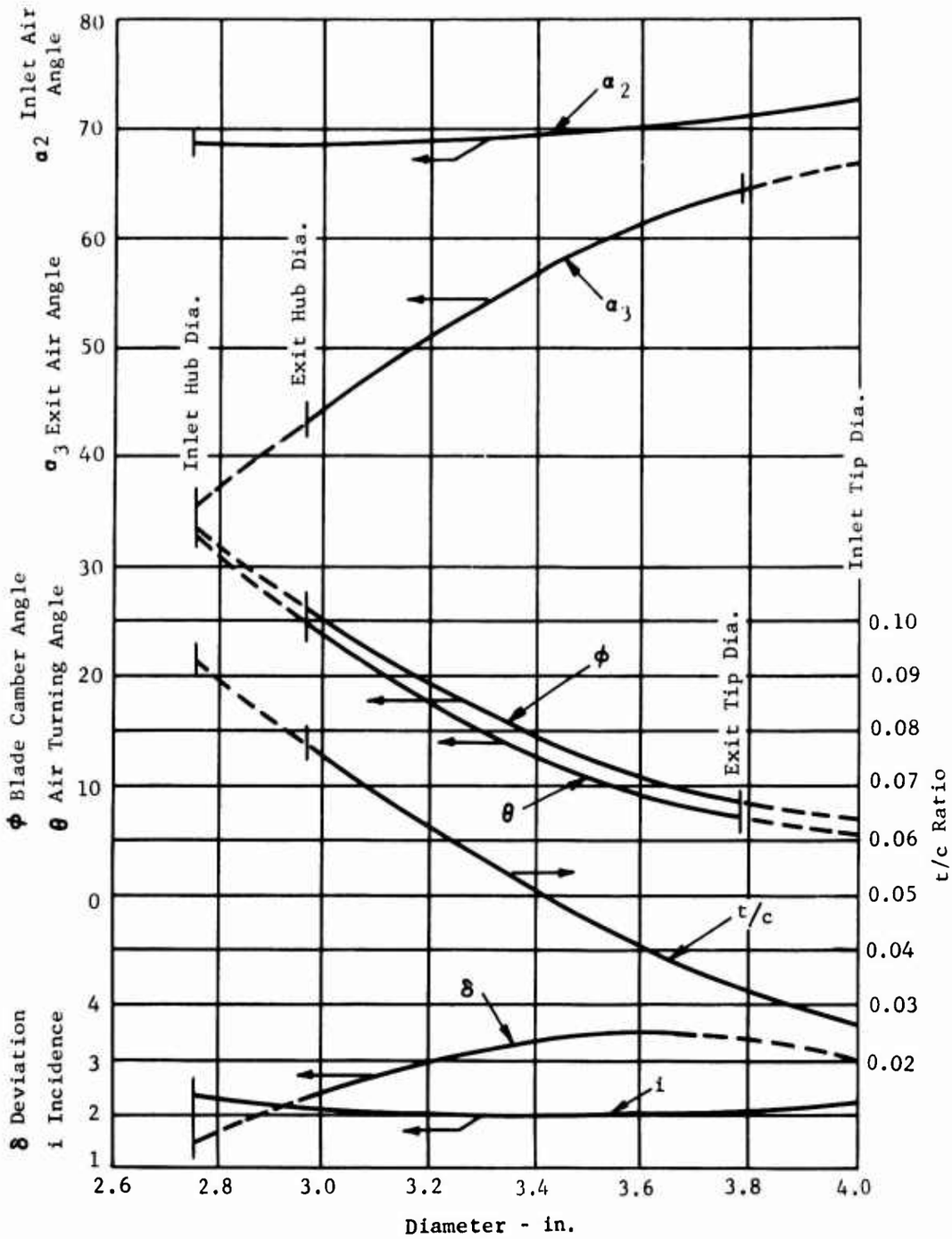


Figure 55. 2:1 Supersonic Compressor - Rotor Design Data.

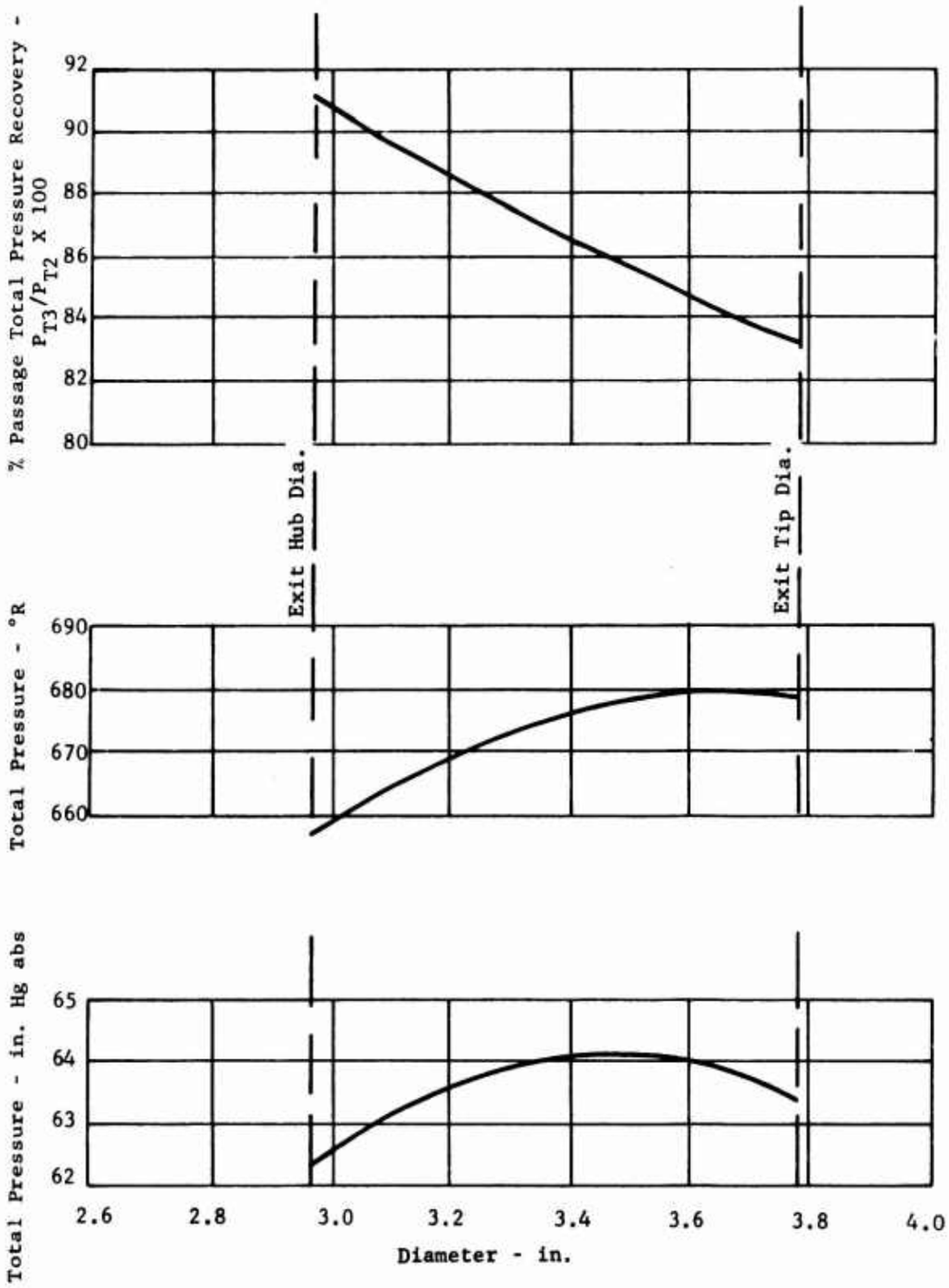


Figure 56. 2:1 Supersonic Compressor - Rotor Design Exit Conditions.

entering total pressures and temperatures. A standard ASME orifice located in the inlet system was used to measure the airflow. The results of this test are presented in Figures 57 through 59. The data are plotted in terms of absolute airflow. At the operating inlet conditions, an absolute airflow of 5.17 pounds per second is comparable to the design corrected airflow of 4.0 pounds per second. The results essentially verify the design parameters with the exception of the deviation in the area of the shroud streamtube being 2 degrees higher than design. The recovery is computed by an area weighted calculation. This results in the lower limit of recovery, since the mass rate in the wake region is lower than that of the mainstream. Figure 60 is a photograph of this test arrangement, and Figure 61 is a photograph of the inlet guide vane.

Rotor Development (SSC 2.0)

The second phase of the test program is for rotor development. The inlet guide vanes and compressor rotor are tested together in this phase, and their overall performance is evaluated. The test procedures and instrumentation for this program are the same as those described in Appendix II.

Figures 62, 63, and 64 are photographs of the rotor, assembled compressor, and compressor installed on test stand respectively. Figures 65 through 67 present the results of testing the first compressor rotor (configuration 1). A second configuration with slightly larger tip diameter ($\approx$ .050 inch) was tested but gave poorer performance due to excessive leading edge thicknesses and bluntness.

The data from these tests indicate that the +6-degree inlet guide vane (IGV) setting provided the highest efficiency at 100 percent speed and a peak pressure ratio higher than for the design IGV setting. The +10-degree IGV setting resulted in the highest airflow but lowest efficiency. The design pressure ratio was achieved in these tests, but the efficiency and airflow were below design values. The efficiencies presented on the maps are based on a direct average of pressure ratio and temperature rise from hub to tip. A mass weighted efficiency was calculated, using a data reduction computer program (described in Appendix II), to be 78.5 as compared to the 77 percent peak efficiency indicated on the compressor map for the +6-degree IGV setting. It should be noted that the inlet guide vane is designed to turn the flow against the direction of rotation, and the +6-degree setting designates turning the IGV 6 degrees further against the rotor rotation than at the design setting.

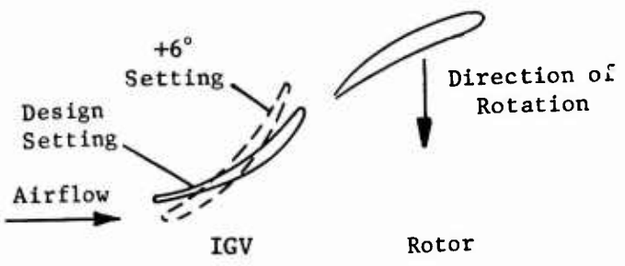

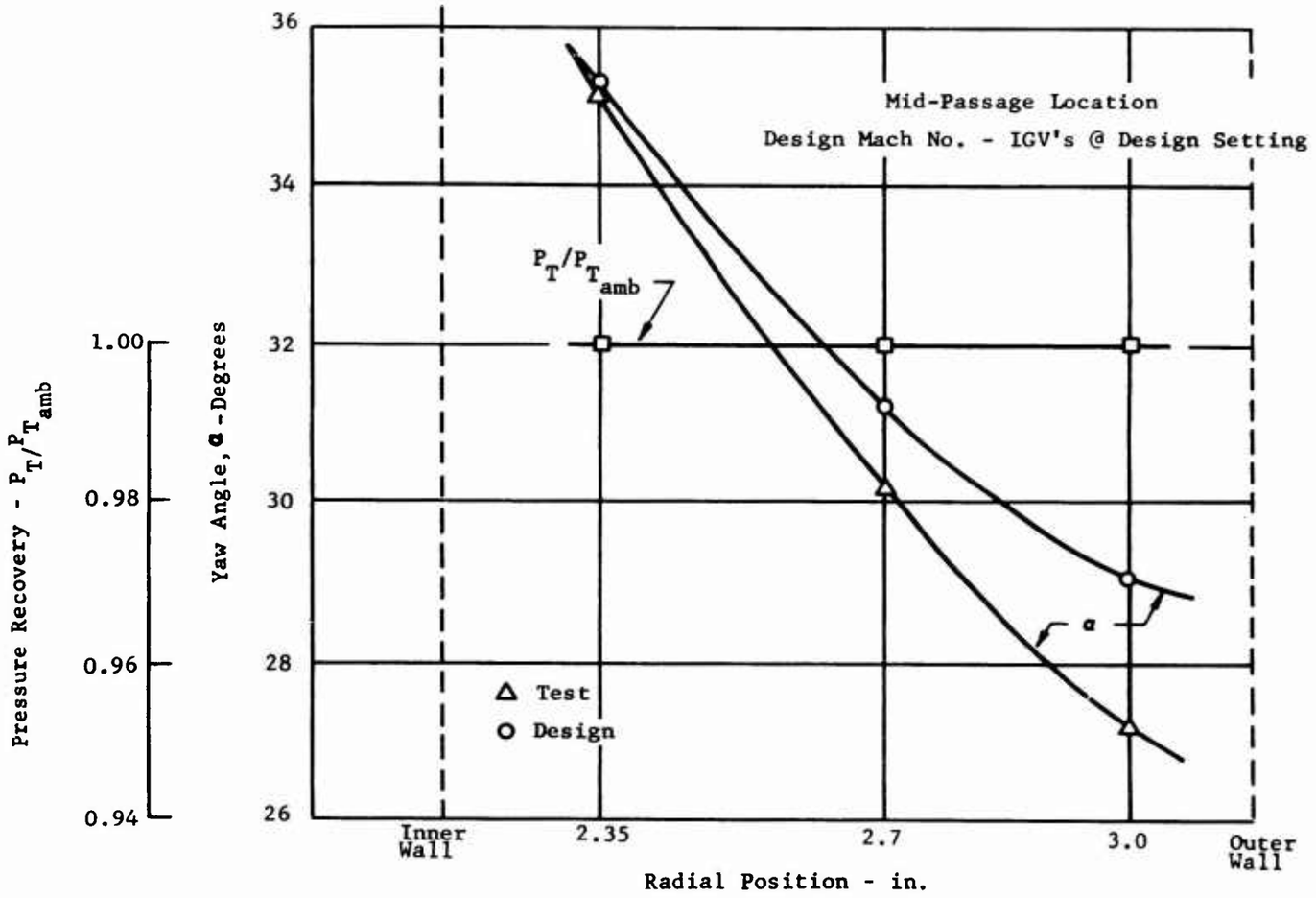


Figure 57. 2:1 Supersonic Compressor Inlet Guide Vane Flow Test - Radial Traverse.

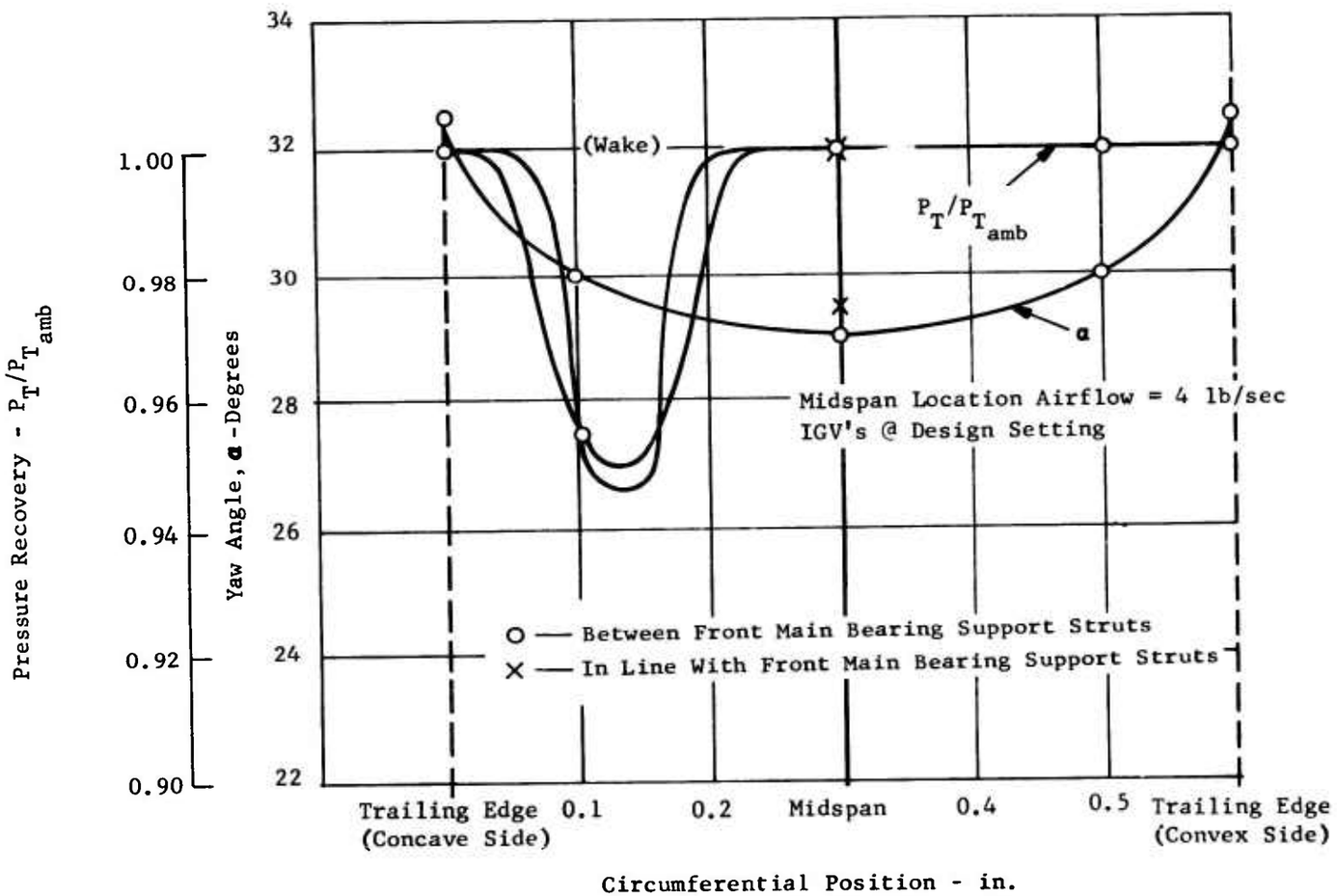


Figure 58. 2:1 Supersonic Compressor Inlet Guide Vane Flow Test - Circumferential Traverse.

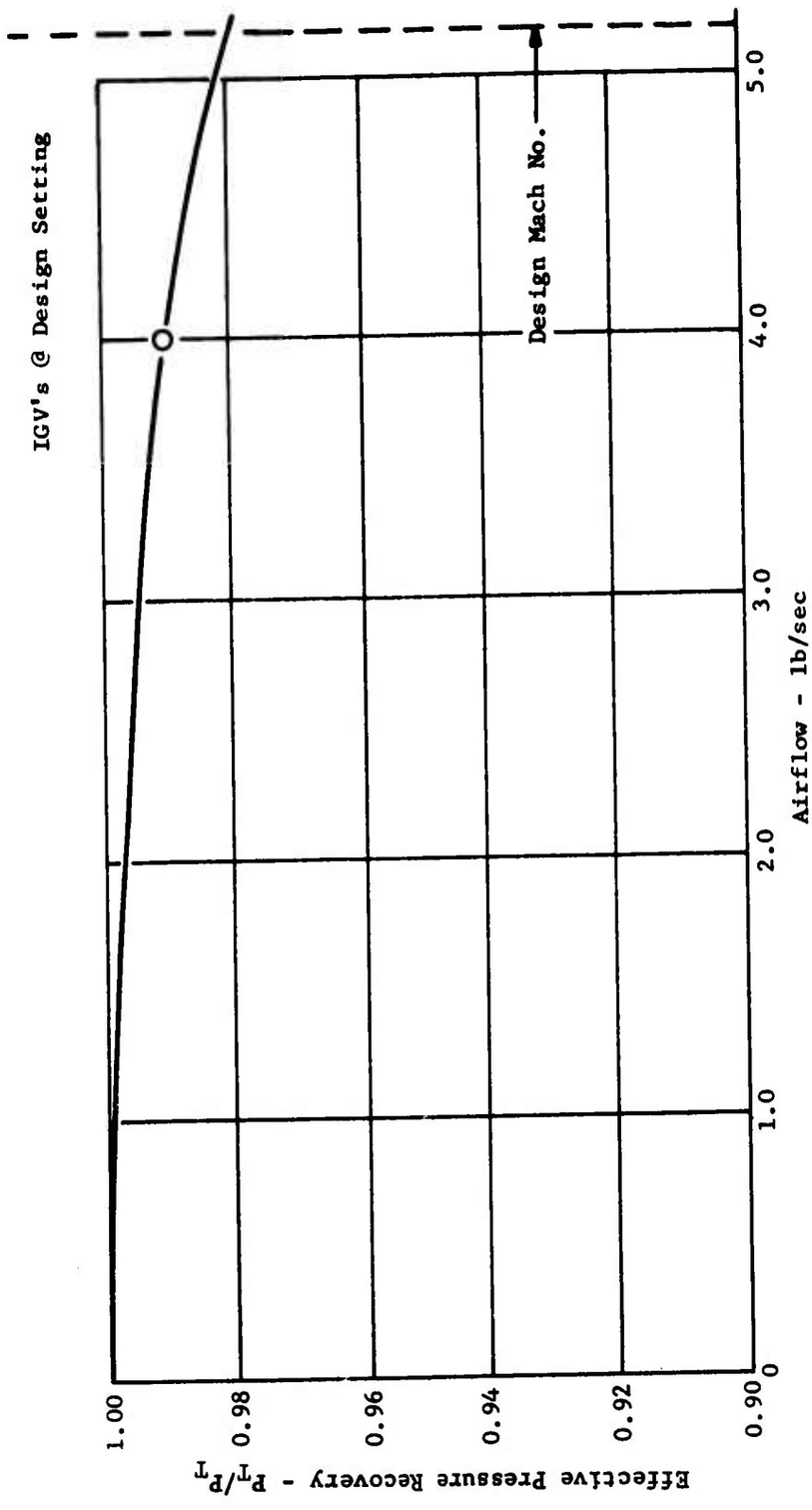


Figure 59. 2:1 Supersonic Compressor Inlet Guide Vane Flow Test - Pressure Recovery.

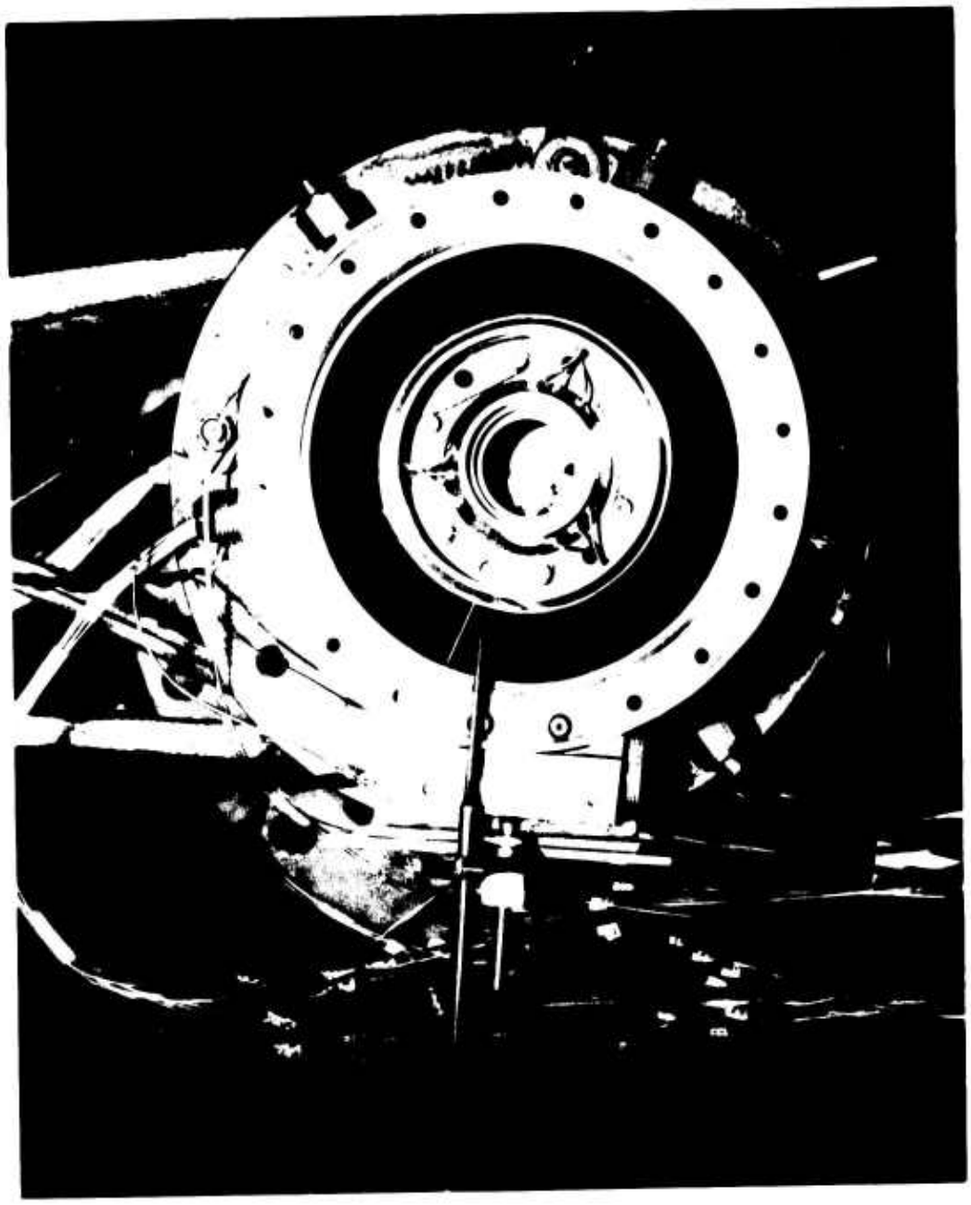

Figure 60. Inlet Guide Vane Flow Test.

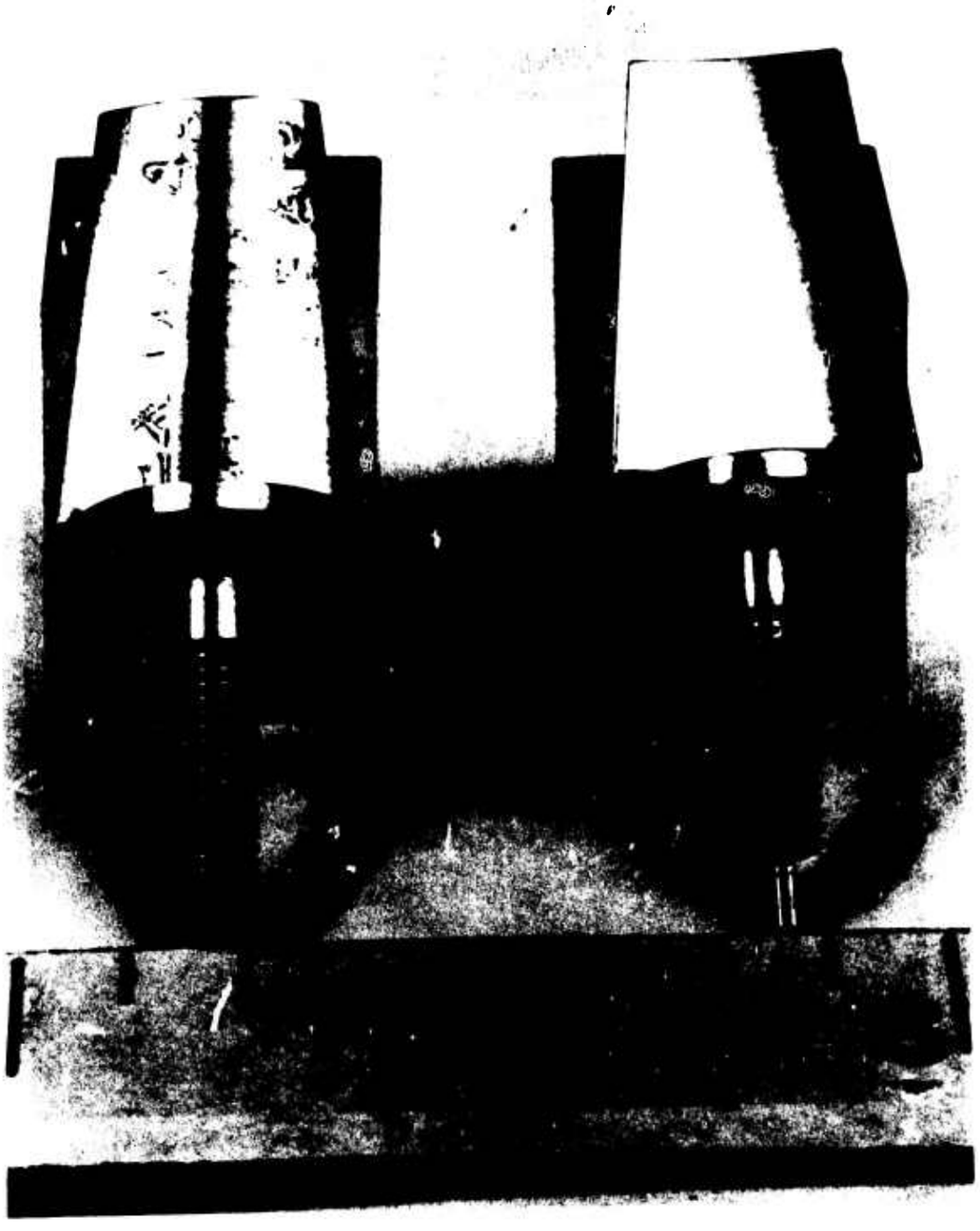

Figure 61. Inlet Guide Vanes.

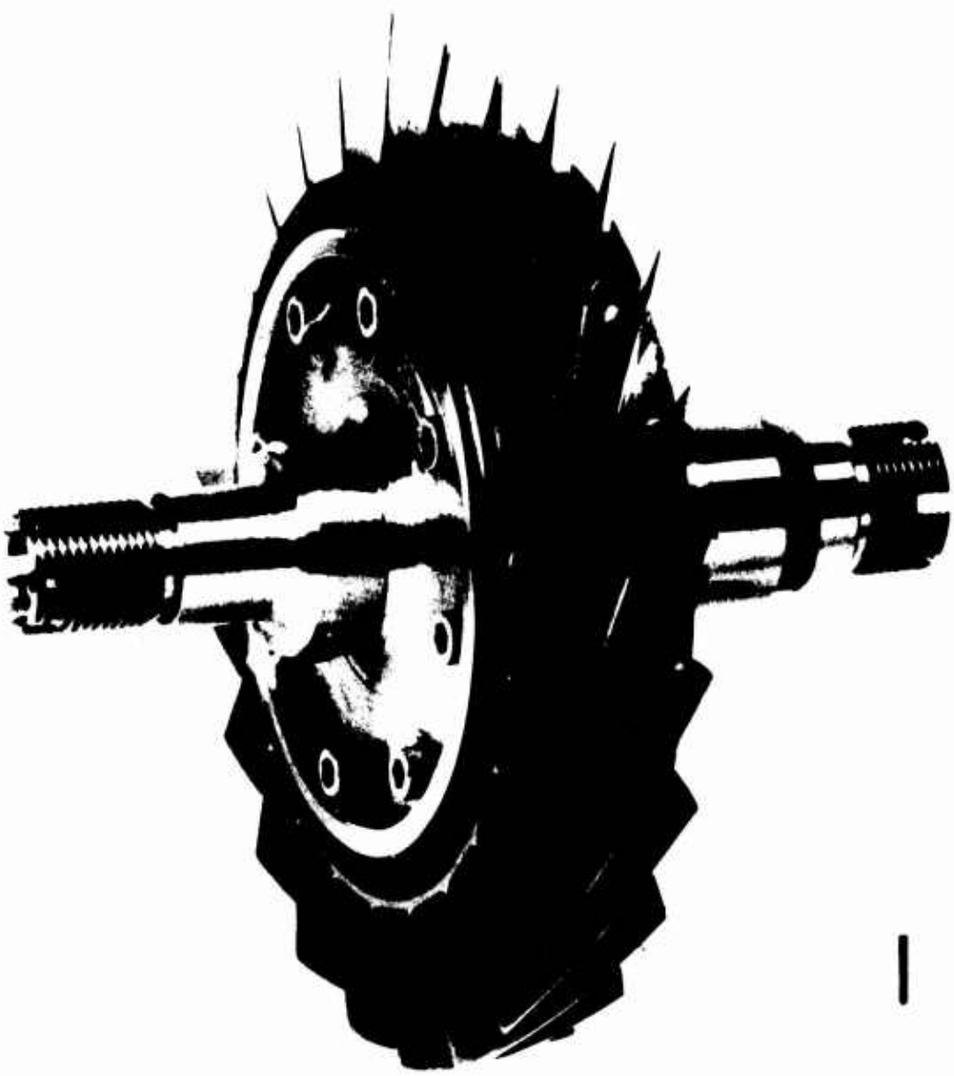

Figure 62. 2:1 Supersonic Compressor Rotor.

Figure 63. 2:1 Supersonic Compressor Assembled.

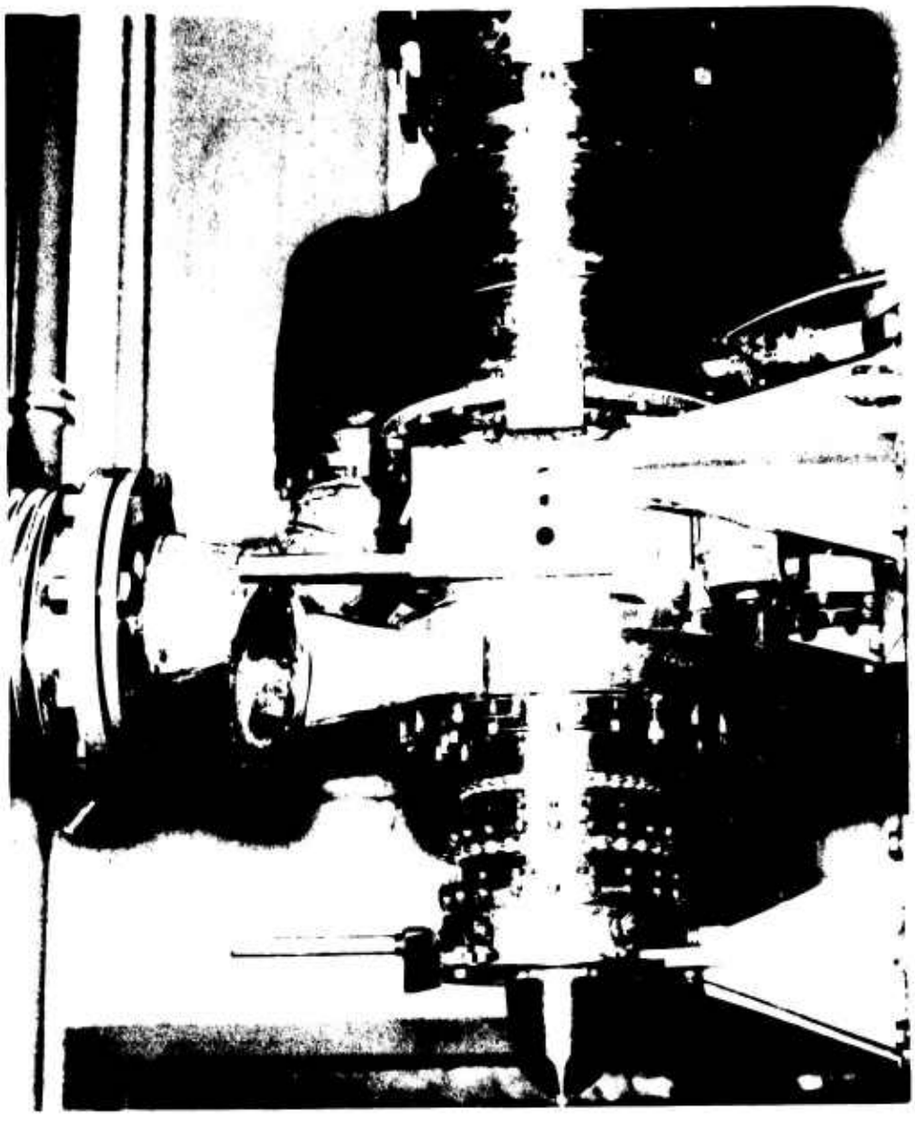

Figure 64. 2:1 Supersonic Compressor and Test Rig.

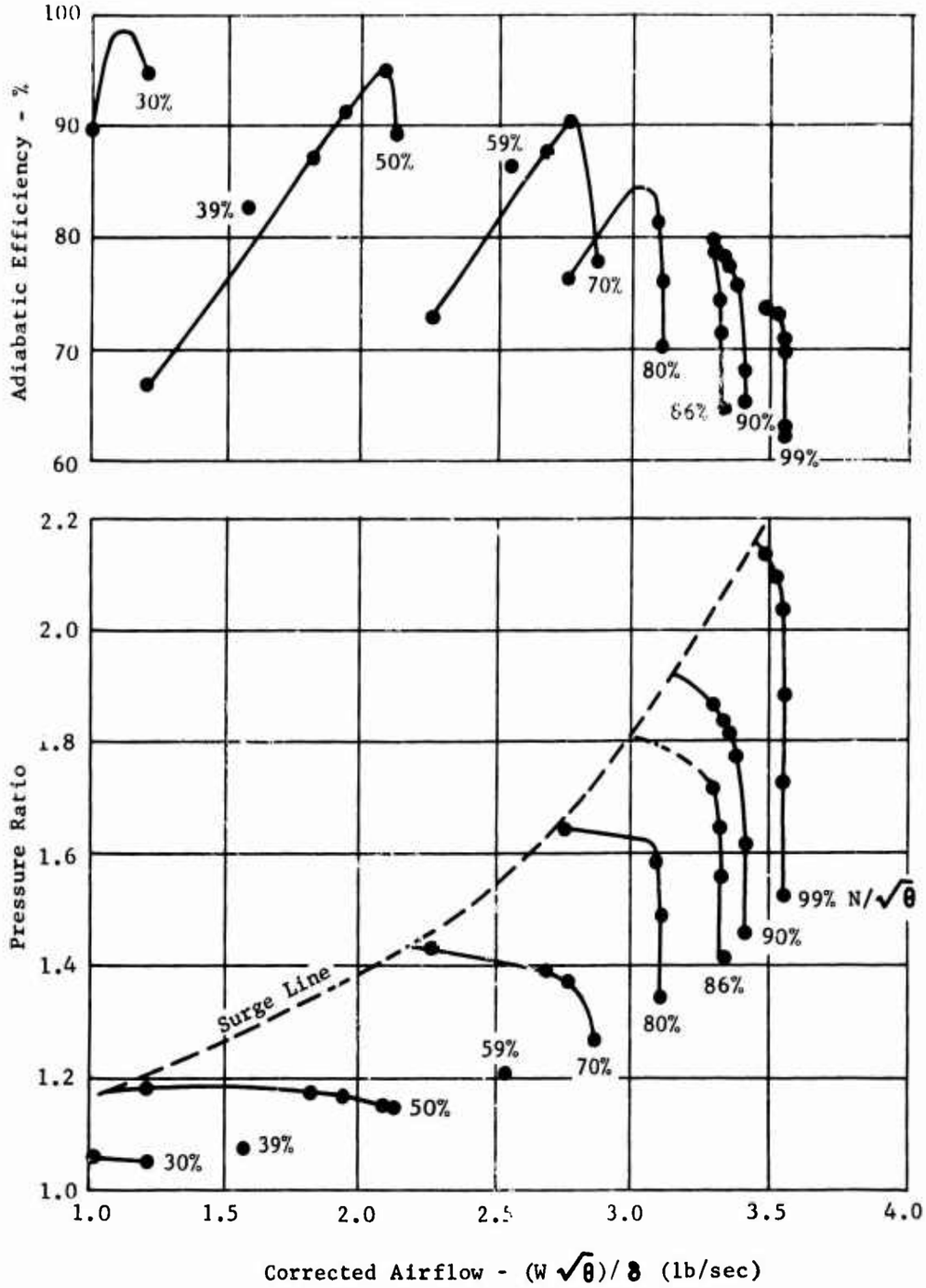


Figure 65. 2:1 Supersonic Compressor - Rotor Test Data - Configuration 1, IGV's @ Design Setting.

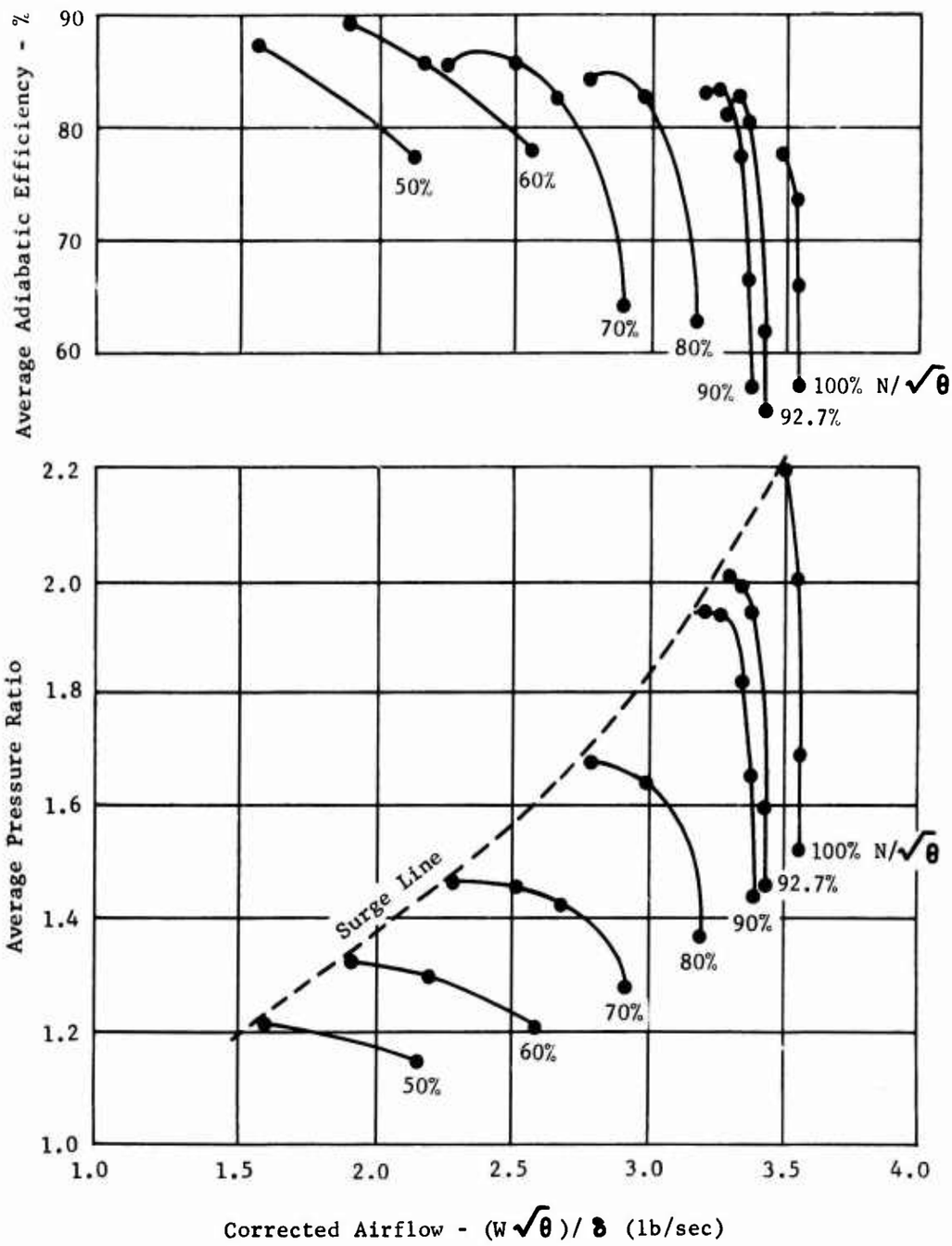


Figure 66. 2:1 Supersonic Compressor - Rotor Test Data - Configuration 1, IGV's @ + 6° Setting.

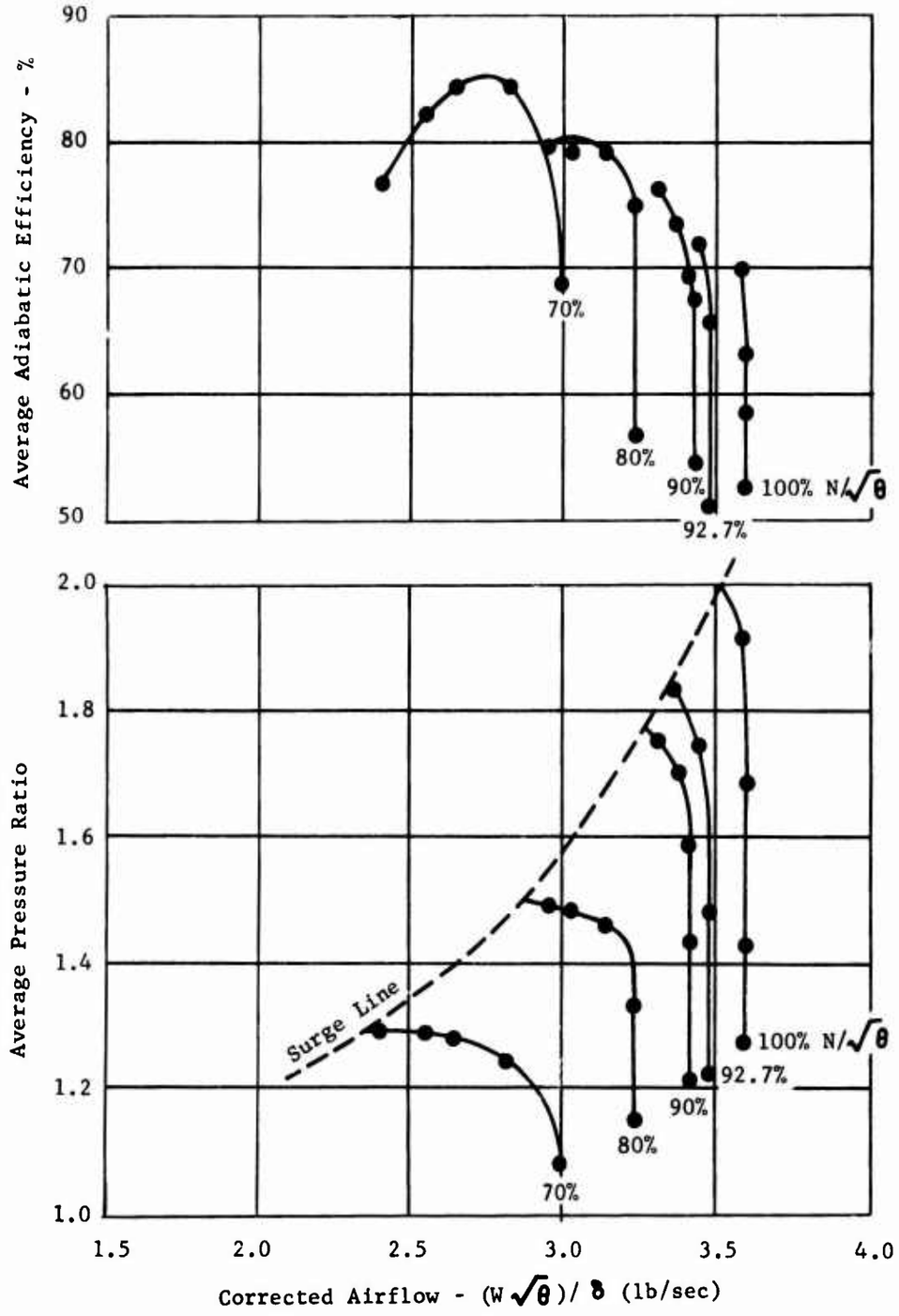


Figure 67. 2:1 Supersonic Compressor - Rotor Test Data - Configuration 1, IGV's @ + 10° Setting.

The plot of the difference between the experimental relative air inlet angle and the angle formed by the expansion surface at the leading edge of the rotor blade is presented in Figure 70. This figure indicates that an incidence angle of between 2.2 degrees and 3.3 degrees with respect to the blade expansion surface should be used to establish an expansion angle which will produce the design flow conditions (reduce the angle). The incidence referred to here differs from the conventional definition in that the conventional approach relates the relative air angle to the mean leading edge angle (average of expansion and compression surface - see Figure 68). It has been concluded that a rework of the leading edge surface angle accordingly on the next configuration is required to achieve design performance. The results of testing configuration 2 have emphasized the importance of maintaining the sharpest practical leading edges to achieve high performance in this type of compressor.

The 2.8 supersonic compressor has been designed for sharper leading edge thicknesses (.007 inch) compared to those of the 2.0 compressor (.015 inch) and has allowed for an additional 1 degree of incidence.

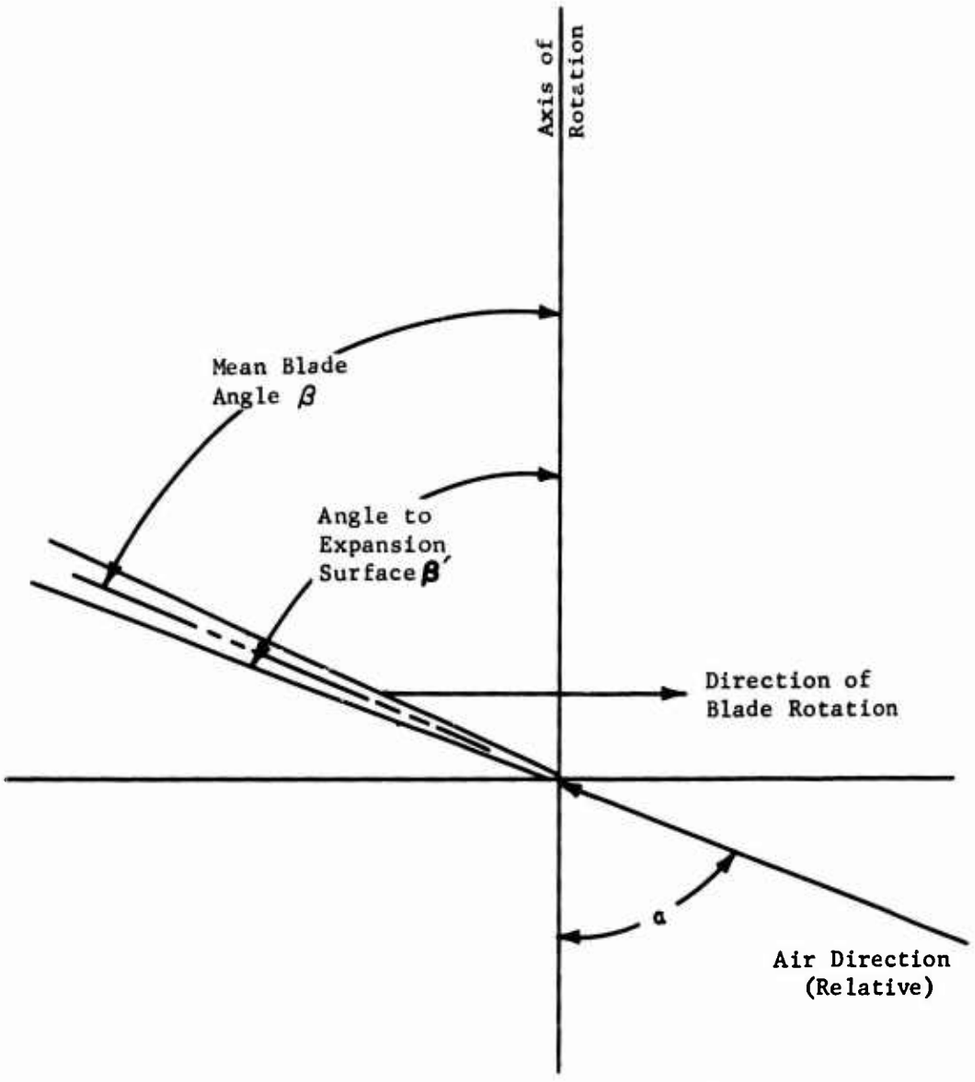


Conventional Incidence Angle $i = \beta - \alpha$

Modified Incidence Angle $i' = \beta - \alpha$

Figure 68. Schematic Illustrating Incidence Angle Definitions.

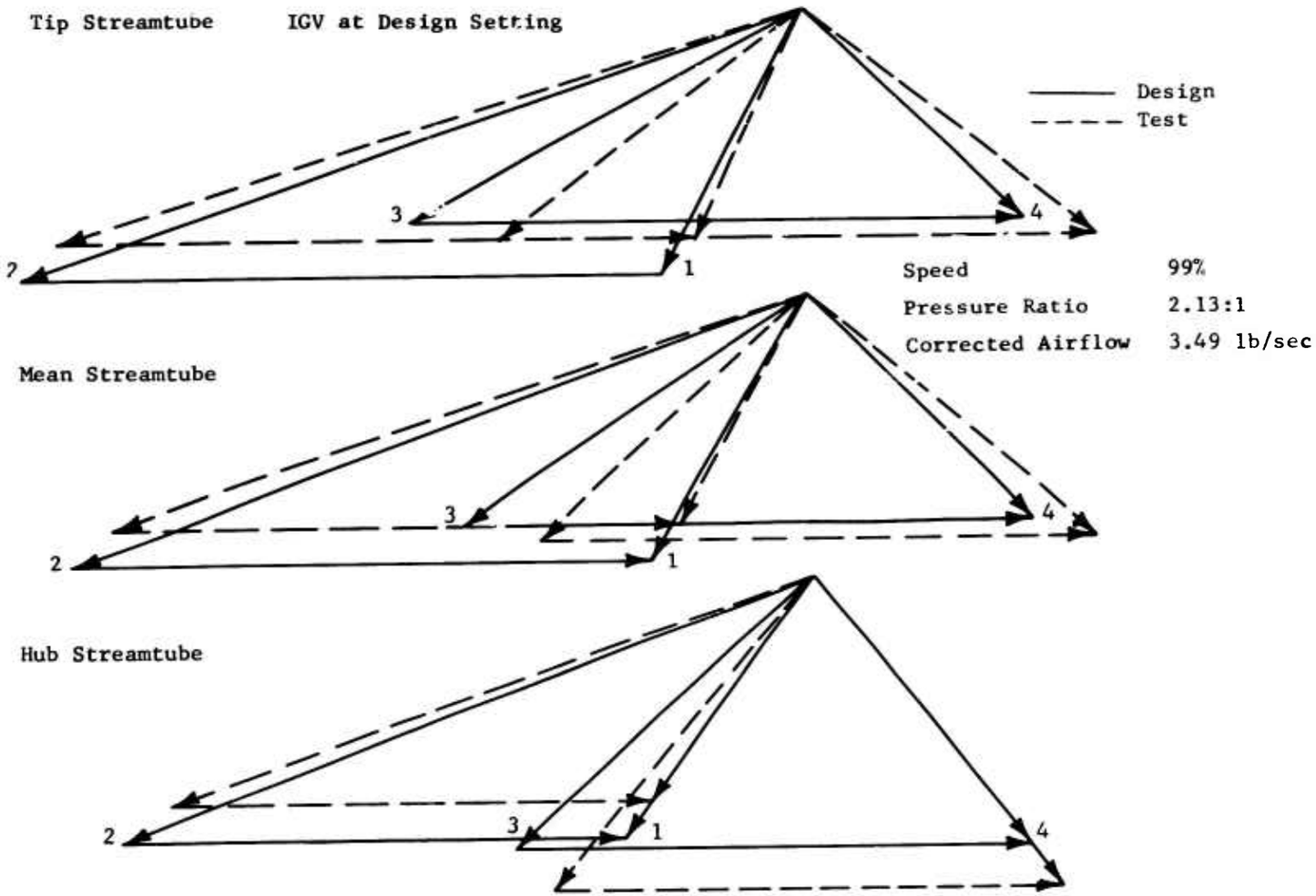


Figure 69. 2:1 Supersonic Compressor Rotor Test - Vector Diagrams.

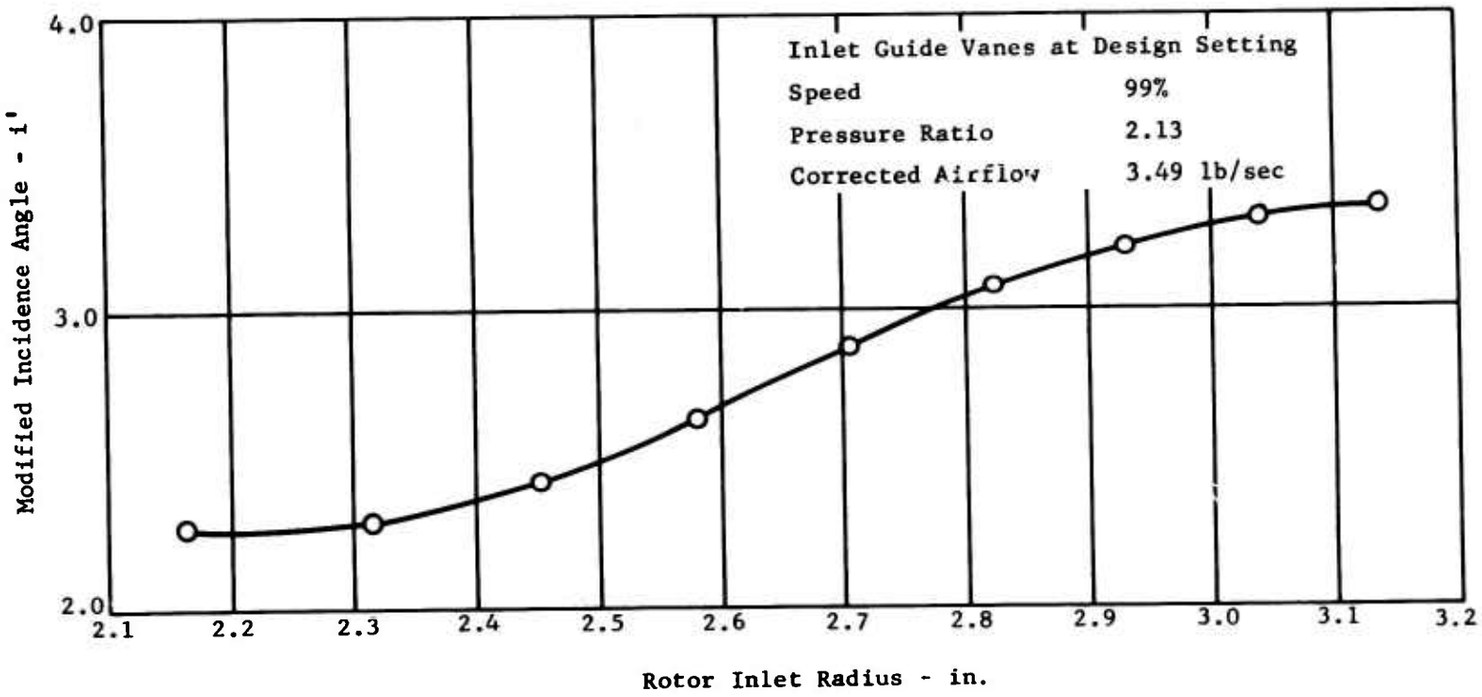


Figure 70. 2:1 Supersonic Compressor Rotor Test - Modified Incidence Angles.

## (U) APPENDIX II
## PHASE II TEST PLAN

### OBJECTIVE

The objective of the rotor development program is to evaluate the combined inlet guide vanes and rotor performance of the 2.8:1 single-stage supersonic compressor design through experimental testing, data analysis, and design modifications. The performance goals for the inlet guide vanes and rotor are:

| | |
|---|---|
| pressure ratio | 2.8:1 |
| adiabatic efficiency | 87.2 percent |
| airflow | 4.0 pounds per second |
| design speed | 50,700 RPM |

### APPROACH

The inlet guide vane performance for this compressor has been established independent of the rotor by a flow test program using an external air supply. These data will be used in the analysis of the combined inlet guide vane and rotor data.

The first step in the program will be to develop a compressor map between 40 and 100 percent speed by obtaining experimental data for the initial design configuration with the inlet guide vanes at their design setting. Compressor maps will also be developed between 70 and 100 percent speed for two other inlet guide vane settings. Complete temperature and pressure data will be recorded during the testing.

The data points in the 90 to 100 percent speed range, which represent peak pressure ratio and peak efficiency, will be analyzed to establish vector diagrams that satisfy the experimental data. The experimental vector diagrams will be compared to the design conditions to pinpoint deficient areas.

Based on the results of the data analysis, design modifications will be established. These modifications will be incorporated in the compressor hardware by machining, blade bending, and similar means.

An experimental map for the modified configuration will be developed at the optimum guide vane setting, and the cycle will be repeated. At least two compressor builds are estimated for this series.

A redesign is planned after the first series of tests to correct deficiencies which require modifications beyond the limits of reworking the existing hardware. It is expected that the key design modifications will be established in the first test series.

A second test series will be conducted with the redesigned component or components in the same manner as the first test series. Three builds are

estimated for the second series, in which final hardware modifications will be made. A complete compressor map will be developed between 40 and 100 percent speed for the final configuration.

## TEST CONFIGURATION

### Compressor

1. The compressor build will include the inlet guide vanes and the 2.8:1 pressure ratio rotor but no exit stators or interconnecting duct. The compressor will be mounted to and powered by the steam-driven Rover Turbine on test stand WX25R. See figures 71 and 72.

2. The inlet guide vanes will be set in the zero position (design setting) initially, but repositioning may be required as indicated by the test results.

3. The rotor blade clearance will be set at .010 inch for the initial build. This setting is expected to result in a .002 to .003 inch running clearance with the abradable shroud surface. Interference of the rotor tips and the abradable shroud is not planned for the first build. The self-grinding feature of the rotor tip and shroud will be included in subsequent builds after the vibrational characteristics of the compressor have proven satisfactory. This should insure tracking in to a minimum running clearance.

4. An external air supply will be used to pressurize the cavity between the front oil seal and the rotor labyrinth seal. This pressurization serves to balance the axial forces on the rotor to minimize bearing loads and to provide a pressure differential across the oil seal to eliminate oil leakage.

### Test Equipment

1. Air Inlet System - The air inlet system consists of an air filter, a calibrated air bottle, a convergent adapter, and approximately seven feet of straight ducting.

2. Exit Air System - The compressor exit scroll is connected to a close-couple valve with a divergent adapter. The exhaust air from the close-couple valve is ducted and dumped into the vertical stack of the steam exhaust system.

3. Turbine Thrust Balance System - Pressurized air is supplied to the downstream side of the turbine balance piston to reduce the thrust load on the bearing. An automatic system maintains the air pressure equal to the steam pressure at the exit of the turbine stator.

4. Oil System - Oil is supplied from a pump to three inlet points on the compressor and turbine at a pressure of 30 psi. The

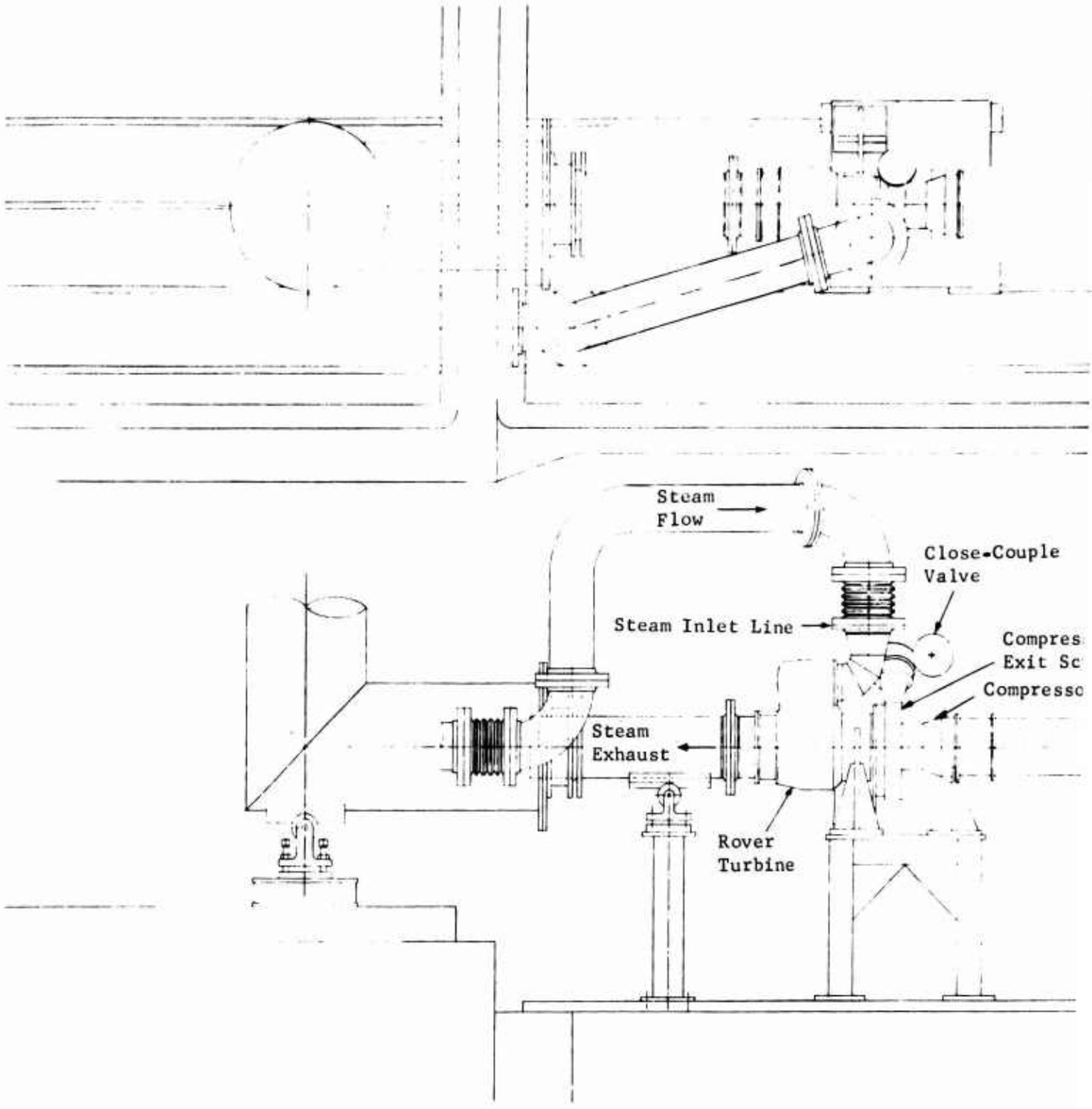


Figure 71. Compressor Test Rig Installation.

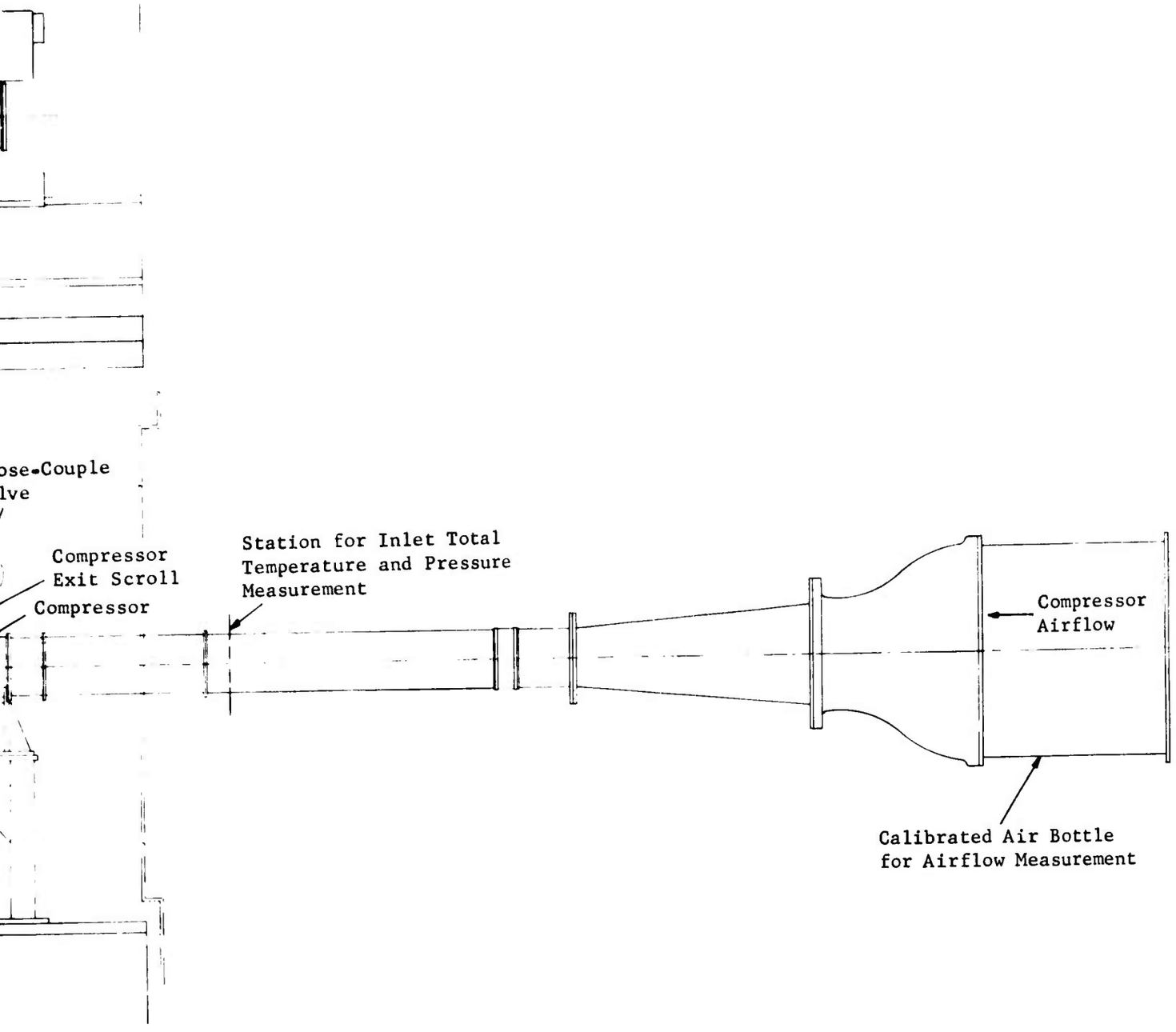
ose-Couple
lve
Compressor
Exit Scroll
Compressor
Station for Inlet Total
Temperature and Pressure
Measurement
Compressor
Airflow
Calibrated Air Bottle
for Airflow Measurement

R

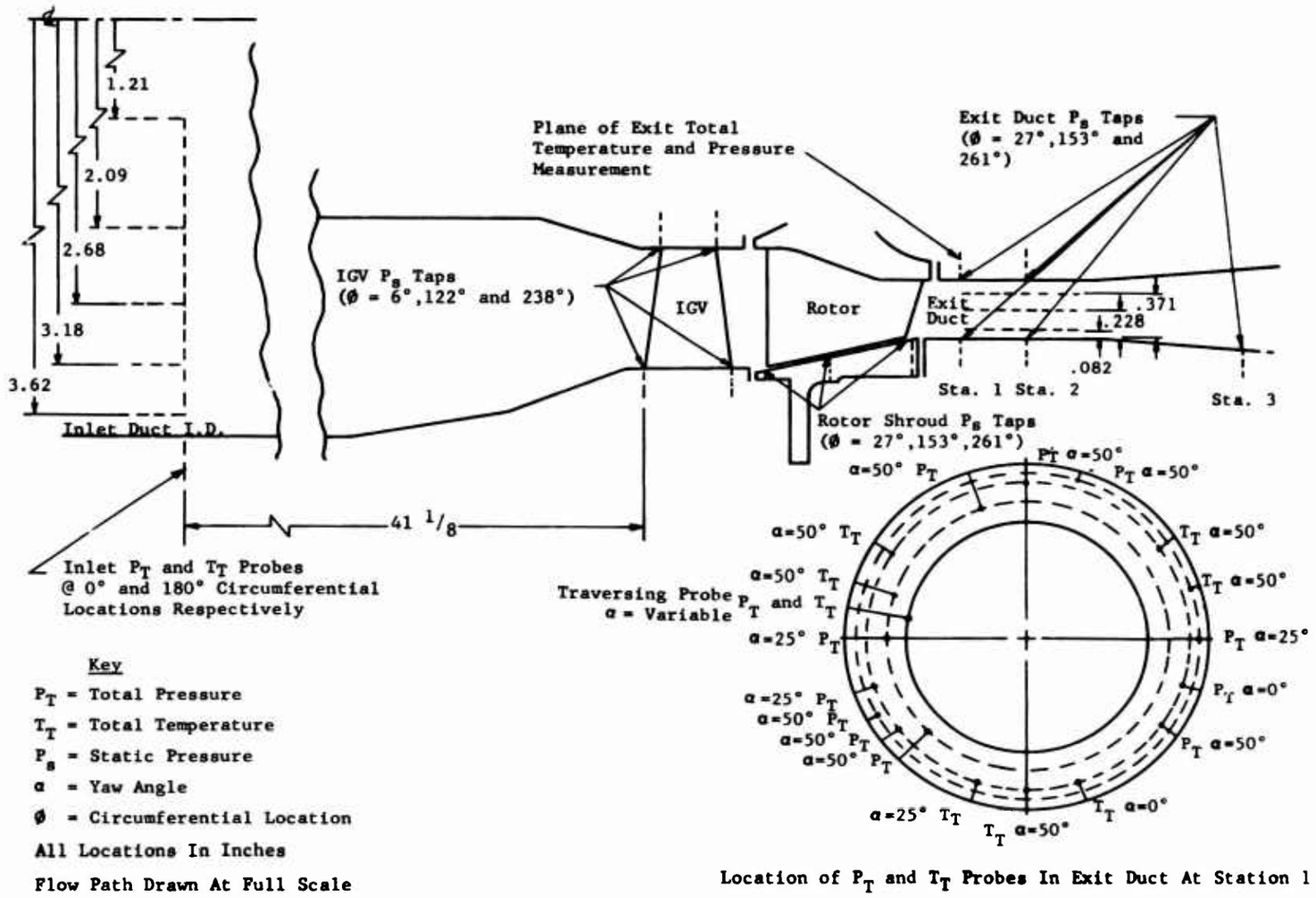


Figure 72. 2.8:1 Supersonic Compressor for USAAVLABS Schematic of Pressure and Temp. Instrumentation.

inlet points feed respectively: (a) compressor front bearing, (b) compressor rear main bearing and turbine front main bearing, and (c) turbine rear main bearing. The oil from the compressor front main bearing collects in the compressor sump, while the remaining oil collects in the turbine sump. The return oil from both sumps is scavenged with a common pump.

## INSTRUMENTATION

### Compressor Speed

A magnetic pickup is set to sense six lobes on the front compressor shaft nut. The signal is fed into an eput meter for direct RPM readout. The signal is also fed into an oscilloscope, and the RPM is periodically checked against a known frequency calibration signal.

### Compressor Airflow

The pressure differential across a standard calibrated air bottle is measured on an inclinometer to determine the compressor airflow. The air bottle is located at the entrance of the compressor inlet air system.

### Compressor Pressures

The compressor pressures to be measured include fixed total pressure probes, a traversing yaw probe, and static pressure taps. All of the pressures, except those from the traversing probe, are recorded on manometer banks which are photographed. The data from the traversing probe is recorded on X-Y plotters. The locations and ranges of all pressures are detailed on Table VII.

1. Inlet Total Pressure - The inlet total pressure is measured by a five-element total pressure rake located in the inlet ducting upstream of the compressor. The probe elements are located at the centers of equal areas along the zero-degree radial position from the duct center line to the I.D.

2. Rotor Exit Total Pressure - The rotor exit total pressure is measured with an array of fixed-position total probes and a traversing yaw probe. These measurements are made at an axial station which represents the leading edge plane of the exit stators.

   The fixed total probes are positioned at yaw angles of 0°, 25°, and 50° to cover the exit flow angle variation expected between wide-open throttle and the surge line and at three radii which represent the hub, mean, and tip streamtubes. These fixed total probes are distributed uniformaly at various circumferential locations.

TABLE VII. INSTRUMENTATION

| Instrumentation | Axial | Location Circumf. | Radial | Operating Range | Quick Look Board |
|---|---|---|---|---|---|
| 5 Inlet Totals (Pressures, Temperatures) | Inlet Duct | 0°, 180° | 1.21", 2.09", 2.68", 3.18", 3.62" | -60 to 0 in. Hg gage | |
| Static Pressure in Labyrinth Cav. | | | | -60 to 0 in. Hg gage | |
| 3 Statics | Leading Edge IGV | 6°, 122°, 238° | Flow Path O.D. | -60 to 0 in. Hg gage | |
| 3 Statics | Leading Edge IGV | 6°, 122°, 238° | Flow Path I.D. | -60 to 0 in. Hg gage | |
| 3 Statics | Trailing Edge IGV | 6°, 122°, 238° | Flow Path O.D. | -60 to 0 in. Hg gage | 1 pressure |
| 3 Statics | Trailing Edge IGV | 6°, 122°, 238° | Flow Path I.D. | -60 to 0 in. Hg gage | |
| 3 Statics | Leading Edge-Rotor | 40°, 166°, 274° | Flow Path O.D. | -60 to 0 in. Hg gage | |
| 3 Statics | Mid Chord Rotor | 27°, 153°, 261° | Flow Path O.D. | 0 to 60 in. Hg gage | |
| 3 Statics | Trailing Edge-Rotor | 14°, 140°, 248° | Flow Path O.D. | 0 to 60 in. Hg gage | 1 pressure |
| 3 Statics | Leading Edge Exit Stator | 27°, 153°, 261° | Flow Path O.D. | 0 to 60 in. Hg gage | |
| 3 Statics | Exit Duct Station 1 (Leading Edge) (Exit Stator ) | 27°, 153°, 261° | Flow Path I.D. | 0 to 60 in. Hg gage | |
| 3 Statics | Exit Duct Station 2 (0.49" Aft ) (of Station 1) | 27°, 153°, 261° | Flow Path O D. | 0 to 60 in. Hg gage | |
| 3 Statics | Exit Duct Station 3 (2.14" Aft ) (of Station 1) | 27°, 153°, 261° | Flow Path O.D. | 0 to 60 in. Hg gage | |
| 3 Pitot, $\alpha$ = 50° | Exit Duct Station 1 (Leading Edge) (Exit Stator ) | 0°, 126°, 234° | 0.228" from Flow Path O.D. | 0 to 60 in. Hg gage | 1 pressure |
| 1 Pitot, $\alpha$ = 50° | Exit Duct Station 1 (Leading Edge) (Exit Stator ) | 18°, 243° | 0.082" from Flow Path O.D. | 0 to 60 in. Hg gage | |

TABLE VII - CONTINUED

| Instrumentation | Location Axial | Circumf. | Radial | Operating Range | Quick Look Board |
|---|---|---|---|---|---|
| 1 Pitot, α = 50° | Exit Duct Station 1 (Leading Edge) (Exit Stator ) | 225°, 342° | 0.371" from Flow Path O.D. | 0 to 60 in. Hg gage | |
| 1 Pitot, α = 0° | Exit Duct Station 1 (Leading Edge) (Exit Stator ) | 108° | 0.228" from Flow Path O.D. | 0 to 60 in. Hg gage | 1 pressure |
| 1 Pitot, α = 25° | Exit Duct Station 1 (Leading Edge) (Exit Stator ) | 252° | 0.228" from Flow Path O.D. | 0 to 60 in. Hg gage | 1 pressure |
| 1 Pitot, α = 25° | Exit Duct Station 1 (Leading Edge) (Exit Stator ) | 90° | 0.082" from Flow Path O.D. | 0 to 60 in. Hg gage | |
| 1 Pitot, α = 25° | Exit Duct Station 1 (Leading Edge) (Exit Stator ) | 270° | 0.371" from Flow Path O.D. | 0 to 60 in. Hg gage | |
| 3 Total ic Thermo α = 50° | Exit Duct Station 1 (Leading Edge) (Exit Stator ) | 54°, 180°, 306° | 0.228" from Flow Path O.D. | 50 to 500°F | |
| 1 Total ic Thermo α = 50° | Exit Duct Station 1 (Leading Edge) (Exit Stator ) | 72° | 0.082" from Flow Path O.D. | 50 to 500°F | |
| 1 Total ic Thermo α = 50° | Exit Duct Station 1 (Leading Edge) (Exit Stator ) | 288° | 0.371" from Flow Path O.D. | 50 to 500°F | |
| 1 Total ic Thermo α = 0° | Exit Duct Station 1 (Leading Edge) (Exit Stator ) | 162° | 0.228" from Flow Path O.D. | 50 to 500°F | |
| 1 Total ic Thermo α = 25° | Exit Duct Station 1 (Leading Edge) (Exit Stator ) | 198° | 0.228" from Flow Path O.D. | 50 to 500°F | |
| Traversing Probe (Total pressure) (Total temperature) (Yaw Angle) | Exit Duct Station 1 (Leading Edge) (Exit Stator ) | 279° | variable | 0 to 60 in Hg gage<br>50 to 500°F<br>0 to 70° | |

The traversing yaw probe senses and automatically aligns the probe along the flow yaw angle and is capable of a continuous traverse from the tip to the hub of the annular passage. During a traverse, the total pressure, yaw angle, and total temperature are recorded on X-Y plotters as a function of radius.

3. Static Pressures - Static pressure taps are located on the O.D. and I.D. of the flow path in the inlet section and at the leading and trailing edges of each of the blade rows. Static taps are also located at the leading edge, mid chord, and trailing edge of the rotor shroud. These pressures are measured at each of three equally spaced circumferential locations.

Compressor Temperatures

The compressor temperatures include fixed total temperature probes and a traversing total temperature probe. The fixed probe total temperatures are read out from a multiple selector Brown recorder, while the traversing probe temperature is recorded on an X-Y plotter. The detailed locations of the thermocouples are presented in Table VII.

1. Inlet Total Temperature - The inlet temperature is measured by a five-element total temperature iron-constantan (I.C.) thermocouple rake, which is located and spaced the same as the inlet total pressure rake.

2. Rotor Exit Total Temperature - The rotor exit total temperature is measured with an array of fixed-position total temperature thermocouples and a total temperature thermocouple on the traversing yaw probe. These measurements are made at an axial station which represents the leading edge of the exit stators.

   The yaw angles and streamtube locations of the thermocouples are the same as those described for the rotor exit total pressures. A switch box arrangement permits the recording of exit temperature both as an absolute value and as a temperature rise with respect to the inlet temperature.

   The traversing thermocouple is a part of the same traversing yaw probe as described for the total pressure.

Vibration

Vibration pickups are located so as to record the vertical and horizontal vibrations at the front compressor support, turbine front support, and turbine rear support. The vibrations are recorded in units of acceleration (g's), since the displacement values are less than 0.1 mil.

### Oil Temperatures and Pressures

The oil temperature is recorded at the inlet and outlet of the compressor rig, and the temperature rise is monitored as an indication of satisfactory bearing operation. The oil inlet pressure is recorded to insure adequate oil flow.

### Steam Pressure

The steam pressure is recorded upstream of the control valve and at the inlet steam jacket for the turbine.

### Blade Stresses

Provisions have been made to incorporate strain gages on the compressor rotor blades. Slip rings are available, and an alternate design for incorporating this unit in the compressor rig has been made. The final decision as to whether or not this instrumentation is necessary will depend on the results of the rotor static natural frequency calibration and subsequent final review of the flutter analysis.

## PRETEST INSPECTIONS

### Dimensional Inspection

Dimensional inspection of the hardware is performed prior to and during assembly to establish and check critical dimensions, clearances, and airfoil geometry.

### Blade Natural Frequencies

The static natural vibrational frequencies of the blades are measured by exciting the blades and calibrating their natural frequencies against a known frequency on an oscilloscope. A microphone is used to sense the blade frequency. The results are compared to the predicted values, and the blade flutter analysis is reviewed.

### Rotor Balancing

The compressor and turbine rotors and shaft assemblies are balanced to within .001 - .003 ounce-inch at 2500 RPM prior to assembly.

### Magnaflux

The compressor rotor is given a Magnaflux inspection prior to assembly.

## TEST PROCEDURES

Table VIII presents the scheduled test points. The following sequence of steps describes the normal test procedure:

TABLE VIII. SCHEDULED TEST POINTS

| Percent Speed | $(W\sqrt{\theta})/\delta$ | P/P |
|---|---|---|
| 40 | Wide-open throttle | |
| | 2.0 | |
| | 1.5 | |
| | 1.2 | |
| | Surge point | |
| 60 | Wide-open throttle | |
| | 2.7 | |
| | 2.5 | |
| | Surge point | |
| 80 | Wide-open throttle | |
| | 3.5 | |
| | 3.4 | |
| | Surge point | |
| 90 | Wide-open throttle | 1.80 |
| | | 2.0 |
| | | 2.2 |
| | Surge point | 2.32 |
| 100 | Wide-open throttle | 2.08 |
| | | 2.3 |
| | | 2.6 |
| | | 2.8 |
| | Surge point | 2.90 |

*The above points are estimated based on predicted performance and are intended as a guide. Deviation from predicted performance may require adjusting the data points to be run.

1. All subsystems such as the oil system and the balance air systems are started and checked for proper operation prior to opening the steam control valve and starting the compressor.

2. The steam control valve is then activated, and the compressor speed is brought slowly up to the first test speed with the close-couple valve for the compressor air system in the wide-open position (maximum airflow). The vibration meter is monitored continuously throughout the test.

3. The inlet temperature is noted after it has stabilized, and the speed is then adjusted to the desired corrected speed ($N/\sqrt{\theta}$).

4. After all instruments are stabilized, a complete set of data is recorded, including a photograph of the manometer banks and full traverse from tip to hub with the traversing yaw probe.

5. A constant speed line is then developed by closing the close-couple valve while maintaining speed, until the next scheduled reduced weight flow is attained. Step 4 is then repeated. Four to five test points are planned for each speed line. The final test point on a given speed line is obtained by closing the close-couple valve until compressor surge is audible. The weight flow at which surge is first detected is noted, and the close-couple valve is opened until a weight flow slightly above surge is attained. This point is then taken as the last data point on the speed line.

6. The close-couple valve is set wide open, and the compressor is then accelerated to the next highest speed. The process is repeated for each of the scheduled speed lines up to 100 percent speed. In the range of 90 to 100 percent speed, where the speed lines are expected to exhibit almost constant weight flow, the constant speed line is developed by closing the close-couple valve to meet prescribed increments of increased pressure ratio rather than increments of reduced weight flow.

## DATA PRESENTATION

### Compressor Map

The standard compressor map in which the adiabatic efficiency and total to total pressure ratio are plotted against corrected weight flow for each of the corrected speed lines will be generated and compared to the predicted map. The predicted stage map is presented on Figure 3. This map will be based on the average compressor inlet conditions and the average rotor exit conditions (measured at the inlet station for the exit stator design). The corrected conditions and efficiency are computed as follows:

$$\text{Corrected airflow} = (Wa\sqrt{\theta})/\delta$$

Where: Wa = actual measured airflow in pounds per second

$$\sqrt{\theta} = \sqrt{\frac{T_{inlet}}{T_{reference}}}$$

$T_{inlet}$ = average total temperature at the compressor inlet (°R)

$T_{reference}$ = 519°R

$$\text{Corrected speed} = N/\sqrt{\theta}$$

Where: N = actual measured speed in revolutions per minute (RPM)

$\sqrt{\theta}$ = same as above

$$\text{Percent speed} = \frac{(N/\sqrt{\theta} \text{ measured})}{(N/\sqrt{\theta} \text{ design})} \times 100$$

Where: $(N/\sqrt{\theta})$ measured = same as above

$(N/\sqrt{\theta})$ design = 50,700 RPM

$$\text{Pressure ratio} = P_{T_4}/P_{T_o}$$

Where: $P_{T_4}$ = Total pressure integrated from hub to tip of the absolute velocity vector leaving the rotor.

$P_{T_o}$ = integrated total pressure at the compressor inlet.

$$\text{Adiabatic efficiency} = \frac{\Delta H'}{\Delta H} \times 100$$

Where: $\Delta H'$ = the isentropic enthalpy rise for the measured pressure ratio (BTU/lb).

$\Delta H$ = the actual enthalpy rise based on the average measured total temperatures at the compressor inlet ($T_{inlet}$) and the total temperature of the absolute rotor exit velocity vector integrated from hub to tip (BTU/lb).

Rotor Exit Conditions

The following rotor exit parameters will be presented as a function of radius from hub to tip:

Total pressure
Total temperature
Absolute Mach number
Absolute flow angle with respect to axial

Vector Diagrams

The velocity vector diagrams representing the rotor inlet and outlet conditions will be presented for three streamtube positions and will be compared to the design vector diagrams.

DATA ANALYSIS

A data analysis computer program will be used to construct the streamline paths, mass flow weighted pressure ratio, and efficiency and vector diagrams which satisfy the test results. The inputs for this program are the measured inlet and outlet radial profiles of total pressure and total temperatures, the measured weight flow, and the compressor geometry. The program computes a solution which satisfies these inputs and radial equilibrium for both tangential velocities and meridional streamline curvature. In addition to the parameters discussed above, numerous other parameters are calculated by the program, such as streamtube diffusion factors, loss coefficients, and incidence and deviation angles.

The data analysis will be run for key test points such as peak pressure ratios and peak efficiencies in the 90 to 100 percent speed range and for any other points which may give some insight into deficiencies in the design. In each case, adjustments will be made to the program inputs until the solution best satisfies all of the measured data (e.g., static pressures and total temperature and pressure profiles). This solution will then be used to analyze deficient areas and to resolve what modifications will improve the performance. The compressor design techniques and empirical data will also be re-evaluated based on these results.

Unclassified
Security Classification

**DOCUMENT CONTROL DATA - R & D**

*(Security classification of title, body of abstract and indexing annotation must be entered when the overall report is classified)*

| | |
|---|---|
| 1. ORIGINATING ACTIVITY (Corporate author)<br>Curtiss-Wright Corporation<br>Wood-Ridge, New Jersey | 2a. REPORT SECURITY CLASSIFICATION<br>Confidential<br>2b. GROUP<br>4 |

3. REPORT TITLE

Single Stage Axial Compressor Component Development For Small Gas Turbine Engines, Volume I, Design (U)

4. DESCRIPTIVE NOTES (Type of report and inclusive dates)

Final Technical Report for period 1/1/66 to 9/30/66

5. AUTHOR(S) (First name, middle initial, last name)

Charles H. Muller, William Litke, Andrew Sabatiuk, Howard W. Weiser

| 6. REPORT DATE | 7a. TOTAL NO. OF PAGES | 7b. NO. OF REFS |
|---|---|---|
| March 1969 | 152 | 23 |

| | |
|---|---|
| 8a. CONTRACT OR GRANT NO. DA 44-177-AMC-392(T)<br>b. PROJECT NO. 1G162203D14413<br>c.<br>d. | 9a. ORIGINATOR'S REPORT NUMBER(S)<br>USAAVLABS Technical Report 68-90A<br>9b. OTHER REPORT NO(S) (Any other numbers that may be assigned this report)<br>68-050223 F, WAD R608/PF-1 |

10. DISTRIBUTION STATEMENT

In addition to security requirements which apply to this document and must be met, each transmittal outside the Department of Defense must have prior approval of US Army Aviation Materiel Laboratories, Fort Eustis, Virginia 23604.

| 11. SUPPLEMENTARY NOTES | 12. SPONSORING MILITARY ACTIVITY |
|---|---|
| Volume I of a 3-volume report | U.S. Army Aviation Materiel Laboratories<br>Fort Eustis, Virginia 23604 |

13. ABSTRACT

The design of a single stage axial supersonic compressor with a predicted performance of 2.8:1 stage pressure ratio at 82 percent adiabatic efficiency and 4 pounds per second airflow is discussed. (U)

The results of a gas generator performance study to evaluate non-regenerated designs with 16:1 pressure ratio compressors and turbine inlet temperatures between 2500°F and 3000°F are presented and discussed. The design point specific fuel consumption of the engines studied ranged from 0.415 to 0.438 pounds per horsepower per hour. At 50 percent power this range increased to 0.465 and 0.534 respectively. The engine configuration which indicated the lowest specific fuel consumption has a two spool gas generator and variable stator free power turbine. (U)

The preliminary designs of a two stage axial/centrifugal compressor and an advanced gas generator which incorporates this compressor are discussed. The predicted performance of the compressor is 16:1 pressure ratio at an adiabatic efficiency of 77.5 percent and an airflow of 4 pounds per second. The predicted design point specific fuel consumption and power at a 2500°F turbine inlet temperature are 0.431 pounds per horsepower per hour and 785 horsepower respectively. (U)

The results of a preliminary design study for a variable geometry axial compressor rotor concept are also discussed. This concept offers the potential for improved part speed compressor performance and stage matching. (U)

DD FORM 1 NOV 68 1473 REPLACES DD FORM 1473, 1 JAN 64, WHICH IS OBSOLETE FOR ARMY USE.

Unclassified

| 14. KEY WORDS | LINK A | | LINK B | | LINK C | |
|---|---|---|---|---|---|---|
| | ROLE | WT | ROLE | WT | ROLE | WT |
| Research and Development<br>Compressor, axial<br>Small Gas Turbines<br>Design and Development | | | | | | |

# GENERAL DECLASSIFICATION SCHEDULE

IN ACCORDANCE WITH
DOD 5200.1 R & EXECUTIVE ORDER 11652

# THIS DOCUMENT IS:

Subject to General Declassification Schedule of Executive Order 11652-Automatically Downgraded at 2 Years Intervals- DECLASSIFIED ON DECEMBER 31, 1972

BY

Defense Documentation Center
Defense Supply Agency
Cameron Station
Alexandria, Virginia 22314